THE CONSTRUCTION OF A WIDE-FREQUENCY RANGE DOUBLE HETERODYNE CONDUCTANCE BRIDGE AND ITS USE IN THE INVESTIGATION OF POLARISATION ERRORS IN CONDUCTANCE MEASUREMENTS

oooooooooooooooo

A thesis submitted in fulfilment of the requirements of RHODES UNIVERSITY for the degree of DOCTOR OF PHILOSOPHY.

By
Herby Silvester Govinden

1961

ACKNOWLEDGEMENTS

Sincere thanks are due to:

The S.A. Council for Scientific and Industrial Research for a scholarship, and also to Rhodes University for a grant, which made it possible for this research to be undertaken;

Professor J.A. Gledhill, M.Sc., Ph.D. (S.A.), Ph.D. (Yale), F.Inst.P., for his able supervision and for invaluable advice and criticism given throughout the period of this research;

Professors W.F. Barker, E.T. Verdier and A.S. Galloway for their encouragement and interest;

Dr. N.P. Finkelstein for assistance in the construction of the electronic thermoregulator;

Mr. F. van der Water and Mr. G. W. Randell for glass-blowing and advice given in technical matters affecting the construction of the conductance bridge;

Mr. G.F. Walters for the photographs and reproduction of the diagrams;

And to many others for help in many ways.

C O N T E N T S

ABBREVIATIONS, SYMBOLS and UNITS

The following are used throughout the text:

a.c.	=	alternating current
c/s	=	cycle per second
kc/s	=	kilocycle per second
R, r	=	resistance
C, c	=	capacitance
X	=	reactance
f	=	frequency in cycles per second
ω	=	$2\pi f$
Z	=	impedance
μF	=	microfarad
pF	=	picofarad = 10^{-12}farad
D.S.C.	=	double silk covered
S.W.G.	=	standard wire gauge
r.m.s.	=	root-mean-square
e.s.u.	=	electrostatic unit
v	=	volt
G.R.	=	General Radio
Q	=	cell constant
D	=	demal = gram equivalent per cubic decimetre
N	=	normal
g	=	gram
mg	=	milligram
ml	=	millilitre
nm per cm	=	nanomho per centimetre

INTRODUCTION

REVIEW

The measurement of the conductivities of electrolytes has been the subject of much research during the past ninety years. With the introduction of alternating currents in the Wheatstone Bridge Network, the first step was taken by Kohlrausch, Wien and others towards increasing the accuracy of measurements by minimising errors due to polarisation. Subsequent research lay in:

(a) Improving the source of the a.c.

For an a.c. conductance bridge, the two conditions of balance may be shown to be functions of the frequency of the current applied to the network (see Section 1.1). Hence good balance in an accurate bridge (i.e. silence in the telephone - if the latter is used as null detector) can only be achieved if the source of current is chosen to have a steady frequency and a wave-form which is as nearly sinusoidal as possible. Now the induction coil - first used by Kohlrausch (1) - clearly does not satisfy these requirements. It produces a current of somewhat irregular wave-form, which may be separated analytically into the sum of a number of sine waves of different frequencies. With such a source, the balance point is characterised by a poor minimum since, when the bridge is balanced for one frequency it is out of balance for another. As soon as this became

recognised, a series of papers were published which reported investigations of the various sources of a.c. available, with a view to finding one with the desired characteristics. In 1913 Washburn and Bell (2) replaced the induction coil with a type of rotary generator; Taylor and Curtis (3) were led to the use of a Vreeland oscillator. In 1916, Taylor and Acree (4) studied the wave-forms of the induction coil, the 60 cycle mains supply, a rotary generator and a Vreeland oscillator. They concluded that the Vreeland oscillator was the best available, but Morgan and Lammert (5) found it unreliable. Meanwhile, Hall and Adams (6) had introduced the vacuum-tube oscillator to the field of conductance measurements. Later workers e.g. Ulich (7), Woolcock and Murray-Rust (8), Jones and Josephs (9), recognising its many advantages, also adopted it as a source of a.c. When properly designed and constructed, it conforms to the requirements of a good source; in addition, its frequency and output voltage are readily variable. Continued developments in electronics have made the vacuum-tube oscillator vastly superior to all other sources for accurate measurements.

(b) Increasing the sensitivity of the null detector

One of the factors determining the accuracy with which the bridge can be balanced is the sensitivity of the null point detector. The early work of Kohlrausch and others

established the use of the telephone as the detecting instrument. Wien effected an improvement in its sensitivity by designing an ''optical telephone'' which may be regarded as the forerunner of the vibration galvanometer. It was simply a magnetic telephone of which the diaphragm could be tuned to be in resonance with the a.c. flowing in the telephone windings. In this way, the amplitude of motion was greatly magnified and was observed by reflecting a beam of light from a mirror operated by the moving diaphragm. Washburn and Bell (2) used a telephone tuned to the frequency of the a.c. source. Subsequent improvements, however, kept pace with those to the oscillator. Hall and Adams (6) considerably increased the sensitivity by adding a thermionic amplifier. This method has also been applied to improve the sensitivity of the various types of visual indicators now in use. Of these, the cathode-ray oscilloscope appears to have gained most favour. Its use as a phase-discriminating null detector was first described in 1938 by Lamson (10). Thus, resistive and reactive components can be balanced separately if the a.c. source is fed to the X plates in correct phase, and the voltage from the detector terminals (suitably amplified) is applied to the Y plates. At balance, a horizontal line is observed on the screen; resistive unbalance tilts this line through an angle while reactive unbalance converts the line to an

ellipse. Jones, Mysels and Juda (11) included this method of detection in a precision conductance bridge and claim to have attained a precision of 0.0005% with it. Less popular are the ''magic eye'' tube described by Ulrey (12), Breazeale (13), Garman (14) and Koehler (15), and the a.c. galvanometer referred to by Quirk and Hall (16). Although the latter can be made phase selective, the instrument is subject, at maximum sensitivity, to transient disturbances which are annoying, as time is required for the galvanometer to return to its original state.

Modern conductance bridges almost invariably include visual indicating devices. Since the observations are visual, they are less nerve-racking and the bridge can be balanced even in noisy surroundings. Another advantage is that measurements may be carried out using supersonic frequencies.

(c) Reducing errors inherent in the design of the bridge

The design and construction of precision conductance bridges was initiated by Jones and Josephs (9) in 1928, after they had subjected the conventional Kohlrausch method of measurement to an exhaustive examination. Various factors affecting the accuracy of measurements were investigated, and the conditions under which errors may become more significant were clearly defined. For instance, they pointed out that the general condition of

balance: $Z_1Z_4 = Z_2Z_3$ (see Section 1.1) is only true if no current escapes from the bridge arms. Since there are capacitances from each point of the bridge to earth, current may flow away through these, and inequalities of capacitances on opposite sides of the bridge will cause errors in setting and probably make zero sound at balance unattainable. This at once threw suspicion on bridges with unequal ratio arms. A particularly troublesome capacity is that between the telephone coils and the head of the observer, which allows current to flow through the phones via this capacity to ground - to which the oscillator and other parts of the bridge are linked capacitatively, even when the bridge is in balance. Taylor and Curtis (3) had observed that these effects could be lessened by putting a high resistance shunt across the oscillator leads and earthing the centre point of this. Jones and Josephs found that the setting of their bridge depended on the setting of a reversing switch in the oscillator leads, and, having traced the error to inequality in the capacitances to earth from these leads, designed the grounding circuit shown in Fig. 1. This is actually a Wagner earthing device (17). In use, the bridge was first balanced in the usual manner with r_3 and C_3, and then the lower end of the phone was grounded by means of the switch S_1. This, in effect, completed a new bridge circuit consisting of r_1, r_2, r_5, r_6 and C_g. This bridge was balanced by adjusting the tap g (i.e. adjusting the ratio

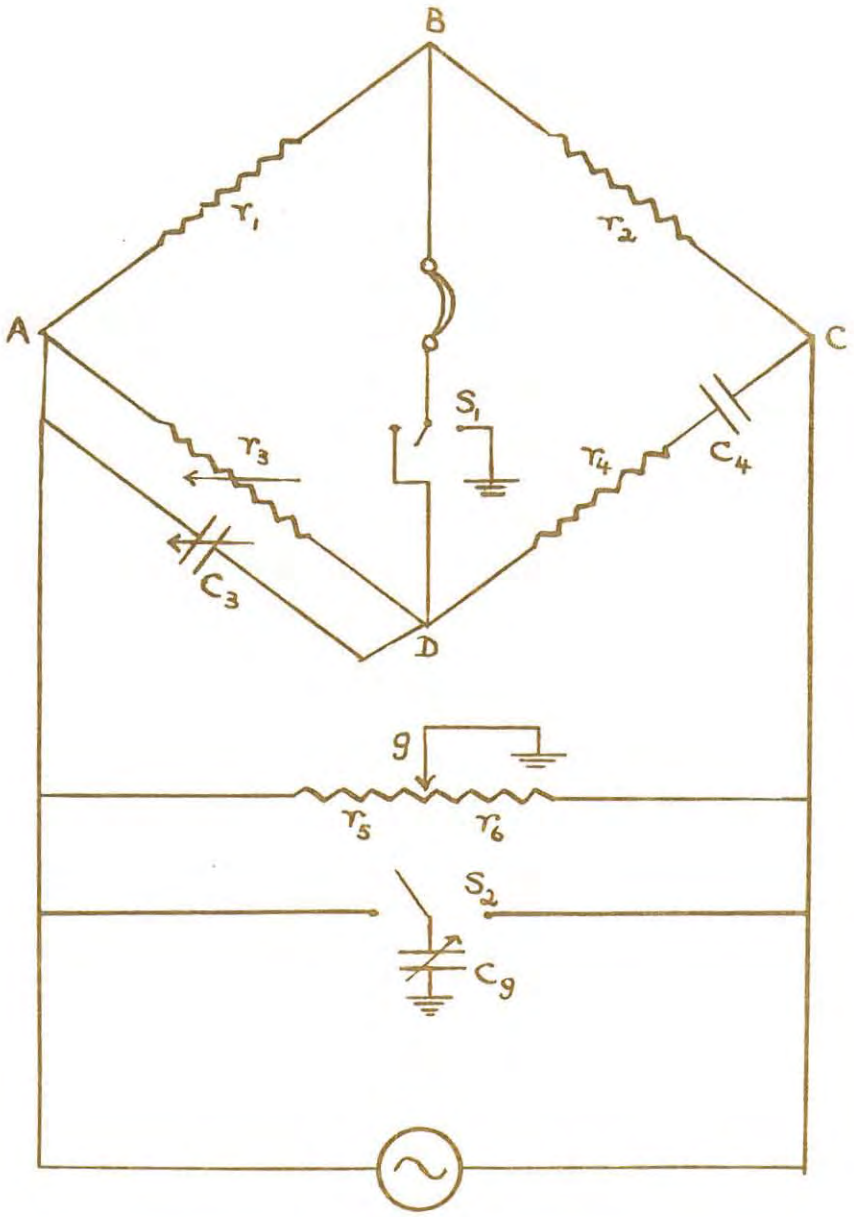

FIG. 1 JONES BRIDGE WITH WAGNER EARTH CIRCUIT

r_5/r_6) and C_g, the latter being put across either r_5 or r_6, as necessary, by S_2. The main bridge was then again balanced, then the ground bridge, and so on alternately until the bridge was balanced for both positions of the switch S_1. Now B and D were at the same potential, which, since g is grounded, is zero. Hence no current could go from B or D to ground. Jones and Josephs, while verifying experimentally that the grounding device introduced no error, did not give the underlying theory.

After an examination of the effects produced by an earthed metal plate in various parts of the bridge, Jones and Josephs concluded that shielding of the bridge caused more error than it cured, and so built an unshielded bridge. Shielding had been in general use in radio-frequency measuring technique before this, however, and its theory had been developed by Campbell and others (18, 19); it had been shown that a grounded shield introduced no error in a properly grounded bridge, and it appears that their summary rejection of shielding in the conductance bridge was based on false conclusions.

As they were building an unshielded bridge, the question arose as to whether or not the thermostat should be grounded. A conductance cell immersed in water which is grounded is quite effectively shielded, and, after a series of experiments, they recommended that oil should be used in place of

water in the vessel. It did not appear to matter then whether the container was grounded or not. In addition to the grounding effect of a water thermostat, they suggested the presence of errors due to eddy-currents in the water and a shunt-path through the wall of the cell near one electrode, through the water in the thermostat, and back through the cell wall near the other electrode. Even in a grounded bridge there would be a possibility of error arising from these causes, and oil is therefore used in all precision measurements.

The condensers used for C_3 next came under scrutiny, and three points were raised. Firstly, losses in the dielectric have the effect of a resistance in series with the condenser. A good air-dielectric condenser should be practically loss-free at 3 kc/s, provided that the supporting insulators are good. Secondly, there is a parallel leak-resistance from one set of plates along the surface of and through the supporting insulators to the other set of plates. This shunts r_3, and may affect its value within the limit of accuracy aimed at. This leak is unfortunately, variable - depending on the temperature of the air and its humidity. It may be measured approximately, however, preferably on a damp day, and if its value exceeds $10^5 r_3$ it will not affect the readings within 0.001%. It may be minimised by coating the insulators with paraffin wax.

The leak cannot be eliminated completely, however, and so sets an upper limit to the resistances which may be measured with a bridge. Thirdly, Jones and Josephs drew attention to the factor $(1 - \omega^2 C_3^2 r_3^2)$ in eqn. 1 (see Section 1.1) which had been ignored by previous workers. It had been argued that the cell is a resistance in parallel with a capacitance - it is a well-known fact in a.c. theory that any condenser and resistance in series may be replaced by an equivalent pair in parallel - and that C_3 would balance out the capacitance, leaving r_3 equal to the resistance. This reasoning does not hold, because the values of the equivalent capacitance and resistance are not equal to those of the parallel combination; in any case, it is the equivalent series resistance which is required for the Jones-Christian polarisation correction (see p. 18), and so the factor must be used whenever that correction is to be applied.

The only remaining portion of the circuit - the resistances - caused Jones and Josephs more trouble than the rest of the circuit together. Those available showed errors depending on the frequency of anything up to 0.02% at 2400 c/s for special boxes, and much greater errors for ordinary boxes. They traced these errors to several causes, of which the two most important are:

(i) Losses due to the dielectric between the binding posts on which the resistance is mounted, due to leakage along the surface, actual loss in the dielectric and the capacitative shunt between the two terminals. They recommended, apparently on empirical grounds, that the distance between two binding posts carrying a resistance R between them should be at least $0.04R^{\frac{1}{2}}$ cm., in order to minimise these errors.

(ii) Appended coils which are not in use have a capacity to those which are, and withdraw energy from the bridge on each cycle in the form of charging current. This error was found to be of importance only in coils of 10,000 ohms or more each, and they recommended that coils of this value should be mounted so that only those actually in use have any connection with the bridge.

Other causes of error were residual inductance in and capacitance between individual coils in the resistance boxes, variable contact resistances, and losses in the cotton and silk insulation round the wires used to connect the various units in the boxes. Jones and Josephs designed and built new resistance boxes to their own specifications, and described a bridge incorporating all the above points, which was probably the most accurate bridge in existence at the time.

In 1930 Shedlovsky (20) set out the theory of the effect of earth capacity on a shielded conductor. Application of the theory to the bridge network made it possible to explain the effects of various methods of grounding the bridge, and particularly, the method of action of the Wagner Earth. Subsequently, Shedlovsky designed a shielded bridge embodying his developments. It is of interest to note that he sets the condition that the shielding of the measuring resistances shall not be closer than $2\frac{1}{2}$ inches at any point. He states: ''this spacing proved to be sufficient by actual test to make the effect of screen capacity on the resistance negligible.'' The ratio arms may, however, be shielded closely provided that they are shielded symmetrically. Slight inequalities in the impedance of the arms may in any case be allowed for by reversing them and taking the mean (geometric) of the two results.

An interesting point in Shedlovsky's bridge is his use of a balanced oscillator. This is more stable than the normal single-ended type, and has the advantage that the capacitances from the output leads to earth may be made nearly equal. In spite of this feature, however, this type of oscillator does not appear to have been much favoured by later workers, who prefer to couple unsymmetrical oscillators up to the bridge by way of doubly-shielded transformers.

It will be seen from Fig. 1 that it is not possible to

have one terminal of the detector grounded permanently in that type of bridge, because it must be possible to connect the detector across the bridge proper without grounding any point of it. Vacuum-tube amplifiers, however, particularly of the high-gain type, are troublesome to operate in the ungrounded condition, being liable to pick up hum from a.c. supply lines in the vicinity. In order to use a grounded high-gain amplifier in the bridge, it is customary therefore to balance the Wagner Earth against r_1 and r_2 by connecting the amplifier input to B, and then to balance arms 3 and 4 against Wagner Earth by switching the grid side of the amplifier input to D, leaving the other input terminal grounded all the time. This process, known as ''separate terminal balancing'', was introduced by Astin (21) on a capacity bridge of the Schering type, and suggested for conductance bridges by Luder (22). It has the disadvantage that the setting of the Wagner Earth must be as precise as that of the bridge proper, but this is soon overcome by experience, and is far outweighed by the sensitivity of a silent, high-gain amplifier.

Further developments in the design of high-precision bridges were those made by Luder (loc. cit.). He describes a bridge incorporating a 10,000 ohm-per-step decade with knife switches. Thus, only those resistances required can be switched in while all the others in the decade are

left out of the circuit completely. Important points from his paper are the suggestion that the oscillator should be supplied from a voltage-stabilised power supply run off the a.c. mains, and the amplifier from batteries. If both are fed from the mains or from the same batteries, trouble is encountered from a note fed from the oscillator into the supply and thence to the plate of the first amplifier tube. High-gain amplifiers run from a.c. supply are also very likely to develop hum and pick up noises from electrical machinery in the neighbourhood. Hence it is better to run the amplifier off batteries and the oscillator from the mains than vice versa.

It may be mentioned that precision conductance bridges, incorporating the improvements introduced by Jones and Josephs, Shedlovsky and Luder, were designed and constructed at this University - and for the first time in South Africa - by Gledhill (23) in 1942 and later by Goddard and Faure (24, 25).

(d) Decreasing errors associated with the design of the conductance cell

In 1916, Washburn (26) derived equations for the design characteristics of the conductance cell on the assumption that heating of the cell by the current passing and the sensitivity of the telephones were limiting factors determining the accuracy. A series of cells of the pipette

type was then designed. These were soon recognised as being both convenient and reliable in use, and were employed practically exclusively for accurate work after that time. Although Washburn's equations have now fallen into disuse - the heating effects and the sensitivity being no longer the limiting factors - his efforts may be regarded as the first attempt towards the really scientific design of cells. Prior to this, it was customary to use cells of either the Ostwald or Kohlrausch type with the electrode area and spacing such as, simple calculation and experience showed, would give a resistance of 50 to 1000 ohms when filled with the liquid in question.

In the course of measurements on solutions of potassium chloride and hydrochloric acid, Parker (27) observed that determinations with different cells led to somewhat different conductance values. In 1923, therefore, he published two papers in which he reported that the ''cell constant'' was not constant, but that it depended in a complicated manner on the nature and concentration of the measured solution. He ascribed this apparent variation to polarisation and to adsorption, as also did Randall and Scott (28) who made a thorough investigation of the effect. Shedlovsky (29), who made similar observations, discounted adsorption as a possible cause but reported that '' measurements with bright Pt electrodes showed fluctuations of a nature suggesting variable polarisation effects''. It was not until

Jones and Bollinger (30) published their third paper of the series on the measurement of the conductance of electrolytes, however, that a satisfactory explanation was advanced. They tracked down the variation which they called the ''Parker effect'', to a capacitance by-pass through the leads of cells of the Washburn type. (Inspection of cells with dipping electrodes show that a similar effect is present). Subsequently, they proceeded to design cells in which the Parker effect was minimised by separating the lead tubes as much as possible. See Figs. 2(a), (b), (c).

Other methods for the elimination of the Parker effect have also been successfully devised. Amongst these may be mentioned the cell designed by Thomas and Gledhill (23). Here, thin lead wires run down two relatively wide lead tubes, which are well separated. Thus, a column of air serves to insulate the lead tubes from the outside liquid. (See Section 2.21). Nichol and Fuoss (31) and Brody and Fuoss (32) have constructed cells - especially for use with dilute non-aqueous solutions, and which represent a departure from conventional cell design - in which the Parker effect becomes evident only at very high values of the cell resistance (see Section 2.21).

(e) Studies of electrolytic polarisation phenomena

Up to the time of Kohlrausch, conductance measurements had been hampered by the fact that the passage of direct

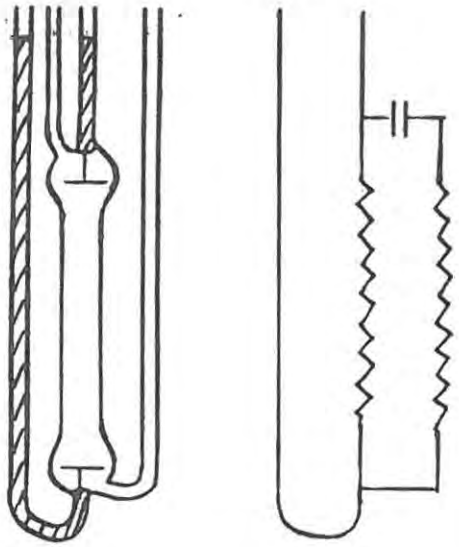

FIG. 2(a) Parker Effect in WASHBURN CELL

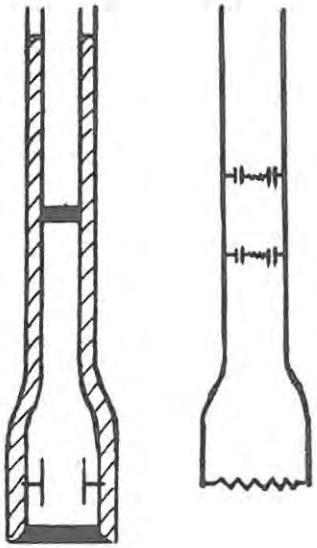

FIG. 2(b) Parker Effect with DIPPING ELECTRODES

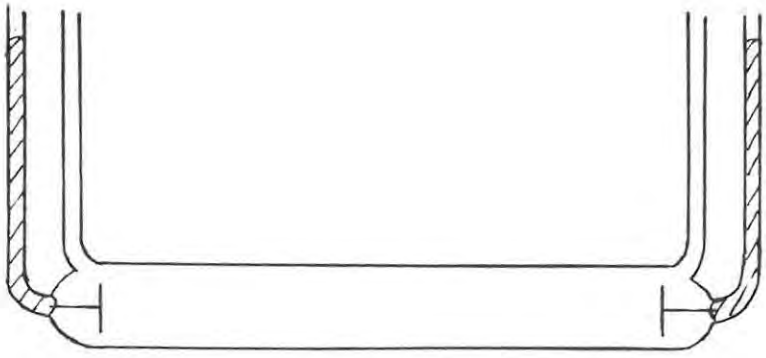

FIG. 2(c) JONES CELL

current through the cell (with two electrodes, usually of platinum) caused electrolytic action at the electrodes, i.e. the formation of gas films on the electrode surfaces, and concentration changes in the vicinity of the electrodes due to transport phenomena (see Section 2.1). Hence results were obtained, which were hardly reproducible. Considerable improvement in accuracy was only made possible when, with the introduction of a.c., these polarisation effects were reduced. Kohlrausch maintained, however, that with the use of such a current the cell no longer behaved like a pure resistance. He believed that, with inert Pt electrodes, hydrogen and oxygen are deposited on the electrodes alternately in every cycle - the electrolysis being strictly reversible chemically and thermodynamically. This reversible transformation of electrical energy into chemical energy would then be electrically equivalent to an electrostatic condenser, whose capacitance (designated as C_s) is in series with the resistance of the electrolyte. C_s is referred to as the polarisation capacitance.

The inclusion of a condenser in parallel with the resistance in the measuring arm of the bridge - suggested by Kohlrausch to compensate for C_s and thus to improve the minimum at balance - did not, however, make for reproducible results. Consistent values could be obtained only when the electrodes were '' platinised'' i.e. giving them a thin

coat of platinum black; other helpful factors were: increasing the frequency of the a.c. to 1 kc/s or more and designing the cell so that the resistance to be measured could be 100 ohms or more.

In 1896, Wien (33) observed -whilst experimenting with Ni, Ag and bright Pt electrodes - that a.c. electrolysis gave rise to a resistance increase (ΔR) over the ''true'' resistance (R_t) of the cell i.e. the resistance calculated from the cell dimensions and the conductance of the electrolyte. The use of the compensating condenser was found to be ineffective against this polarisation resistance, ΔR. It was then suggested by Wien that ΔR might be the result of incomplete reversiblity of the electrode processes. Continued investigations by Wien showed ΔR to be independent of frequency in the range 64 to 256 c/s, while C_s was almost independent of frequency although a slight decrease with frequency had been noted.

Wien's researches were followed up by Warburg (34) who, in 1899, published a paper in which he put forward the idea that diffusion was responsible for the incomplete reversibility of the electrode reactions. By applying Fick's Law of Diffusion, he concluded that polarisation causes a capacitance in series with the resistance of the cell and that this capacitance (C_s) varies indirectly with $f^{\frac{1}{2}}$, and also that there is a phase displacement of 45° at the electrodes.

Now, it can be easily deduced from the diagram below that

$$\tan \psi = \Delta R C_s \omega = 1$$

since $\psi = 45°$.

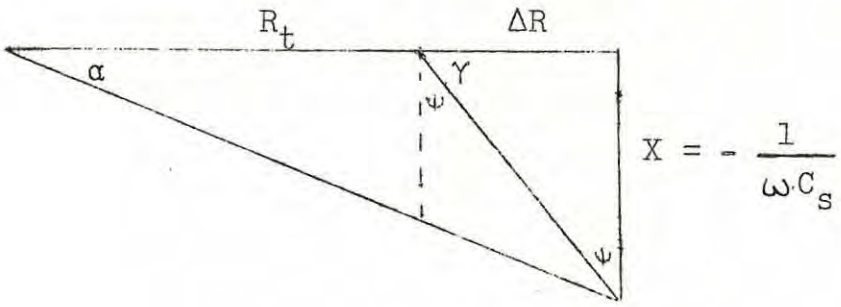

Note: α = phase displacement across complete cell
γ = phase displacement across the electrodes
ψ = complement of γ and it, therefore, represents the change in phase displacement across the electrodes due to the irreversibility of the electrode processes.

Warburg's theory was then extended to show that, if $\psi = 45°$ and C_s is inversely proportional to $f^{\frac{1}{2}}$, ΔR must also be inversely proportional to $f^{\frac{1}{2}}$. Experiments with Hg and Ag electrodes indicated that these relationships were valid as rough approximations.

A paper which aroused considerable interest was presented by Jones and Christian (35) in 1935. In it, they reviewed the foregoing theories of Kohlrausch, Wien and Warburg, and proceeded to report on their measurements of the conductance of electrolytes - particular attention being paid to galvanic polarisation effects. A most in-

genious cell was used, based on a design by Miller (36). The latter, in a new experimental attack on the problem of polarisation studies, had devised a cell with movable electrodes, but the data he obtained were lacking in precision. Jones and Christian improved on the design and construction so that the spacing between the electrodes could be accurately measured and the area of cross-section was uniform. By moving the electrodes a distance d and subtracting the readings at either end, the resistance of a length d of electrolyte of known cross-section could be found, and hence R_t was calculated, assuming that the difference between the polarisation effects for the two sets of readings was negligible. The data which they obtained gave ''definite evidence that polarisation causes a positive resistance which is not located in the body of the solution but is one aspect of the phenomena which occur at the electrodes''. They also concluded that ''polarisation resistance is inversely proportional to the square root of the frequency '' and that ''polarisation causes a capacitance in series with the resistance which decreases with increasing frequency''. Two interesting mathematical expressions were then derived, based on the above results:

(i) $$R_s = R_t + \Delta R = \frac{d}{a\kappa} + \Delta R$$

where R_s = equivalent series resistance
a = area of cross-section of electrode
κ = specific conductance of electrolyte

Hence, a plot of R_s values at any frequency, against corresponding $\underline{d}$ values should give a straight line with the value of ΔR given by the intercept on the R axis.

(ii) $$R_s = R_t + \Delta R = \frac{d}{a\varkappa} + \frac{k}{f_2^{\frac{1}{2}}}$$

where k is a constant.

Hence, a plot of R_s values for any $\underline{d}$, against $1/f^{\frac{1}{2}}$ should give a straight line whose intercept on the R axis would be R_t.

Except for a small positive curvature observed when R_s values were plotted against $1/f^{\frac{1}{2}}$, Jones and Christian found the experimental points to lie approximately on a straight line. (It may be added that the solutions investigated had resistances which varied between 50 and 2000 ohms, whilst the frequency ranged from 50 to 4000 c/s). Hence they recommended that R_s should be measured at a series of frequencies (they suggested three frequencies) and plotted against $1/f^{\frac{1}{2}}$, and extrapolation to infinite frequency would yield R_t. This has, therefore, been standard practice since 1935.

Nichol and Fuoss (31), in their measurements on dilute non-aqueous solutions, have found that '' when the resistance is of the order of 10^4 ohms, the curvature becomes extremely pronounced and linear extrapolation on an R - $f^{\frac{1}{2}}$ scale becomes impossible''. These workers state, however, that

their data can be represented by the quadratic equation

$$R_s = R_t + af^{-\frac{1}{2}} + bf^{-1}$$

Thus, when the coefficients a and b have been evaluated, R_t can be calculated directly from the above equation.

It will be seen that this equation reduces to

$$R_s = R_t + af^{-\frac{1}{2}}$$

if b = 0, i.e. the higher terms in $f^{-\frac{1}{2}}$ being negligible. This is found to be so for aqueous solutions which do not have very high resistances; in such cases, then, the linear extrapolation recommended by Jones and Christian is applicable.

Investigations carried out at this University (see p. 21) have shown that, in certain instances, linear extrapolation is only possible with $R - f^{-\frac{1}{4}}$ plots, while, in other cases, approximately straight lines are obtained on $R - f^{-1}$ plots. This strongly suggests that, under certain conditions (see under Section 2.6), both a and b become equal to zero, and a lower term in $f^{-\frac{1}{2}}$ must be introduced; whilst, sometimes, a = 0, making the term $f^{-\frac{1}{2}}$ negligible.

PURPOSE OF PRESENT RESEARCH

Conductance research pursued at this University has been greatly facilitated by the construction of precision conductance bridges by Gledhill (23), and by Goddard and A. Faure (24, 25). Coupled with improvements effected in cell design and in the methods of temperature control, it has been found possible to measure with great accuracy the solubilities of sparingly soluble salts, the resistance of ultra-pure water, and the conductances of dilute potassium chloride solutions, and of mixed electrolytes.

However, a disturbing feature of the measurements noted by P.K. Faure (37), Goddard (24), A. Faure (25) and Taylor (38), amongst others, is that the true resistance cannot always be reliably deduced by the Jones and Christian extrapolation procedure, due to a marked deviation from linearity. This was found to be particularly so with the use of bright Pt electrodes and when the resistance measured is below 100 ohms.

Further investigation into the problem is, therefore, necessary and the present research was undertaken with these aims in mind:

(i) to construct a bridge capable of giving accurate readings of resistance and capacitance over a wide range of frequencies, and thereby

(ii) to develop a satisfactory theory to account for the variation of electrolyte resistance with frequency.

CONSTRUCTION

OF

THE CONDUCTANCE BRIDGE

1.1 THE DOUBLE-HETERODYNE PRINCIPLE

As has already been mentioned, one of the factors influencing the accuracy of measurements with an a.c. Wheatstone Bridge Network is the frequency of the current applied to the bridge. The reason for this becomes obvious on analysing the circuit, and hence examining the conditions for balance.

Although the exact equivalent circuit of the conductance cell is not known, it is generally assumed that the cell can be represented by a resistance (i.e. the true resistance of the electrolyte) and a capacitance, C_s, in series with it. On this basis, the circuit of the network is as shown in Fig. 3 (a).

The general condition for balance is obtained by applying the vector Ohm's Law, and is

$$\frac{Z_1}{Z_2} = \frac{Z_3}{Z_4}$$

Now, $Z_1 = Z_2$ (approximately)

At balance, therefore

$$Z_3 = Z_4$$

But, inspection of the circuit shows that the expression for Z_4 is complex. However, the solution may be simplified by imagining Z_4 to consist of an impedance Z_4' with a

capacitance C_4 connected in parallel and, similarly, imagine Z_3 to consist of Z_3' with C_4 in parallel. The network is thus transformed to the circuit shown in Fig. 3 (b). The complex impedances of Z_3 and Z_4 may then be written respectively as

$$1/Z_3 = 1/Z_3' + j\omega C_4$$

and $$1/Z_4 = 1/Z_4' + j\omega C_4$$

Since $Z_3 = Z_4$ at balance, it is obvious from the above equations that $Z_3' = Z_4'$, and that the solution of this equation will give the conditions for balance of the bridge.

Now let, $C_3 - C_4 = C$

The complex impedances of Z_3' and Z_4' will be respectively,

$$1/Z_3' = 1/R_3 + j\omega C$$

or $$Z_3' = \frac{R_3}{1 + \omega^2 C^2 R_3^2} - \frac{j\omega C R_3^2}{1 + \omega^2 C^2 R_3^2}$$

and $$Z_4' = R_4 - \frac{j}{\omega C_s}$$

On equating the resistive components, we get,

$$R_4 = \frac{R_3}{1 + \omega^2 C^2 R_3^2}$$

Equating the reactive components, we have

$$\frac{1}{\omega C_s} = \frac{\omega C R_3^2}{1 + \omega^2 C^2 R_3^2}$$

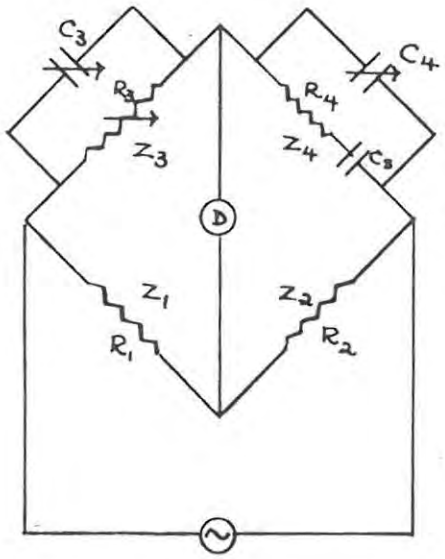

FIG. 3(a) SIMPLIFIED BRIDGE CIRCUIT

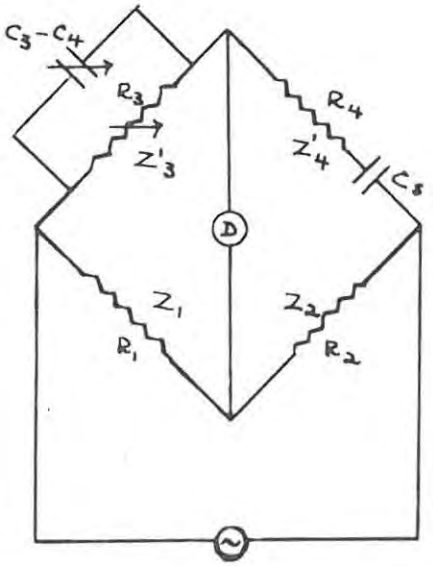

FIG. 3(b) EQUIVALENT CIRCUIT

Using the binomial theorem to clear of fractions and ignoring the higher powers of $\omega^2C^2R_3^2$ in comparison with 1 gives for the final equations of balance

$$R_4 = R_3(1 - \omega^2C^2R_3^2) \quad \ldots\ldots\ldots\ldots(1)$$

and

$$C_s = C(1 - \omega^{-2}C^{-2}R_3^{-2}) \quad \ldots\ldots\ldots\ldots(2)$$

Since ω occurs in both equations, we may conclude that good balance of the bridge depends on the frequency. Although the vacuum-tube oscillator is capable of generating current having an excellent wave-form and good frequency stability, it is difficult to design one which will meet with these requirements over a range of frequencies, such as that in which measurements in the present research were contemplated i.e. over a range of 75 to 100 kc/s.

Now Baker (39), it had been noted, successfully constructed a bridge - based on the double-heterodyne principle - for measuring dielectric constants over a wide range of frequencies. It was suggested to the author, therefore, that this method could equally well be adapted and applied to the construction of a wide-frequency range conductance bridge. The principle, as incorporated in the present bridge assembly, is clearly illustrated in the block diagram shown in Fig. 4.

The beat-frequency oscillator (consisting of a fixed-frequency oscillator, a variable-frequency oscillator, the first mixer and a low-pass filter), together with the

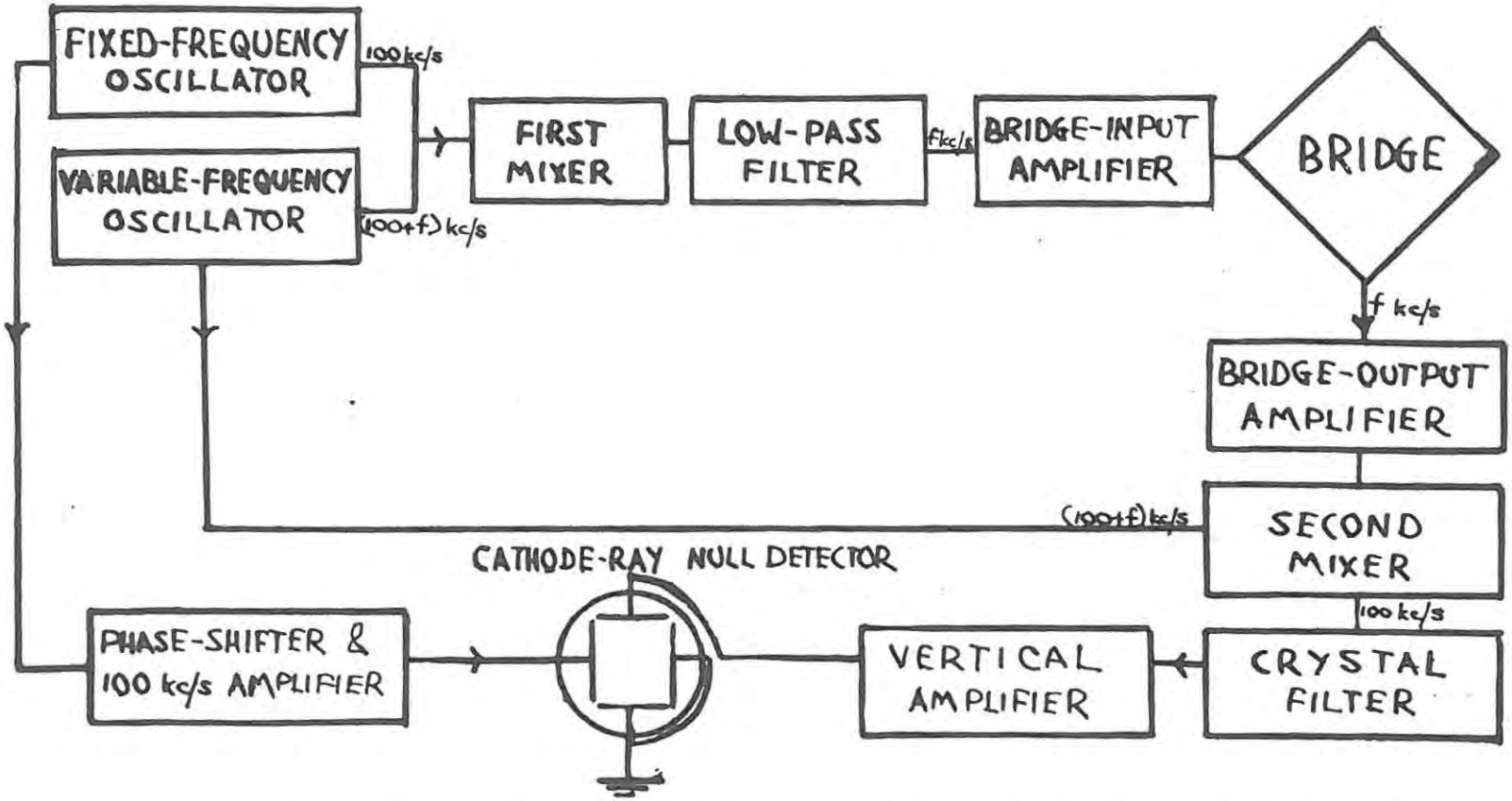

FIG. 4 BLOCK DIAGRAM of DOUBLE HETERODYNE CONDUCTANCE BRIDGE

bridge-input amplifier, constitutes the a.c. generator; while the detector comprises the bridge-output amplifier, the second mixer, the crystal filter with its amplifier and the cathode-ray oscilloscope. Here, the output from the variable-frequency oscillator is heterodyned with the bridge output in the second mixer to produce a constant difference-frequency i.e. 100 kc/s.

The above arrangement offers several advantages:

(a) Although the frequency applied to the bridge can be varied at will, only a constant frequency is detected when balancing the bridge. A highly selective detector tuned to this frequency can, therefore, be designed, and the presence of harmonics in the input to the bridge is thereby nullified. Thus accurate balance is possible at all frequencies - despite the fact that the current applied may not be a pure sine wave throughout the whole frequency range - since the crystal filter, if well designed, will only transmit a pure 100 kc/s signal which is detected.

(b) A wide range of frequencies is obtainable by a simple adjustment of the tuning condenser in the variable-frequency oscillator.

(c) The combination of generator and detector in one apparatus makes for a compact assembly.

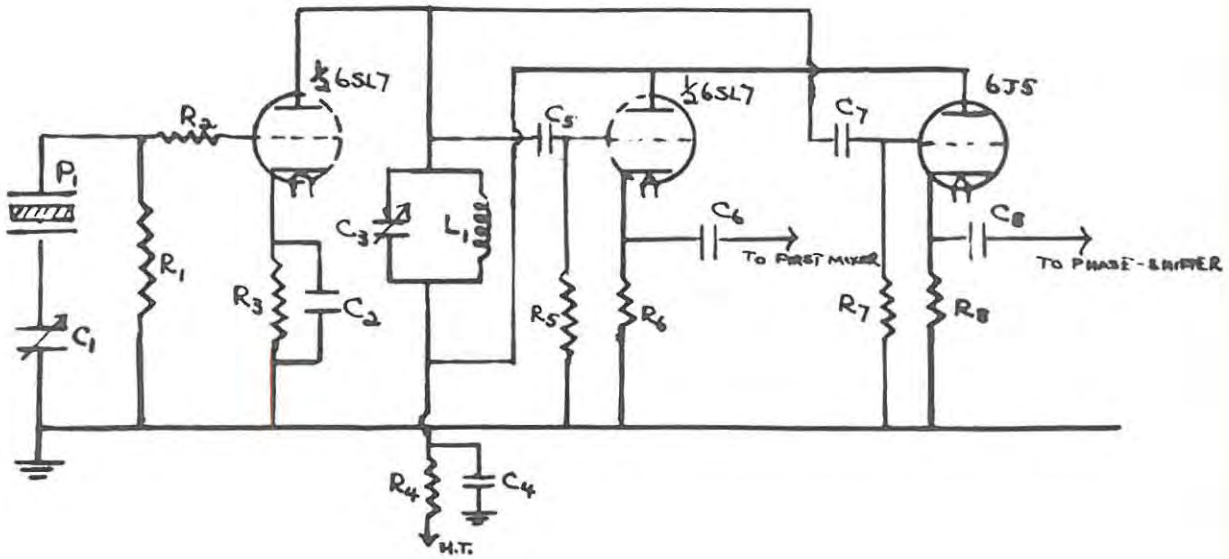

FIG. 5 CIRCUIT of FIXED-FREQUENCY OSCILLATOR

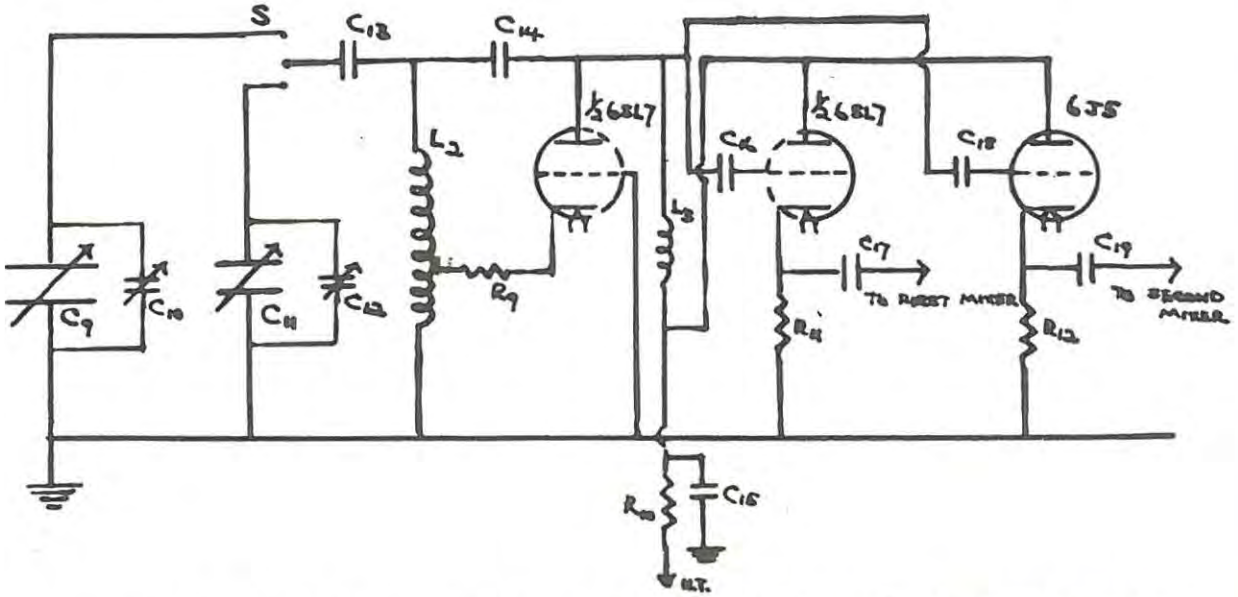

FIG. 6 CIRCUIT of VARIABLE-FREQUENCY OSCILLATOR

FIG. 5 CIRCUIT OF FIXED-FREQUENCY OSCILLATOR

R_1 =	500K ohms	C_1 =	100 pF
R_2 =	47K ohms	C_2 =	0.1 μF
R_3 =	10K ohms	C_3 =	50 pF + padding cap.
R_4 =	10K ohms	C_4 =	0.1 μF
R_5 =	500K ohms	C_5 =	40 pF
R_6 =	20K ohms	C_6 =	500 pF
R_7 =	500K ohms	C_7 =	40 pF
R_8 =	20K ohms	C_8 =	500 pF
P_1 =	100 kc/s Crystal	L_1 =	5 millihenries

FIG. 6 CIRCUIT OF VARIABLE-FREQUENCY OSCILLATOR

R_9 =	160 ohms	C_9 =	1400 pF
R_{10} =	10K ohms	C_{10} =	100 pF
R_{11} =	20K ohms	C_{11} =	100 pF
R_{12} =	20K ohms	C_{12} =	100 pF + padding cap.
		C_{13} =	5000 pF
L_2 =	3.3 millihenries	C_{14} =	1000 pF
L_3 =	R.F. choke	C_{15} =	0.1 μF
		C_{16} =	40 pF
S =	S.P.D.T. switch	C_{17} =	250 pF
		C_{18} =	40 pF
		C_{19} =	250 pF

1.2 DESIGN CHARACTERISTICS AND CIRCUIT DATA

1.21 THE BEAT-FREQUENCY OSCILLATOR

The output from a 100 kc/s crystal-controlled oscillator was heterodyned with that from a variable-frequency oscillator operating from about 100 kc/s to about 200 kc/s. The mixer output was then fed into a low-pass filter, which had been suitably designed to pass a range of frequencies covering the best part of 100 kc/s.

1.211 THE FIXED-FREQUENCY OSCILLATOR (See Fig. 5)

Excellent frequency stability is obtained with a crystal as the frequency-controlling component. Fig. 5 shows a simple tuned-grid tuned-plate circuit with the quartz crystal, P_1, supplying the grid-tuned circuit. The condition for oscillation is obtained when the reactance in the plate circuit is inductive at the crystal resonance i.e. at 100 kc/s. Thus was achieved by tuning the plate resonant circuit - with the aid of the trimmer condenser C_3 - to a frequency slightly higher than 100 kc/s.

The wave-form of the output was, at first, found to be slightly distorted: this was traced to the large amplitude of oscillation driving the grid positive. Insertion of the grid-limiting resistance R_2 remedied this.

The trimmer condensers C_1 and C_3 are located at the front end of the chassis and are easily adjustable with a

screw-driver which can be inserted through small openings in the front panel. Variation of the former condenser serves to bring the frequency into alignment with that of the crystal filter circuit. (See bandwidth measurement: p. 39).

The output was fed to the 1st mixer through a cathode-follower which, as buffer amplifier, isolates the crystal oscillator from the variable-frequency oscillator so that cross-coupling through the mixer is negligible. Since the 6SL7 is a twin-triode valve, half of it was used as the buffer tube. A separate cathode-follower (using a 6J5) has been added to feed the horizontal amplifier (see p. 44).

The oscillator is shielded from external fields by means of a copper box (containing separate compartments for the tube and crystal) which may be seen on the right-hand side of Plate 1.

1.212 THE VARIABLE-FREQUENCY OSCILLATOR (See Fig. 6)

The circuit is of the well-known Hartley type wherein enough positive feed-back to sustain oscillations is obtained by tapping a coil, which forms part of the grid tank-circuit. It was essential to ground the rotor plates of the tuning condensers (C_9 and C_{11}) to prevent the effect of hand-capacity on the frequency.

The resonant circuit was designed as follows:

(i) The Coil: L_2

The former, on which the coil was wound, was taken from

an old radio-frequency choke, is 2" long and has a core diameter of $\frac{1}{2}$". To reduce self-capacitance, 660 turns of of No. 32 D.S.C. copper wire were wound onto six pie-sections, each section consisting of 110 turns. The number of turns and the tapping point were determined by experiment to give the desired range of frequencies, with a reasonably pure wave-form throughout. After impregnating with wax, the coil was firmly bolted to the chassis and shielded with an aluminium can. The can may be seen on the left-hand side of Plate 1.

(ii) The Tuning Condensers

A range of frequencies from about 95 kc/s to about 205 kc/s is generated by varying C_9, which is an ordinary radio condenser. It was desired to take readings more closely spaced at the low frequencies - consequently, C_{11} was included to enable precise settings of difference-frequencies up to about 3.5 kc/s. Each condenser can be switched into the resonant circuit as required (by means of S), and is fitted with a slow-motion drive to facilitate accurate settings.

In addition to the padding capacitances, there are two trimmer condensers C_{10} and C_{12} by means of which the frequency calibration may be standardised on the high- and low-frequency ranges respectively by setting to zero beat; the trimmers may be adjusted through openings in the front

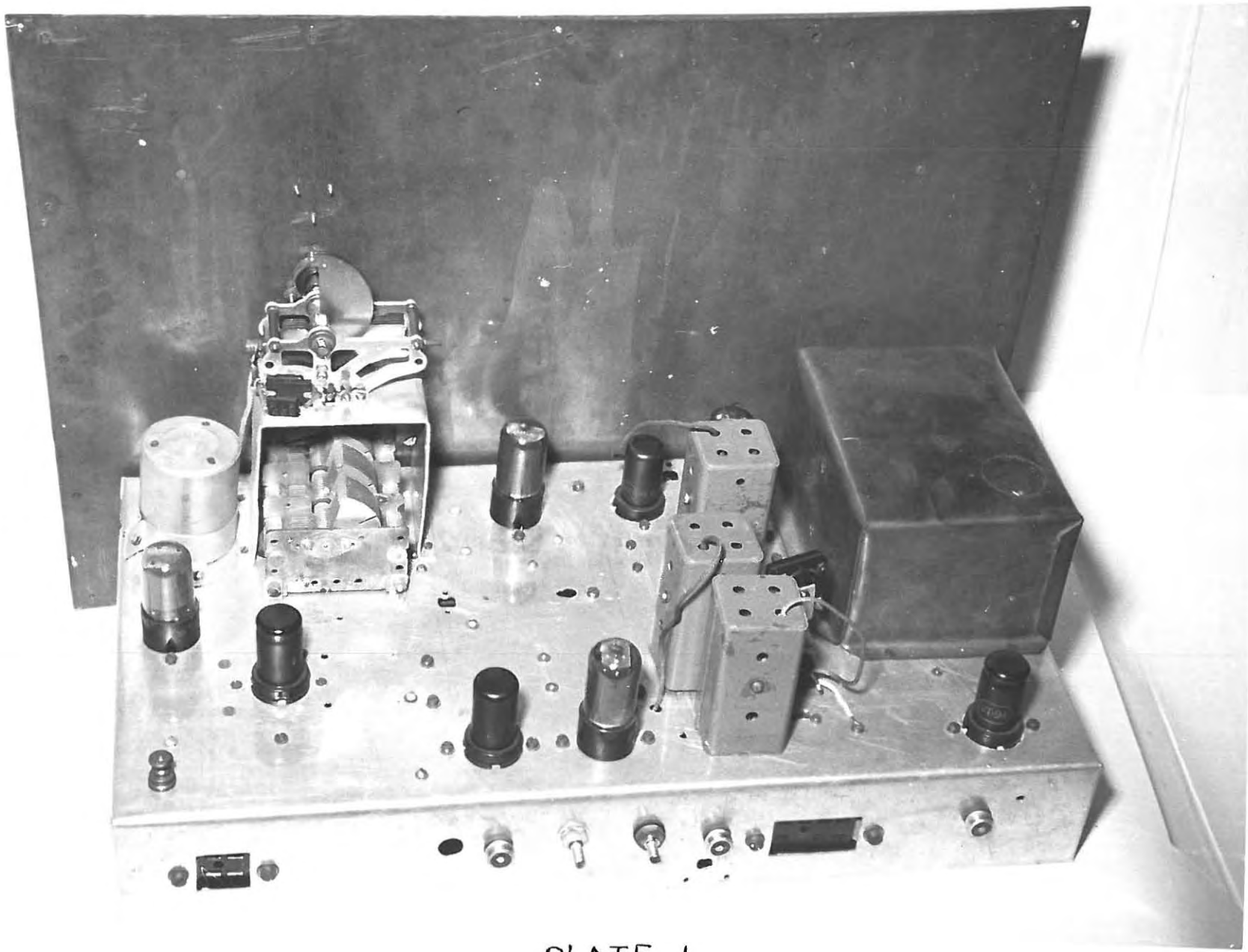

PLATE 1

panel.

The oscillator gives an output with a reasonably constant amplitude from about 2 kc/s to about 70 kc/s. Here again, the output is applied to the 1st mixer through a cathode follower. A separate cathode-follower, including a 6J5 tube, was added in order to feed the 2nd mixer (see p. 37).

1.213 THE FIRST MIXER (See Fig. 7)

The operation of frequency converter and mixers for super-heterodyne reception has been thoroughly investigated by Herold (40). The design considerations can be applied to low-frequency conversion as well, and optimum performance of the mixer constructed was, therefore, obtained by experimentation along the lines suggested.

The pentagrid converter tube 6SA7 was selected because of its special structural arrangement which permits of a comparatively high conversion transconductance, and considerably reduces coupling between the circuits supplying the signal voltages.

The plate and screen are operated at voltages prescribed for the tube (41), while the bias voltages on the grids were adjusted until maximum stability and good wave-form of the output frequencies were achieved. The 100 kc/s signal was injected on grid No. 3 while the variable-frequency oscillator output was impressed on grid No. 1.

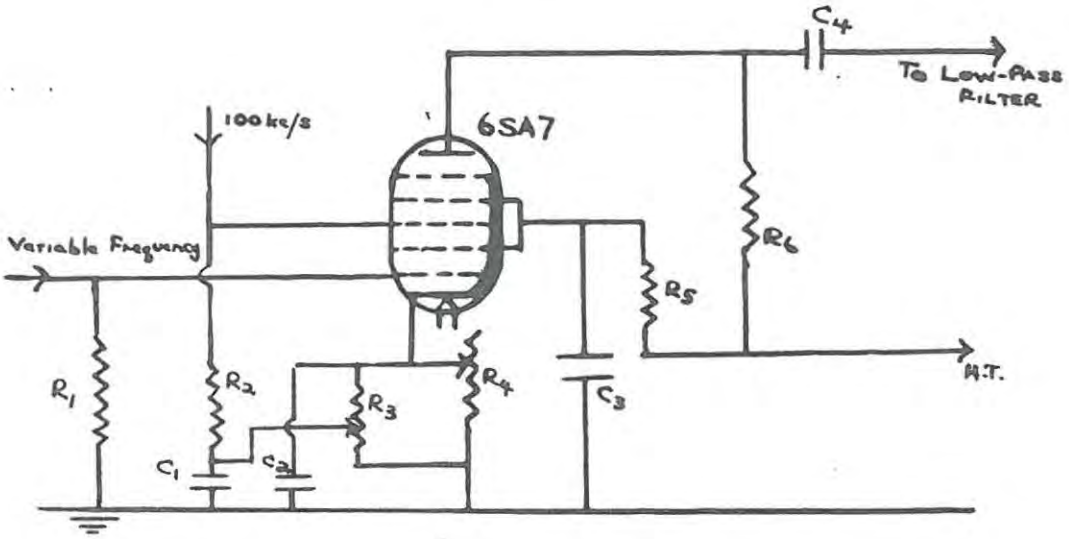

FIG. 7 CIRCUIT of FIRST MIXER

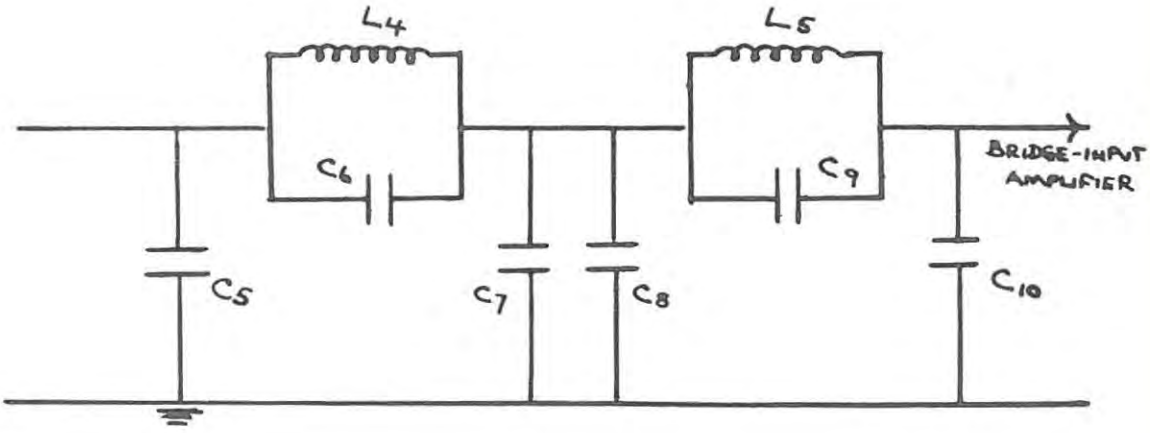

FIG. 8 CIRCUIT of LOW-PASS FILTER

FIG. 7 CIRCUIT OF FIRST MIXER

R_1 = 20K ohms
R_2 = 100K ohms
R_3 = 10K ohms
R_4 = 750 ohms
R_5 = 10K ohms
R_6 = 50K ohms

C_1 = 0.1μF
C_2 = 50μF
C_3 = 0.1μF
C_4 = 0.5μF

FIG. 8 CIRCUIT OF LOW-PASS FILTER

L_4 = 70 millihenries
L_5 = 110 millihenries

C_5 = 20 pF
C_6 = 30 pF
C_7 = 20 pF
C_8 = 20 pF
C_9 = 20 pF
C_{10} = 120 pF

An interesting feature of the circuit is the unusual biasing arrangement (42), which proved helpful in keeping the distortion of the mixer output down to a minimum. Although both grids are biased through a common cathode resistor R_4 - which is a rheostat - the bias voltage on grid No. 3 can be set at an independent value by means of potentiometer R_3 connected across R_4. The shafts of both components (R_3 and R_4) were brought out through the front panel to enable the bias voltages to be adjusted when necessary.

Note: The 100 kc/s input is about 1 volt r.m.s. as compared with the variable-frequency oscillator input which measures 5.5 volts r.m.s. These voltages were found to be optimum values for low distortion of the mixer output.

1.214 THE LOW-PASS FILTER (See Fig. 8)

The main considerations in designing such a filter were that it should:

(i) pass difference-frequencies covering the best part of 100 kc/s

(ii) offer high discrimination against frequencies in the range 100 kc/s to 300 kc/s.

It was necessary that the latter requirement be satisfied in order to block the sum-frequencies and reduce possible leakages from the oscillators to a minimum.

A filter of the constant-k type was initially constructed but an examination of its transmission characteristic revealed that the attenuation did not increase rapidly enough beyond the cut-off frequency which was set, tentatively, at 90 kc/s. Consequently, the circuit diagram in Fig. 8 was worked out according to Zobel's theory of wave filters (43). The filter is composed of two shunt-derived sections and proportioned to operate with a load resistance of 50,000 ohms. To ensure that the attenuation rose rapidly beyond the cut-off frequency, and that high attenuation was maintained for the unwanted frequencies, the values of m for the two sections were fixed at 0.4 and 0.7 respectively.

Langford-Smith (44) states that '' it is generally desirable for good attenuation characteristics, that the ratio of the cut-off frequency to the frequency of peak attenuation in a low-pass filter, should be as low as possible and not greater than 0.8''. On applying the suggestion, it was found that this lowered the cut-off frequency considerably, as can be seen from the transmission characteristic (Fig. 9). Nevertheless, the output - after amplification - is sufficient to enable measurements to be carried out at frequencies up to 75 kc/s.

It is usual to terminate filter networks at either end with suitably designed half-sections in order to provide constant image impedance characteristics in the pass band. Omission of these half-sections (to simplify construction

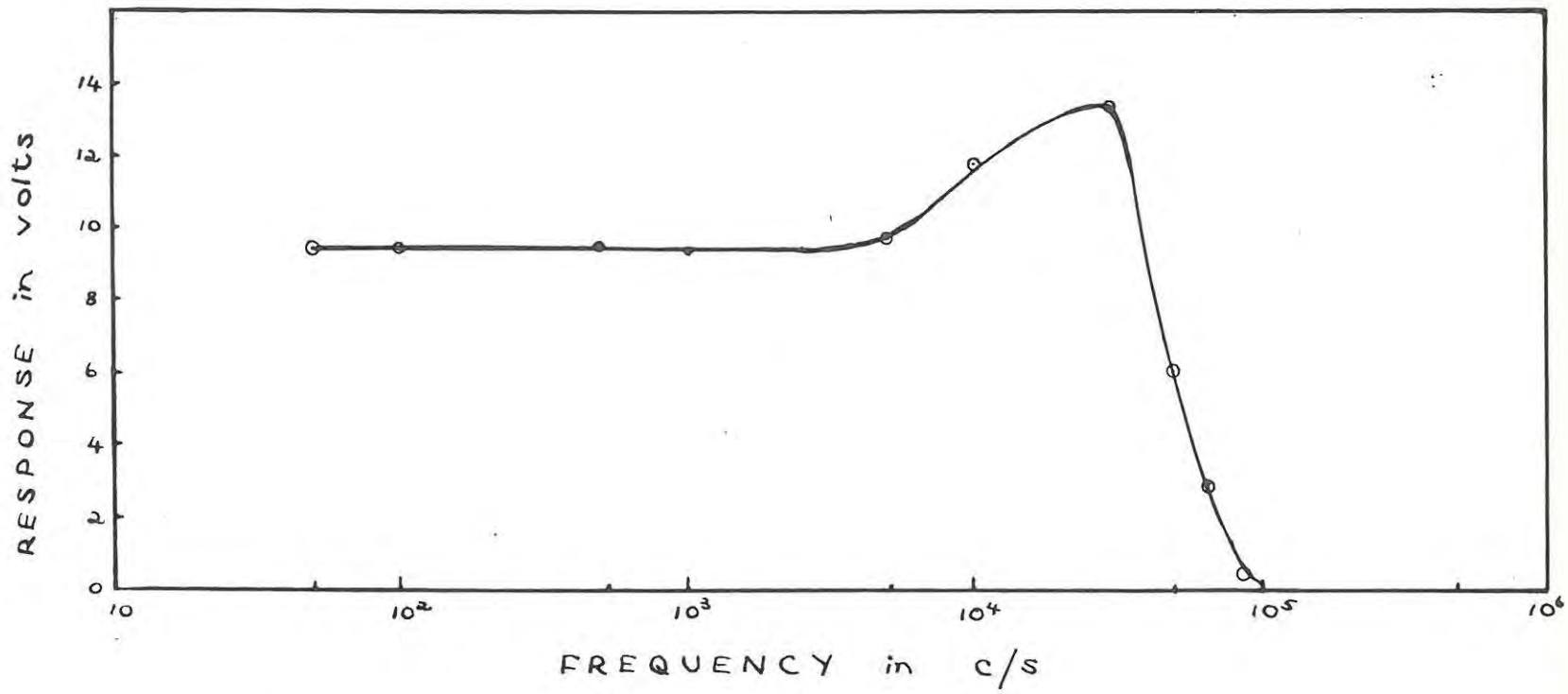

FIG. 9 TRANSMISSION CHARACTERISTIC of LOW-PASS FILTER

of the filter), did not, however, affect its performance significantly.

The coils, L_4 and L_5, were wound onto the former of an old intermediate-frequency transformer with No. 41 S.W.G enamelled wire, impregnated with wax and screened from each other with a strip of aluminium to prevent undesirable coupling. The whole filter was then enclosed in a steel box and suitably mounted on the underside of the chassis.

1.22 MECHANICAL CONSTRUCTION OF THE BEAT-FREQUENCY OSCILLATOR

The following are considerations, as to maximum stability of operation and minimum distortion of the output, which were borne in mind during the process of designing and constructing the beat-frequency oscillator:

1.221 CIRCUIT LAYOUT AND MECHANICAL STABILITY OF COMPONENTS

(a) The oscillators were constructed on opposite ends of the chassis to reduce coupling and ''pulling'' at the low-difference frequencies.

(b) Undesirable heating of the oscillators was avoided by placing the power supplies in a separate compartment. The minor heat sources in the oscillators themselves (i.e. tubes) were either screened or placed as far as possible away from the frequency-determining elements i.e. crystals, coils and tuning condensers.

(c) The frequency drift, due to the internal effects of the tubes heating up, was minimised by the use of steatite bases.

(d) The circuit wiring - especially of resonant circuits - was restricted to short, thick leads.

(e) All coils were impregnated with wax to offset the effects of changes in humidity.

(f) Good mica capacitors were used throughout.

1.222 SHIELDING

(a) The circuits of each stage on the underside of the chassis were screened from one another by transverse strips of aluminium.

(b) Coils in the resonant and filter circuits were enclosed in shielding cans.

(c) All interstage connections were made with coaxial cable. Leads from one chassis to another were taken through coaxial (microphone) connectors.

Note: All the compartments in the framework housing the complete double-heterodyne unit (see p. 47 and Plate 2) were lined with sheet copper and properly earthed to ensure electrostatic shielding from one another and from stray external fields.

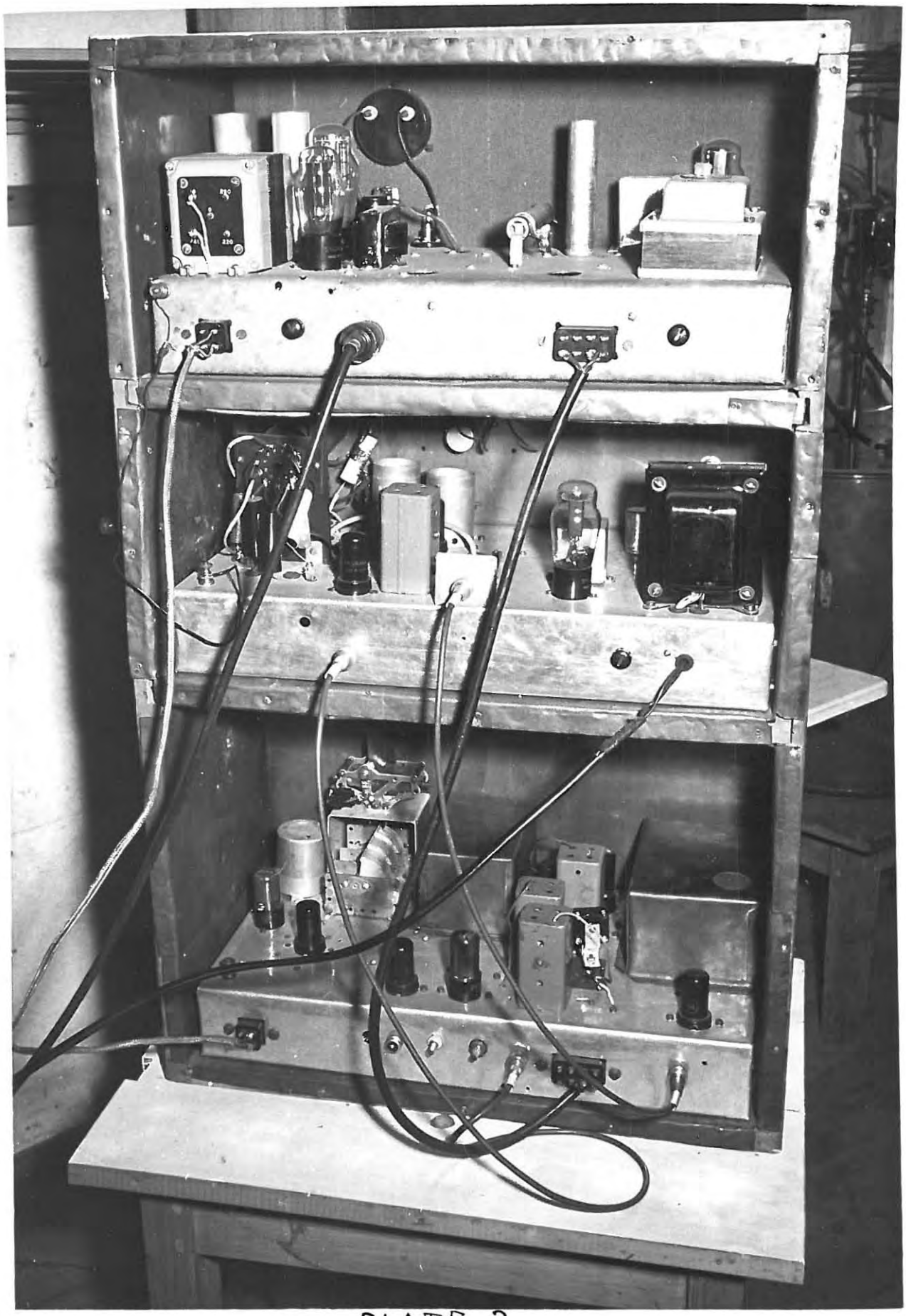

PLATE 2

1.23 THE BRIDGE-INPUT AMPLIFIER (See Fig. 10)

The theory and design of wide-band amplifiers have been worked out by Wheeler, Everest and others (45, 46). By the addition of a network of resistive and reactive elements to the ordinary resistance-coupled audio-amplifier, the characteristics at the low and high frequencies can be considerably improved, and constant amplification is obtained over a wide range of frequencies.

Accordingly, an attempt was made to construct an amplifier with circuit proportions for a two-terminal network suggested by Terman (47). However, the frequency-response curve for this amplifier proved to be unsatisfactory since the fall-off in amplification was too gradual to give negligible output at a frequency of 100 kc/s. No doubt, the introduction of a four-terminal network would have given a sharper cut-off, but such networks are difficult to adjust and require more care in construction.

Since the low-pass filter already constructed was shown to have the desired frequency response, it occurred to the author that a similar filter could be conveniently inserted in the plate circuit of the amplifier, in place of the two-terminal network. The amplifier was, therefore, rebuilt on the lines just mentioned, and the frequency-response determined over the range 50 c/s to 200 kc/s. This is shown in Fig. 11. The fall-off is seen to occur at about 30 kc/s, but the output at about 75 kc/s is still large enough to permit measure-

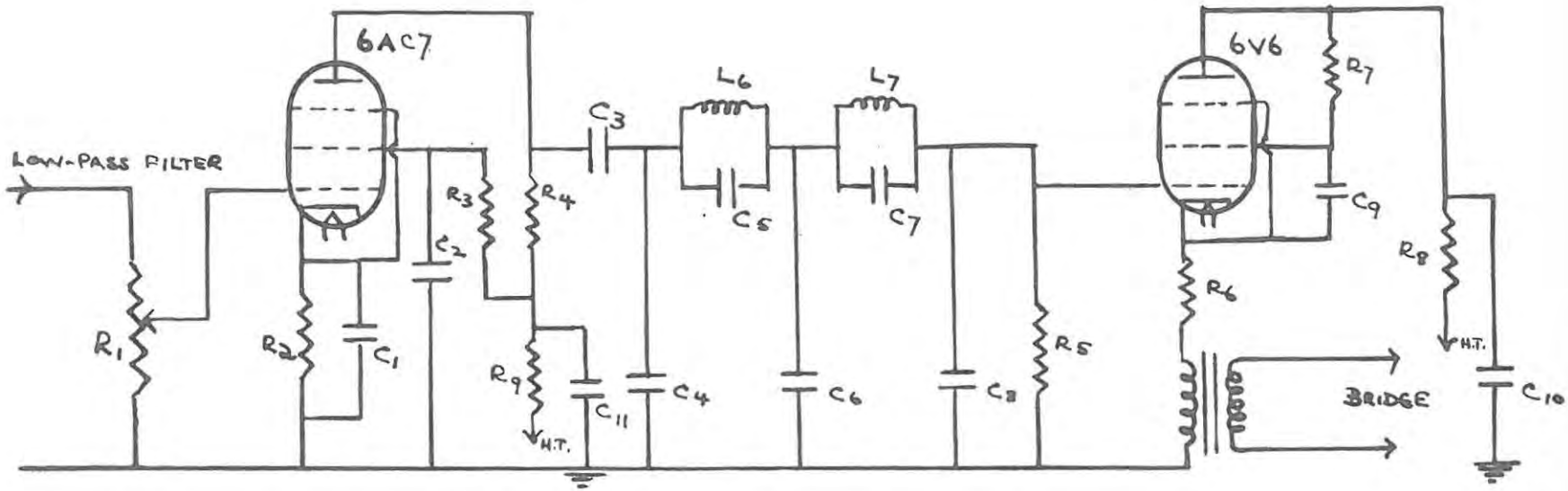

FIG. 10 CIRCUIT of BRIDGE-INPUT AMPLIFIER

FIG. 10 CIRCUIT OF BRIDGE-INPUT AMPLIFIER

R_1	= 50K ohms	C_1	= 50 μF
R_2	= 1K ohms	C_2	= 0.1 μF
R_3	= 220K ohms	C_3	= 0.25 μF
R_4	= 50K ohms	C_4	= 20 pF
R_5	= 50K ohms	C_5	= 30 pF
R_6	= 15K ohms	C_6	= 20 pF
R_7	= 220K ohms	C_7	= 20 pF
R_8	= 3K ohms	C_8	= 120 pF
R_9	= 2K ohms	C_9	= 8 μF
L_6	= 70 millihenries	C_{10}	= 8 μF
L_7	= 110 millihenries	C_{11}	= 8 μF

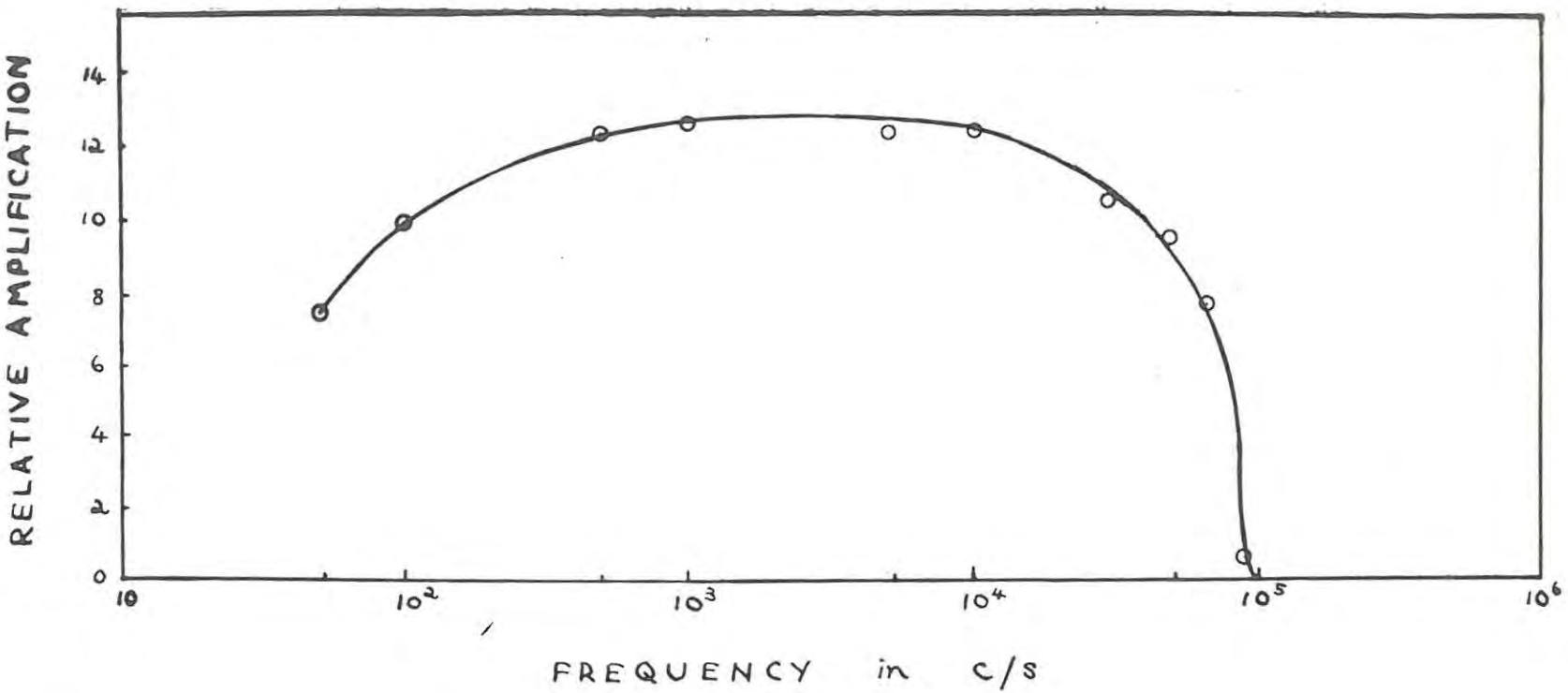

FIG. 11 FREQUENCY-RESPONSE of BRIDGE-INPUT AMPLIFIER

ments with the bridge.

The output is applied to the bridge via the 6V6 which has been connected as cathode-follower to prevent changes in loading from affecting the frequency and stability of the oscillators.

R_1 is a wire-wound potentiometer, governing the input to the amplifier. Variation of it serves to regulate the output of the beat-frequency oscillator. The maximum undistorted output was found to be 15 volts r.m.s. - measured at the cathode of the buffer tube (6V6).

To isolate the bridge from changes of electrostatic potential in the external circuit, the a.c. is supplied via two bridge-coupling transformers:

(i) G.R. Type 578-B: Frequency Range: 20 c/s to 5 kc/s.
(ii) G.R. Type 578-C: Frequency Range: 2 kc/s to 500 kc/s.

The transformers were connected in series with the cathode resistor R_6 - the coaxial cable being taken through a microphone connector situated on the front panel. (See Plate 5). A multiple switch located immediately below the wooden flap attached to the Wheatstone Bridge section, connects the bridge across either of the transformers. {Distortion of the waveform results if the cathode resistor is shunted by the transformer through a capacitance - an effect also observed by Goddard and A. Faure (24, 25) }.

1.24 THE DETECTOR

1.241 THE BRIDGE-OUTPUT AMPLIFIER (See Fig. 12)

As it is convenient that this amplifier should have the same characteristics as the bridge-input amplifier, the circuit diagram is the same as that for the first stage of the latter.

The amplifier was constructed towards the rear end of the chassis on which the beat-frequency oscillator had been built. R_1 is a wire-wound potentiometer which regulates the input from the bridge. (See p. 46, under description of Wheatstone Bridge Network). Connection is made through a coaxial connector which can be seen on the extreme left of chassis shown in Plate 1.

1.242 THE SECOND MIXER (See Fig. 13)

It has already been mentioned that the express function of the second mixer is to produce a constant difference-frequency by heterodyning the bridge-output with that from the variable-frequency oscillator.

In order to isolate the circuit from that of the first mixer, the input from the variable-frequency oscillator was taken from a separate cathode-follower using a 6J5 as the buffer tube - see Fig. 6 - and injected on grid No. 3. The bridge output was applied to grid No. 1.

It must be noted that the coupling transformer, in the plate circuit, constitutes the first stage of the crystal

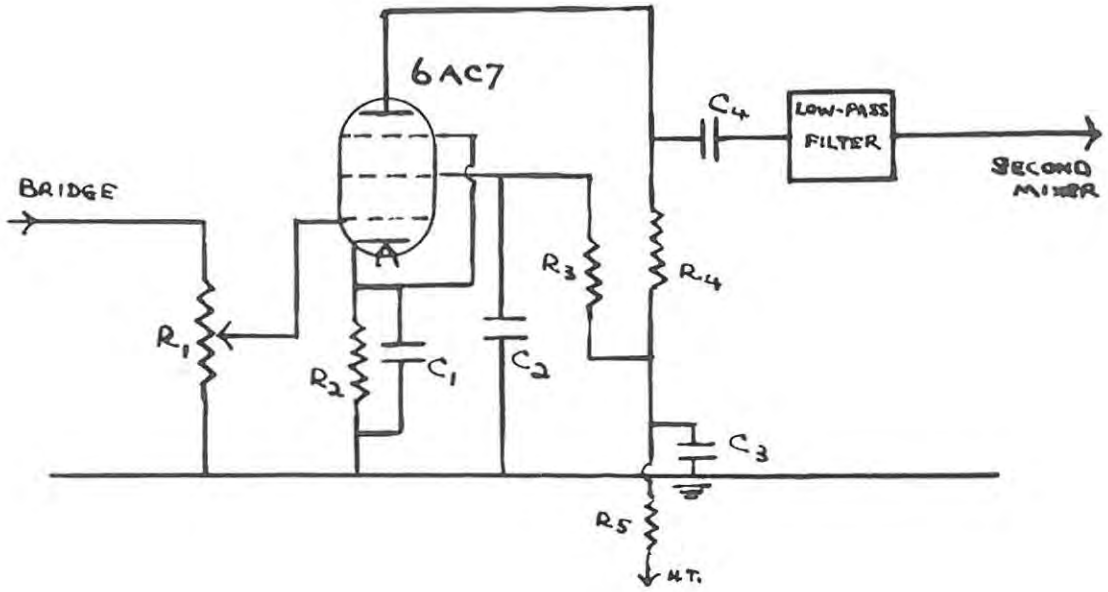

FIG. 12 CIRCUIT of BRIDGE-OUTPUT AMPLIFIER

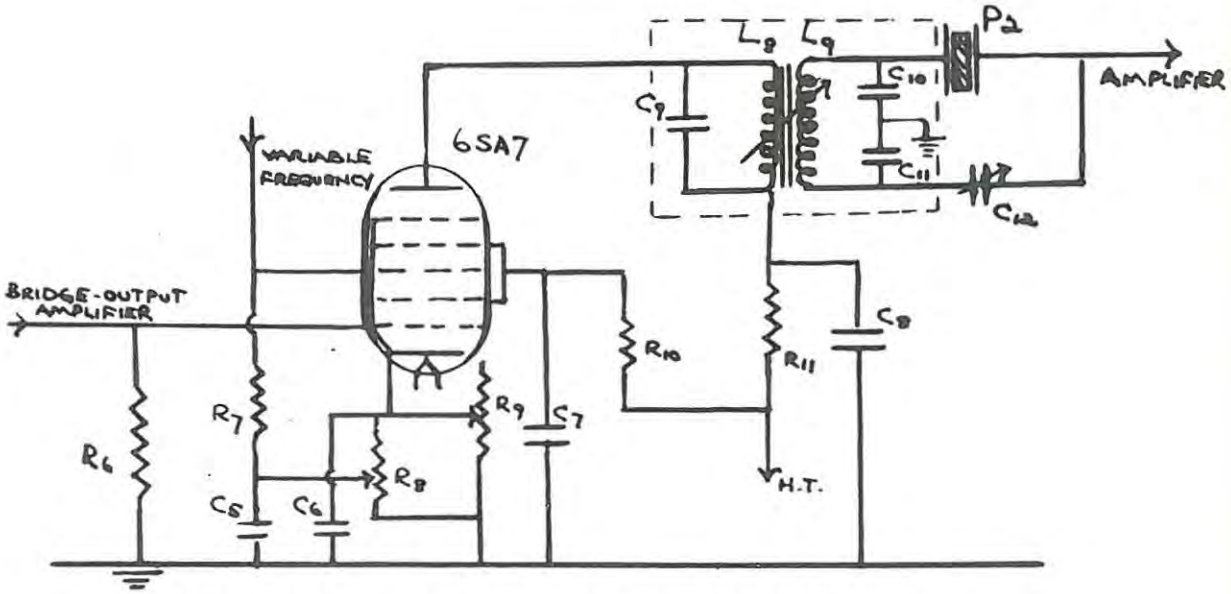

FIG. 13 CIRCUIT of SECOND MIXER and 1ST STAGE of CRYSTAL FILTER

FIG. 12 CIRCUIT OF BRIDGE-OUTPUT AMPLIFIER

R_1 = 50K ohms
R_2 = 1K ohms
R_3 = 220K ohms
R_4 = 50K ohms
R_5 = 2K ohms

C_1 = 50 μF
C_2 = 0.1 μF
C_3 = 8 μF
C_4 = 0.25 μF

FIG. 13 CIRCUIT OF SECOND MIXER and 1st STAGE OF CRYSTAL FILTER

R_6 = 50K ohms
R_7 = 100K ohms
R_8 = 10K ohms
R_9 = 5K ohms
R_{10} = 10K ohms
R_{11} = 10K ohms
P_2 = 100 kc/s Crystal
L_8 = 10 millihenries
L_9 = 10 millihenries

C_5 = 0.1 μF
C_6 = 50 μF
C_7 = 0.1 μF
C_8 = 16 μF
C_9 = 250 pF
C_{10} = 500 pF
C_{11} = 500 pF
C_{12} = 20 pF

filter. R_8 and R_9, the grid-biasing resistors, were brought out through the rear end of the chassis as can be seen in Plate 1, to facilitate adjustments as required.

1.243 THE CRYSTAL FILTER (See Fig. 13 and Fig. 14)

It will be appreciated that the double-heterodyne principle can be successfully applied only if the crystal filter is designed to serve as a highly selective detector i.e. it should have a very narrow bandwidth at the frequency to be transmitted - in this case 100 kc/s.

To this end, considerable time was spent in examining circuits and constructing filters which would give the desired transmission characteristics. The analysis of crystal filter networks by Stanesby and Mason (48, 49) takes into account the values for the equivalent electrical constants of a crystal but, unfortunately, these were not known for the crystals available. A further search of the literature (50) revealed that selective fixed amplifiers, used in wave analysers, incorporate filters having a bandwidth of only four cycles! The circuit diagram, shown in Fig. 14 (and part of Fig. 13), is derived therefrom, and was the filter finally constructed.

There are two stages of filtering - each being succeeded by a stage of amplification. The output is fed directly to the vertical plates of the cathode-ray oscilloscope. The amplifier and the second stage of the filter were constructed on the chassis housing the cathode-ray null detector. The

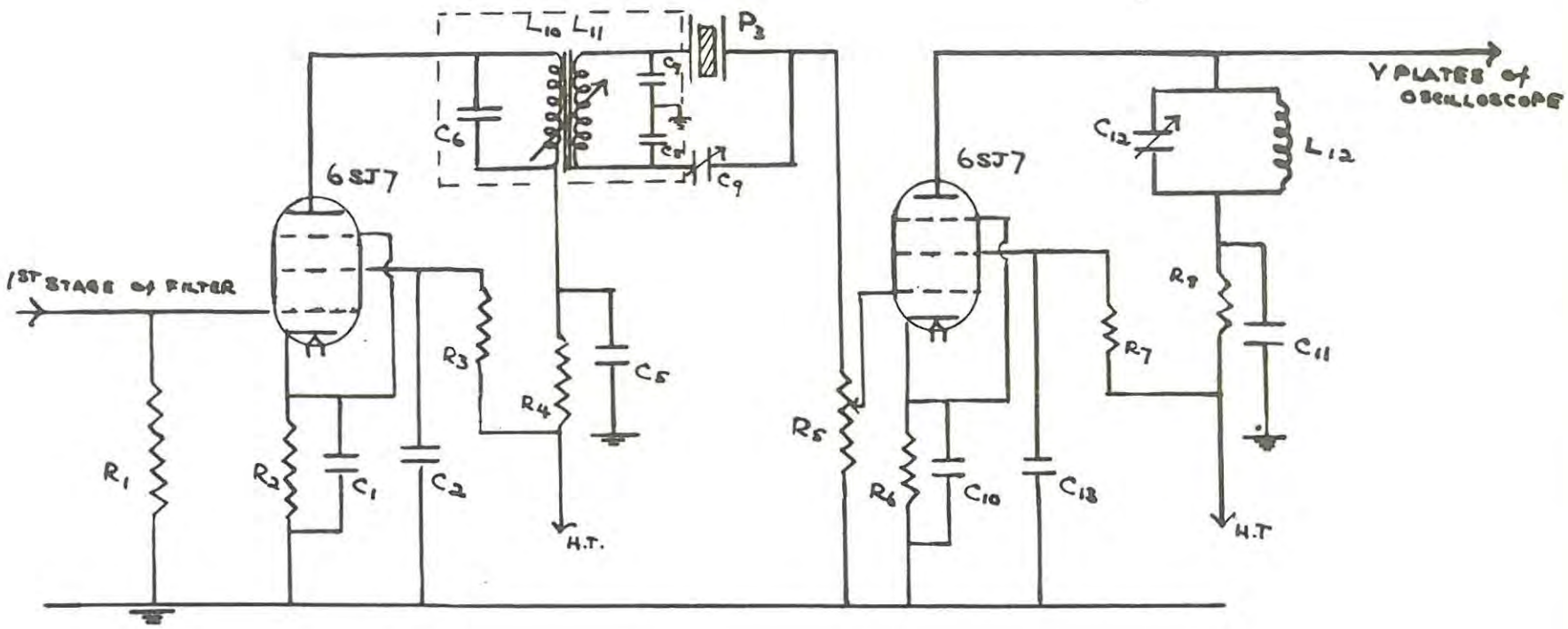

FIG. 14 CIRCUIT of 2ND STAGE of CRYSTAL FILTER and AMPLIFIER

FIG. 14 CIRCUIT OF 2nd STAGE OF CRYSTAL FILTER and AMPLIFIER

R_1 =	1 Megohm	C_1 =	0.05 μF
R_2 =	560 ohms	C_2 =	0.1 μF
R_3 =	100K ohms	C_5 =	0.1 μF
R_4 =	10K ohms	C_6 =	250 pF
R_5 =	2 Megohms	C_7 =	500 pF
R_6 =	600 ohms	C_8 =	500 pF
R_7 =	100K ohms	C_9 =	20 pF
R_8 =	10K ohms	C_{10} =	0.02 μF
L_{10} =	10 millihenries	C_{11} =	0.1 μF
L_{11} =	10 millihenries	C_{12} =	500 pF
L_{12} =	9 millihenries	P_3 =	100 kc/s Crystal

coaxial connector which is shown situated second from the right in Plate 1, serves to link the first stage of the filter with the amplifier.

Old slug-tuned intermediate-frequency transformers were stripped off their coils and capacitors, and used as a basis for wiring the coupling transformers (shown in between dotted lines in the circuit diagram). The coils were wound with No. 41 S.W.G. enamelled wire to the required values of inductance, and the capacitors soldered into position. Each transformer was then enclosed in a metal can and accurately tuned to 100 kc/s by adjusting the position of the movable slug. The tuned circuit - $L_{12}C_{12}$ - in the final stage of the amplifier consists of a radio-frequency choke and a compression trimmer which was used for tuning the circuit to 100 kc/s.

The coupling transformers can be clearly seen towards the rear end of the chassis shown in Plates 1 and 4.

MEASUREMENT OF THE BANDWIDTH

At zero beat-frequency, the variable-frequency oscillator is tuned to 100 kc/s. If the tuning condenser is moved slightly about the position of zero beat, i.e. a few cycles off 100 kc/s, the response of the filter can be detected on a vacuum-tube voltmeter (since the variable-frequency oscillator output is applied to the filter through the second mixer). The deviation from 100 kc/s (up to 50 c/s on either side of

100 kc/s) can be accurately measured by means of Lissajous figures, if the beat-frequency is applied to the Y-plates of a cathode-ray oscilloscope, while a 50 c/s signal (mains supply) is applied to the X-plates.

Hence the following method was devised to assess the performance of the filter:

(a) The apparatus is disconnected from the bridge, the variable-frequency oscillator is disconnected from the second mixer by pulling the 6J5, and the filter output is applied to a vacuum-tube voltmeter.

(b) Alignment of the filter is now effected as follows:
With both crystals (P_2 and P_3) in the filter short-circuited, the 100 kc/s output (taken from the crystal oscillator, preferably through a potentiometer to vary the amplitude of the signal as required) is linked to the grid of the the second 6SJ7 in the second stage of the amplifier, and the tuned circuit ($L_{12}C_{12}$) peaked for maximum response. Next, the output is connected to the grid of the first 6SJ7 in the second stage of the amplifier, and the coupling transformer ($L_{10}C_6$-$L_{11}C_7C_8$) carefully tuned for maximum response. The same process is applied to the coupling transformer (L_8C_9-$L_9C_{10}C_{11}$) in the plate circuit of the second mixer. The crystals are then switched in, and the crystal oscillator frequency varied a few cycles back and forth with the aid of the trimmer C_1 in Fig. 5, until a sharp rise in the output of the filter is indicated.

Lastly, the neutralising trimmers C_{12} in Fig. 13 and C_9 in Fig.14 are adjusted for peak response. The tuned circuits should then be re-tested for alignment. (The necessary re-adjustments should be small if the initial alignments have been properly effected).

(c) The 100 kc/s input is now removed, and the 6J5 replaced.

(d) By means of Lissajous figures (with the beat-frequency and a 50 c/s signal applied to the Y- and X- plates of the cathode-ray oscilloscope), the tuning condenser is set to zero-beat position - adjustment of the trimmers C_{10} and C_{12} in Fig. 6 may also be necessary - and the response in volts read on the meter. The tuning condenser is then carefully adjusted to give beat-frequencies up to 50 c/s on either side of 100 kc/s and the response in volts checked at each setting of the frequency.

(e) Thus, from the response curve so obtained, the bandwidth may be determined at the half-power points, i.e 0.7 of the peak voltage recorded.

By following the procedure outlined, it was possible to adjust the filter to give a bandwidth of 8 cycles. However, since this was associated with an undesirably large decrease in amplification, the bandwidth was finally increased to about 20 c/s. The transmission characteristic of the filter is depicted in Fig. 15. It will observed that the curve is

unsymmetrical about the resonant frequency i.e. 100 kc/s: this was due to a slight maladjustment of the neutralising trimmers.

1.25 THE POWER SUPPLIES

Two power packs were constructed on one chassis as follows:

1.251 THE REGULATED POWER SUPPLY (See Fig. 16)

This is used to supply a steady plate voltage to the oscillators. The circuit makes use of a resistorless neon tube as stabiliser, and is conventional. Regulation was found to be within 1% for a variation of ± 25% in the input voltage.

Since the fixed-frequency oscillator is crystal-controlled, the supply was restricted to 200 volts by adjusting R_5. A voltmeter was wired into the circuit to enable checking of the voltage when the unit is switched on.

1.252 THE UNREGULATED POWER SUPPLY (See Fig. 17)

This supplies plate voltage to the first and second mixers, and the bridge-input and bridge-output amplifiers. Heater voltage for all the tubes on the chassis, housing the beat-frequency oscillator, was tapped from the heavy-duty transformer T_3. The circuit is a typical one for full-wave rectification. R_7 is a high-wattage rheostat used for adjusting the output voltage as required.

Note: The power switches S_1 and S_2, the pilot lights, the

FIG. 16 CIRCUIT OF REGULATED POWER SUPPLY

R_1	=	250K ohms	C_1	=	16 μF
R_2	=	500K ohms	C_2	=	16 μF
R_3	=	2.5K ohms	C_3	=	1 μF
R_4	=	10K ohms	C_4	=	1 μF
R_5	=	10K ohms	L_1	=	20 henries
R_6	=	10K ohms	T_1	=	2.5v transformer
S_1	=	mains switch	T_2	=	mains transformer
N	=	resistorless neon tube			

FIG. 17 CIRCUIT OF UNREGULATED POWER SUPPLY

R_7	=	10K ohms (100 watt)	L_2	=	20 henries
S_2	=	mains switch	C_5	=	16 μF
T_3	=	heavy duty mains transformer	C_6	=	16 μF

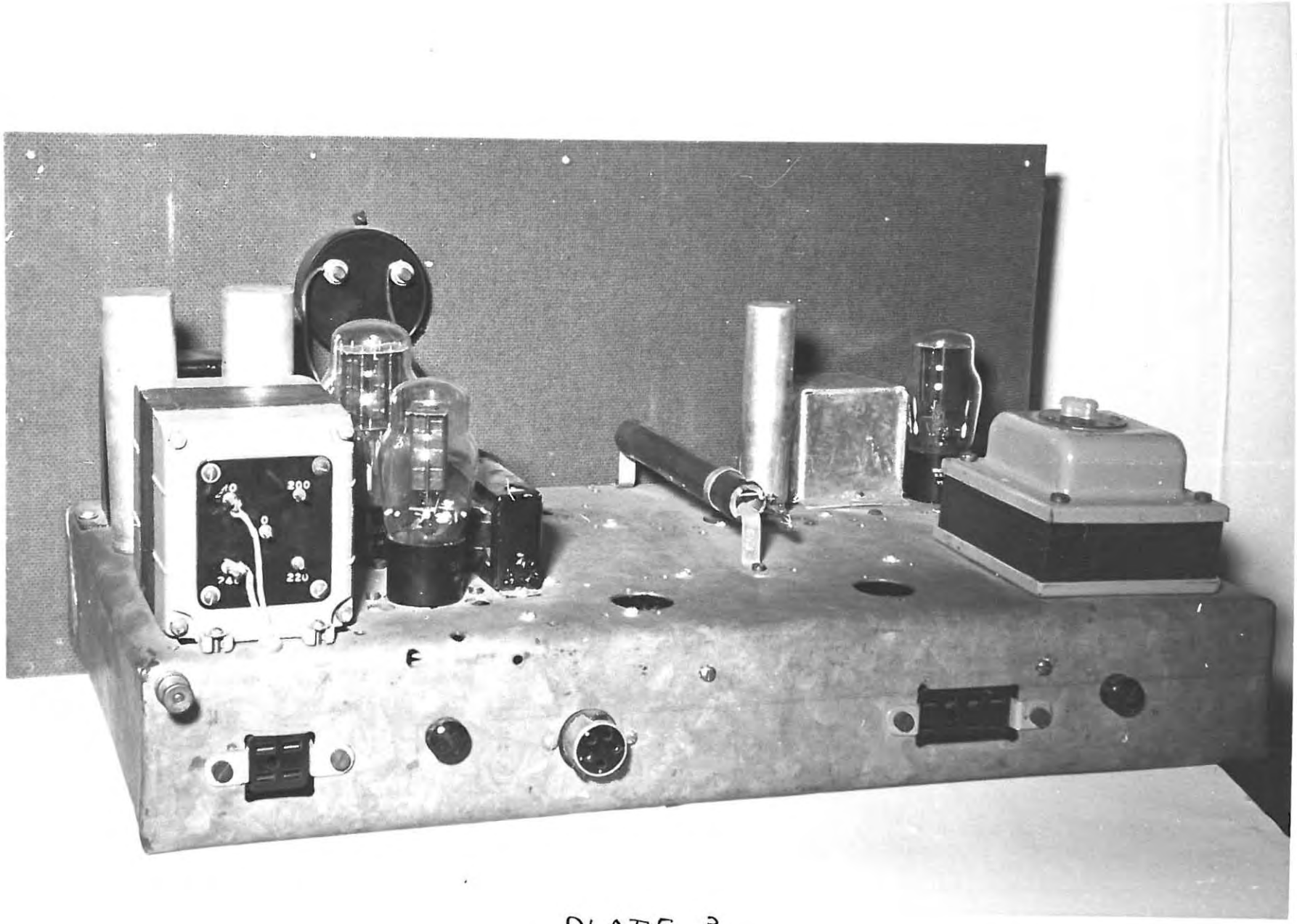

PLATE 3

rheostat R_5 and the voltmeter have been brought out to the front panel, while the fuses were fitted into screw-type holders which were bolted to the rear end of the chassis.

Plate 3 gives a rear view of the power packs.

1.26 THE CATHODE-RAY NULL DETECTOR

1.261 THE OSCILLOSCOPE (See Fig. 18)

The Du Mont oscilloscope in the Goddard-Faure bridge is used simply as a null-point detector, but it is much more elaborate than necessary. Furthermore, it has proved to be a troublesome heat source. It had, therefore, been suggested that a small oscilloscope (of simple design) be constructed, which would dissipate the minimum amount of heat.

The circuit is seen to be a straightforward one, and the absence of an internal time-base has much simplified the construction. Four control potentiometers for adjusting the focus (R_8) and intensity (R_{10}), and for centering the beam horizontally (R_1) and vertically (R_2), are mounted - on the front panel - in pairs on each side of the face of the cathode-ray tube. The blocking capacitors C_7 and C_8 isolate the vertical and horizontal inputs from the deflection plates, and are rated to stand 1000 volts.

A rear view of the oscilloscope can be seen in Plate 4 The cathode-ray tube was placed as far from the power transformer as possible, and shielded with a mu-metal screen to reduce the effects of the magnetic field on the electron beam.

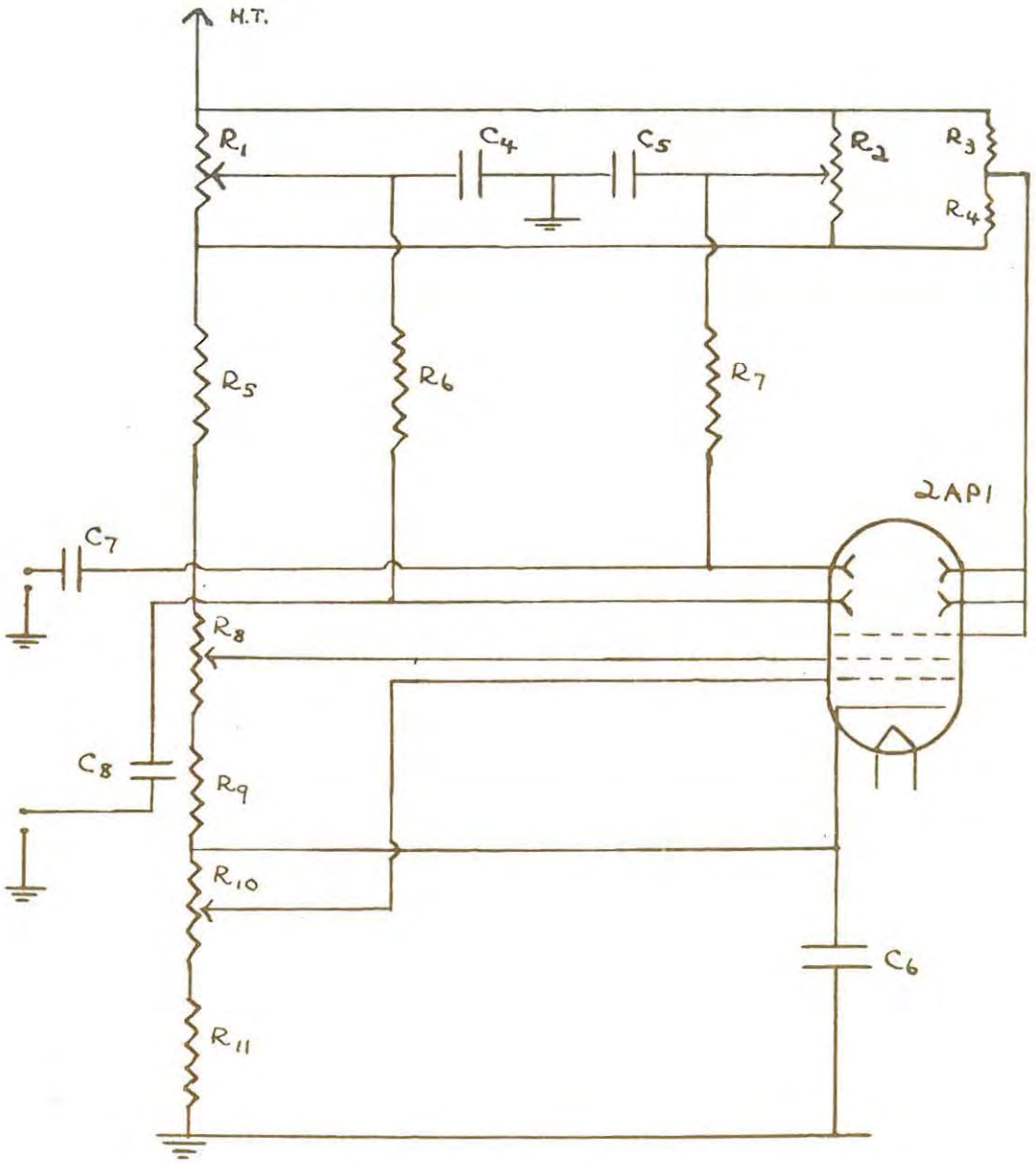

FIG. 18 CIRCUIT of CATHODE-RAY OSCILLOSCOPE

FIG. 18 CIRCUIT OF CATHODE-RAY OSCILLOSCOPE

R_1 = .2 Megohms
R_2 = 2 Megohms
R_3 = 82K ohms
R_4 = 82K ohms
R_5 = 750K ohms
R_6 = 2.2 Megohms
R_7 = 2.2 Megohms
R_8 = 250K ohms
R_9 = 100K ohms
R_{10} = 250K ohms
R_{11} = 250K ohms

C_4 = 0.02 μF
C_5 = 0.02 μF
C_6 = 0.5 μF
C_7 = 0.02 μF
C_8 = 0.02 μF

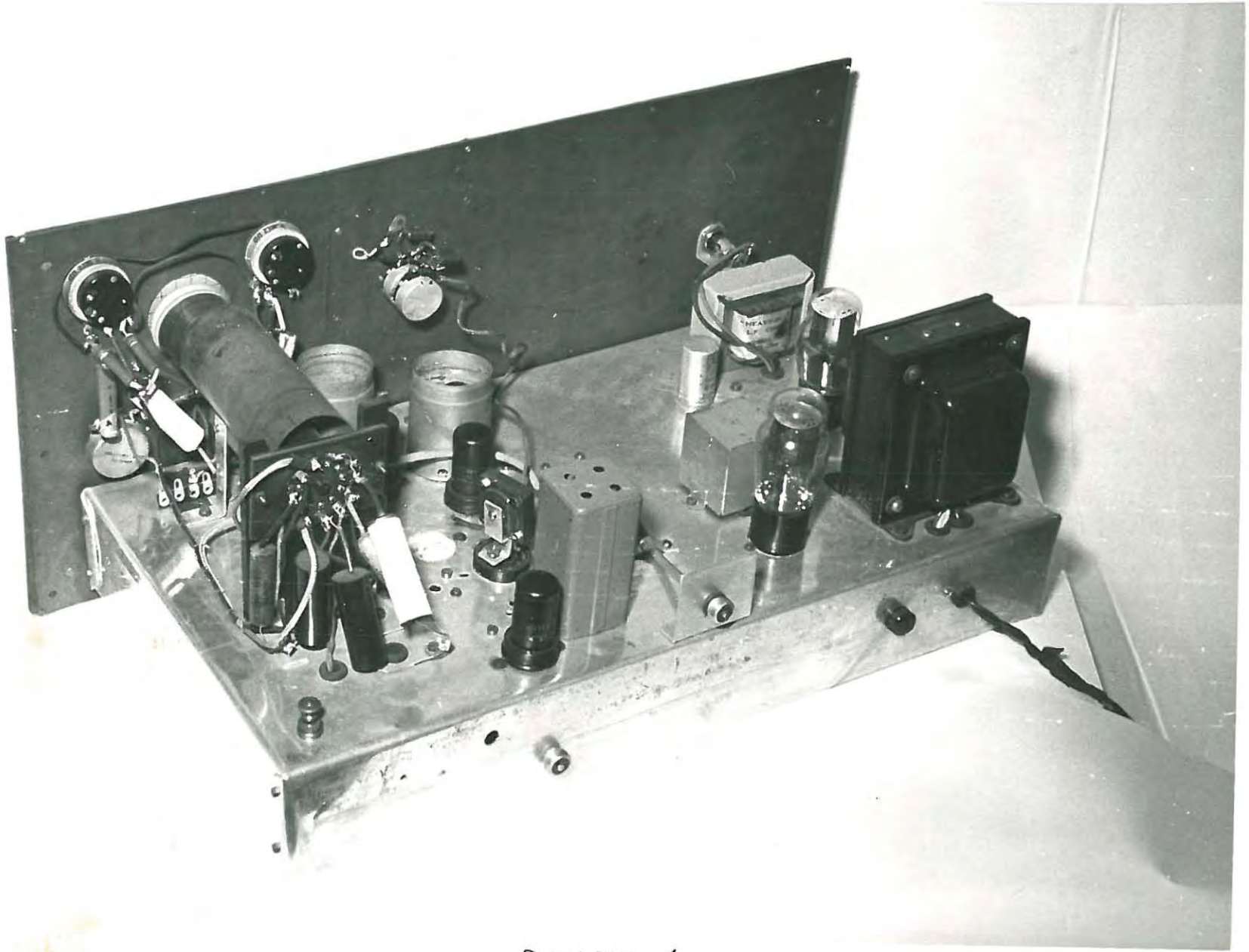

PLATE 4

As much time had already been spent in building the conductance bridge, a proposed electronic switching circuit to give a double-beam oscilloscope could not be included. Such a device would have enabled the operator to balance the Wagner Earth and measuring arm simultaneously.

1.262 THE PHASE-SHIFTER AND HORIZONTAL AMPLIFIER (See Fig. 19)

Circuits for phase-shifting up to 360° have been reviewed in a paper by Everest (51). An attempt was made to construct one of the phase-shifters suggested, but the effort had to abandoned in view of the time available. Instead, a phase-shifter of simple design was used for balancing at frequencies up to about 60 kc/s. In order to isolate the circuit from the first mixer, the input was taken from the crystal oscillator through a separate cathode-follower which uses a 6J5 as its buffer tube (see Fig. 5). The coaxial connector seen on the extreme right in Plate 1 is used for this purpose.

The circuit for the horizontal amplifier is identical with that for the last stage in the crystal filter amplifier.

1.263 THE POWER SUPPLY (See Fig. 20)

The transformer used in this power pack was especially wound so as to cater for the requirements of both the cathode-ray tube and its amplifiers.

The 600 volts necessary for operating the 2AP1 tube is obtained by single-wave rectification, while the plate voltage is supplied to the amplifiers by the usual type of circuit.

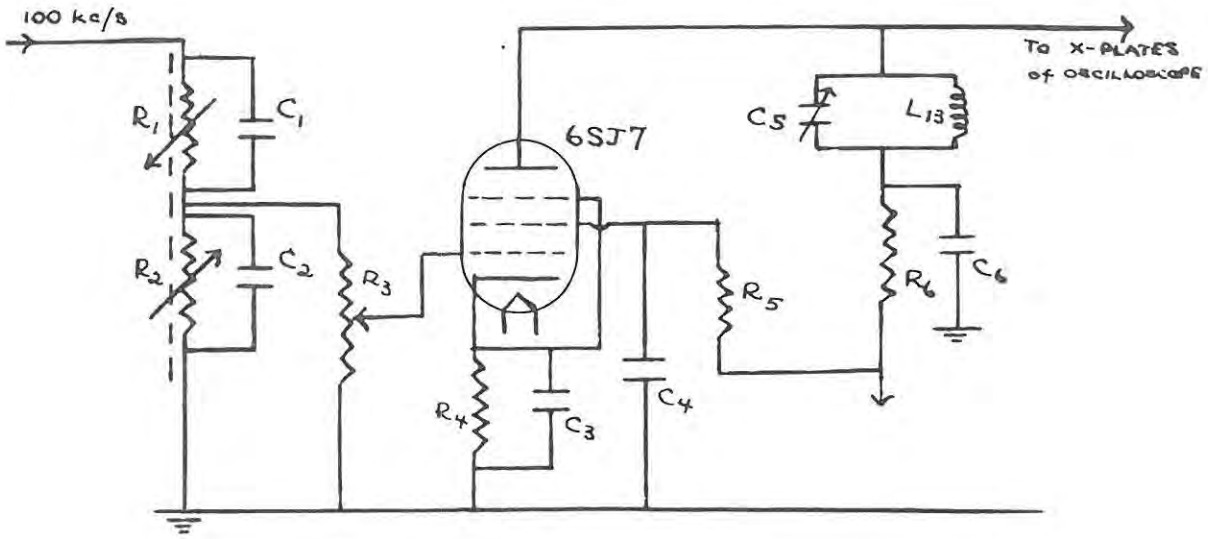

FIG. 19 CIRCUIT of PHASE-SHIFTER and HORIZONTAL AMPLIFIER

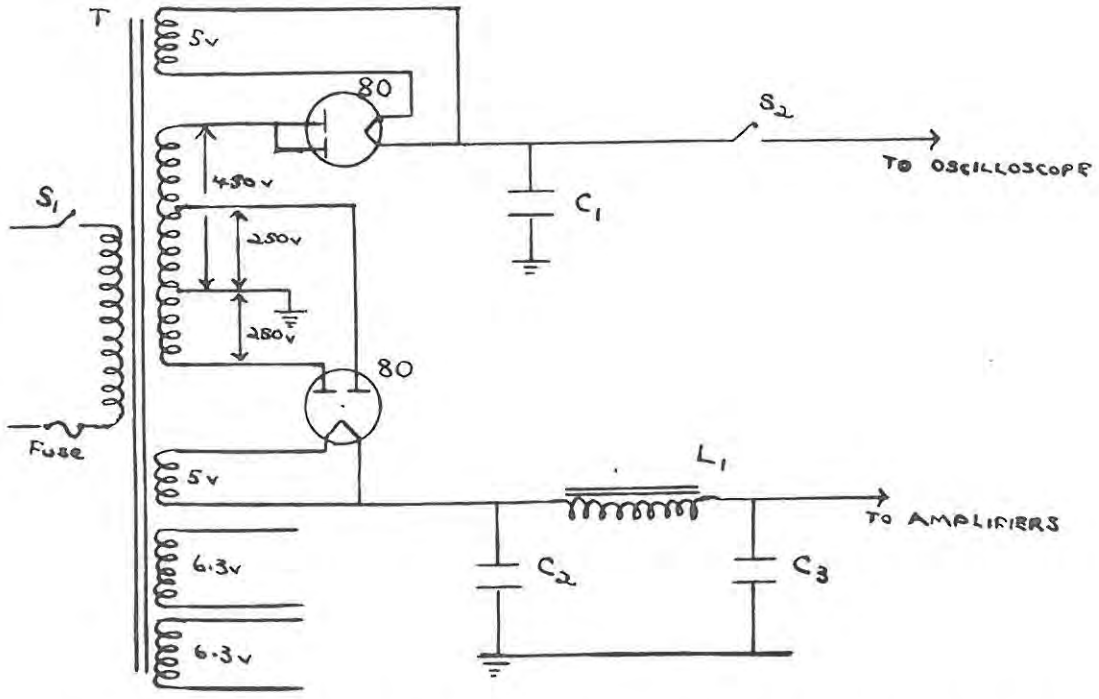

FIG. 20 CIRCUIT of POWER SUPPLY

FIG. 19 CIRCUIT OF PHASE-SHIFTER and HORIZONTAL AMPLIFIER (100 kc/s)

R_1	= 250K ohms	C_1	= 50 pF
R_2	= 250K ohms	C_2	= 50 pF
R_3	= 250K ohms	C_3	= 0.05 μF
R_4	= 600 ohms	C_4	= 0.02 μF
R_5	= 100K ohms	C_5	= 750 pF
R_6	= 10K ohms	C_6	= 0.1 μF
		L_{13}	= 9 millihenries

FIG. 20 CIRCUIT OF POWER SUPPLY

L_1	= 20 henries	C_7	= 0.5 μF
T	= mains transformer	C_8	= 8 μF
S_1	= mains switch	C_9	= 8 μF
S_2	= beam switch		

The switch S_2 was included to cut off the electron beam during the long periods when the cathode-ray oscilloscope was not in use.

1.27 THE WHEATSTONE BRIDGE NETWORK (See Fig. 21)

The bridge network constructed by Gledhill (23), in accordance with the principles laid down by Shedlovsky, Dike and Luder (20, 22, 52), proved to be very satisfactory in use. This has been confirmed by Goddard and Faure (24, 25) who built their bridge on similar lines. Except for the following minor additions, of which the first three were made because of the extended frequency range, the Wheatstone Network remains essentially the same as in the original Gledhill bridge:

(a) A wire-wound 5000 ohm variable resistance (R_7) was included in the Wagner Earth circuit to enable balancing at the higher frequencies.

(b) Wherever possible, ordinary shielded wiring was replaced with shorter lengths of coaxial cable to improve sensitivity and give lower stray capacities.

(c) In order to eliminate hand-capacity effects - which become more pronounced at higher frequencies - the rotor plates of the condensers C_3 and C_4 were insulated from the slow-motion drives with short lengths of ebonite rod.

(d) Silver contacts were riveted into the arms of the cell selector switch, the ratio arms switch and the first

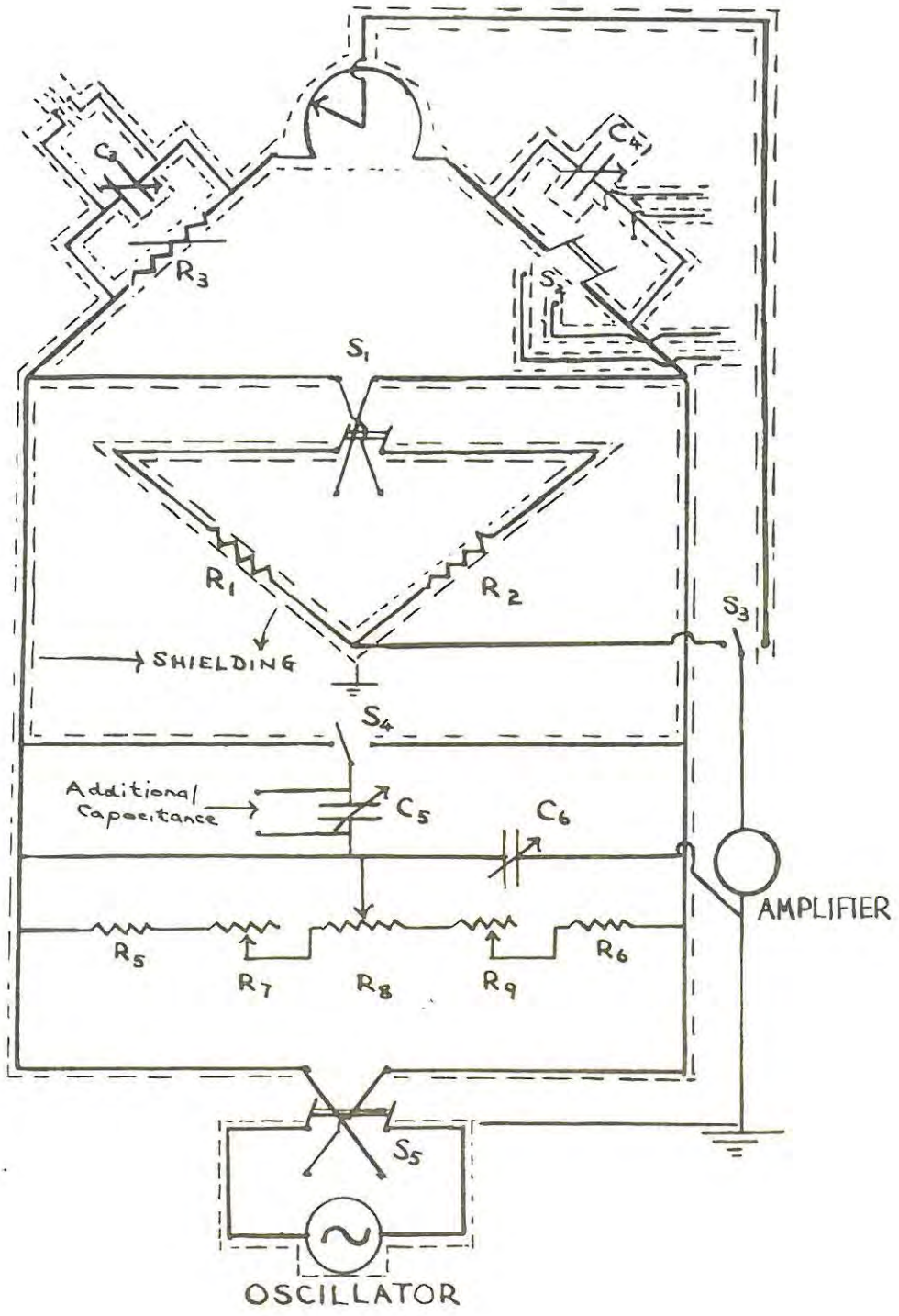

FIG. 21 CIRCUIT of BRIDGE

FIG. 21 CIRCUIT OF WHEATSTONE BRIDGE

R_1 = 10,000 ohms

R_2 = 10,000 ohms

R_3 = Measuring arm:
(Max. 111,111 ohms)

R_5 = 10,000 ohms

R_6 = 10,000 ohms

R_7 = 5,000 ohms

R_8 = 400 ohms

R_9 = 6 ohms

C_3 = 910 pF (max)

C_4 = 170 pF (max)

C_5 = 1000 pF (max)

C_6 = 100 pF (max)

switch of the 10,000 ohm decade resistance, to reduce variable contact resistance.

(e) The bridge output was taken through a 50,000 ohm wire-wound potentiometer (R_1 in Fig. 12). At extreme unbalance, it can be used to decrease the output, and thus avoid overloading the bridge-output amplifier.

Note: Since the measuring arm resistances are mounted at a distance of $2\frac{1}{2}$'' from the shielding which, in Shedlovsky's opinion, is sufficient if the upper frequency range does not exceed 4 kc/s, the effect of this was carefully investigated at frequencies above the recommended limit. When testing the performance of the bridge, no effects became apparent. It might be mentioned that no errors were reported by A. Faure (25) who, however, only took measurements up to 9 kc/s.

1.3 THE BRIDGE ASSEMBLY

The conductance bridge was assembled, as shown in Plate 5, in the constant-temperature room built by Gledhill (23).

A wooden framework measuring 24'' x 39'' x 12'' was erected alongside the Wheatstone Bridge section; it houses the following units:

(a) Top compartment: Power supplies for the beat-frequency oscillator, the bridge-input and bridge-output amplifiers and the second mixer.

(b) Middle compartment: The cathode-ray null detector (with its power supply), the second stage of the crystal filter and its amplifier, the phase-shifter and the 100 kc/s horizontal amplifier to the oscilloscope.

(c) Bottom compartment: The beat-frequency oscillator, the bridge-input and bridge-output amplifiers, the second mixer and the first stage of the crystal filter.

This arrangement conveniently reduces undesirable heating of the oscillators, and possesses a distinct advantage over the Goddard-Faure bridge in that there is no heating of the Wheatstone Bridge components, since the latter are completely isolated from the power supplies.

The two bridge-coupling transformers are located in the space immediately below the Wagner Earth section of the bridge.

In the lower left-hand corner of Plate 5 can be seen a Du Mont cathode-ray oscilloscope and a G.R. 1000 c/s oscillator,

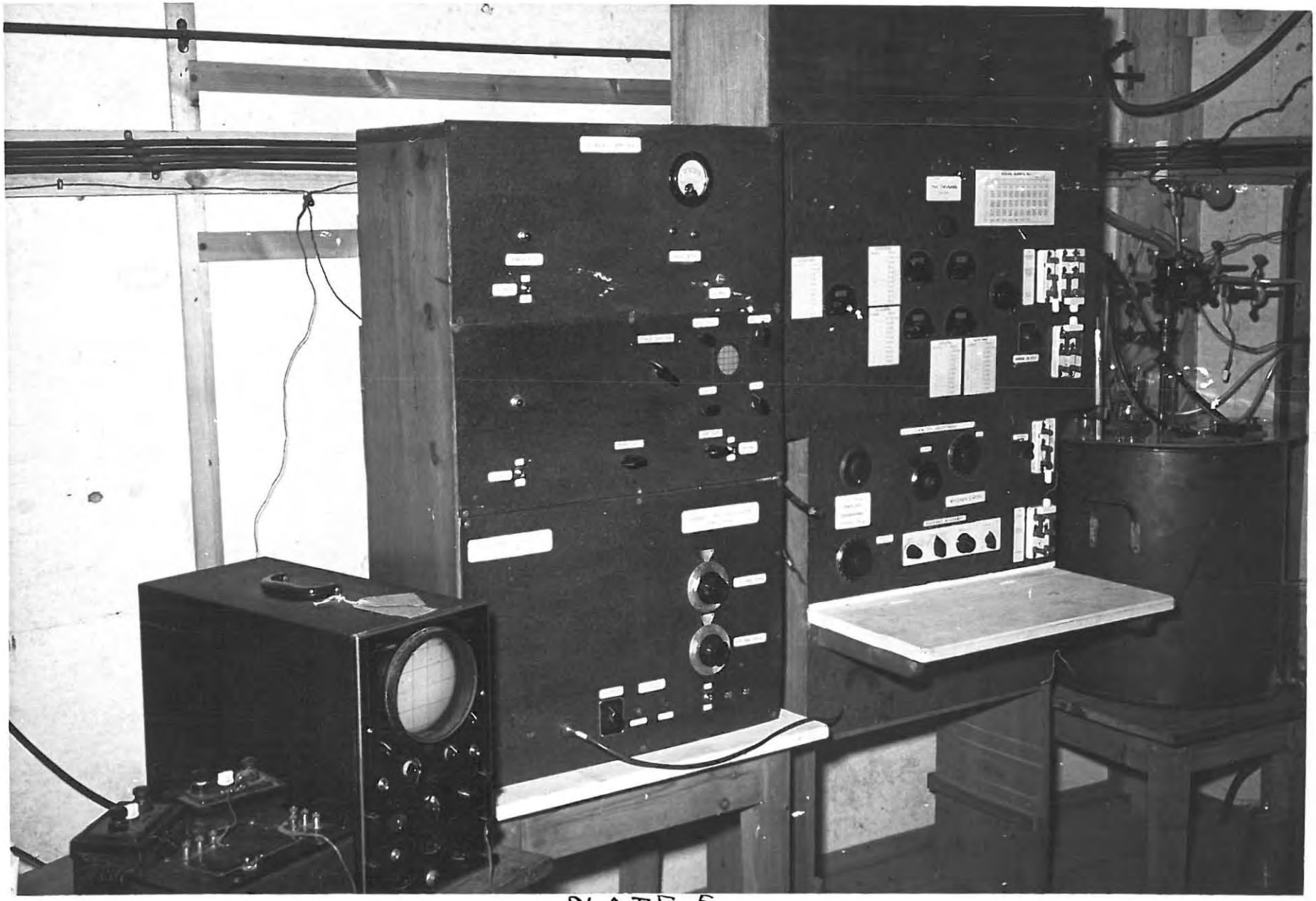

PLATE 5

which were used for checking the oscillator frequencies (see p. 55).

Plate 2 gives a rear view of the double-heterodyne units in the wooden framework. It will be seen that, apart from the mains connection, there are only four inter-connecting leads: two supply power to the oscillators, the third connects the two stages of the crystal filter, while the fourth feeds a 100 kc/s signal to the cathode-ray oscilloscope horizontal amplifier. The leads are easily detachable and, once the front panel screws and earth leads are removed, each unit can be readily withdrawn for adjustments or repairs.

1.4 PERFORMANCE OF THE CONDUCTANCE BRIDGE

With the crystal filter carefully aligned and accurately tuned to 100 kc/s, the bridge has proved to be satisfactory in operation over a wide range of frequencies. Since it was anticipated that the potassium chloride solutions - which were to be used for measurements - would have resistance values well within the range 10 ohms to 10,000 ohms, preliminary measurements, with a G.R. decade resistance box as standard, were confined to these limits. Thus, it was deduced that an accuracy of, at most, 0.01% is attainable, in the resistance measurements.

Attention should, however, be drawn to the following limitations:

(a) Difficulty was experienced in balancing at frequencies <500 c/s due to unstable oscillations.

(b) Owing to the frequency-response of the low-pass filters - but this may be only one of the reasons - the bridge proved to be insensitive at frequencies higher than about 75 kc/s.

Note: Subsequent calibration of the beat-frequency oscillator also provided a means of checking the performance of the bridge.

1.5 MANIPULATION OF THE BRIDGE

Experience has shown that the following procedure should be adopted when carrying out measurements:

(a) The beat-frequency oscillator must be switched on and left to warm up for, at least, one hour, after which the frequency drift should be at a minimum.

(b) By adjusting the tuning condenser, the oscillator is set at the desired frequency, which can be checked with the aid of Lissajous figures (see p. 55).

(c) With the oscilloscope vertical amplifier set at low gain, the measuring arm resistances and capacitances are adjusted until the image on the oscilloscope is almost a horizontal line. (Additional capacitances may be necessary).

(d) After switching over to ''Ratio Arms'', the Wagner Earth is approximately balanced.

(e) The switch is then thrown back to ''Measuring Arms'' and, again, the latter is adjusted to give balance. {This is the ''separate terminal'' balancing procedure suggested by Luder (22)}.

(f) This alternate process of balancing is repeated until there is no change on switching from one position to the other.

(g) At this juncture, the phase-shifter is adjusted as follows: With the switch on ''Ratio Arms'', the coarse resistance (of the Wagner Earth section) is varied to give a large

unbalance. There will now be a tilted ellipse; by adjusting the phasing control, the ellipse can be made to collapse into a line. Then the coarse resistance is used to return the line to its horizontal position.

(h) The frequency should now be checked, and the tuning condenser adjusted if necessary - to get a steady Lissajous pattern.

(i) With the oscilloscope turned up to high gain, final balance is obtained by rapidly following the steps already outlined.

(j) Further readings may be obtained by repeating the balancing with the voltage supply reversed, and then with the ratio arms reversed for the two positions of the supply voltage reversing switch. The average of all four readings is taken as the measurement at the set frequency.

(k) The whole balancing procedure is repeated for measurements at other desired frequencies. It must be remembered, however, that the set frequency should be checked at the beginning and at the end of a particular measurement.

1.6 CALIBRATION

In view of the proposed application, it was necessary that the resistances and capacitances in the measuring arm - as well as those used in conjunction with the bridge - and the beat-frequencies should have accurately known values.

1.61 BRIDGE RESISTANCES

The decade resistances and the slide-wire in the measuring arm of the bridge had not been previously calibrated as an accurately known standard could not be obtained. Fortunately, a 10 ohm oil-immersed standard resistance became available, and this was sent to the S.A. National Physical Laboratory for calibration.

The procedure adopted for calibrating the resistances has been comprehensively dealt with by P.K. Faure (37), and will not, therefore, be given here. However, it might be stated that the method is analagous with that which is employed for calibrating weights, viz: by intercomparison.

1.62 THE G.R. DECADE RESISTANCE BOX

With the box placed in the cell arm, the bridge was balanced at each step, from the lowest to the highest nominal value of resistance. Thus, with the absolute values of the resistances in the measuring arm known, the calibrated values for the box were obtained.

1.63 BRIDGE CONDENSERS

With the condenser in parallel with the cell arm disconnected (i.e. C_4 in Fig. 21), balance was obtained for various settings of C_3 (i.e. condenser in parallel with the measuring arm) against a standard Cambridge variable condenser. The latter was connected across the cell arm and in parallel with a G.R. 10,000 ohm non-inductive resistor (Type 500-J). The standard condenser was then removed, C_4 reconnected, and the bridge balanced for various settings of C_4. This gave the calibration of C_4 in terms of that for C_3. Hence calibration curves were plotted for each of the condensers.

Note: In using these curves, it must be remembered that the values which correspond to the scale readings are not necessarily the absolute capacitances, since the condensers do not generally have zero capacitance at a setting of zero. The capacitances read off from the curves are actually increments above the ''zero value'' as the setting is changed from zero position. As P.K. Faure (37) points out, '' the 'in situ' method (which was used for calibration) does not allow the residual capacitances of the individual condensers, at zero setting, to be measured. Fortunately, however, such values are of no real significance: the only important factor is the difference between the zero values of the condensers in the two arms, and this can be determined''. This difference was found by setting C_3 at zero position and balancing

with C_4: the value obtained was 13 pf. For any given settings of the two condensers, therefore, the effective capacitance in parallel with the measuring arm is

$$C = C_3 - C_4 + 13 \text{ pf}$$

This is the value to be used in the $(1 - \omega^2 C^2 R^2)$ correction term

1.64 ADDITIONAL CAPACITANCES

(a) Two G.R. decade condenser boxes - type 219M and 219K - were calibrated by the method of intercomparison. A G.R. 0.1 μF capacitor was used as a standard for this purpose.

(b) Small mica capacitors were connected in parallel with C_3 (set at a specified value) and the bridge balanced for various settings of a standard condenser in the cell arm.

Note: The calibrated values of the decade resistances, the slide-wire and the decade condenser boxes are given in the Appendix.

1.65 THE BEAT-FREQUENCY OSCILLATOR

Robinson (53) and Kurokawa and Hoashi (54) have shown that the Wien Bridge (a network used for comparing two condensers) can be made to afford a simple, yet accurate method for determining the frequency of the a.c. source. Although a direct reading frequency bridge was not actually set up as suggested by these workers, the basic Wien Bridge Network was, nevertheless, used for purposes of calibrating the oscillator.

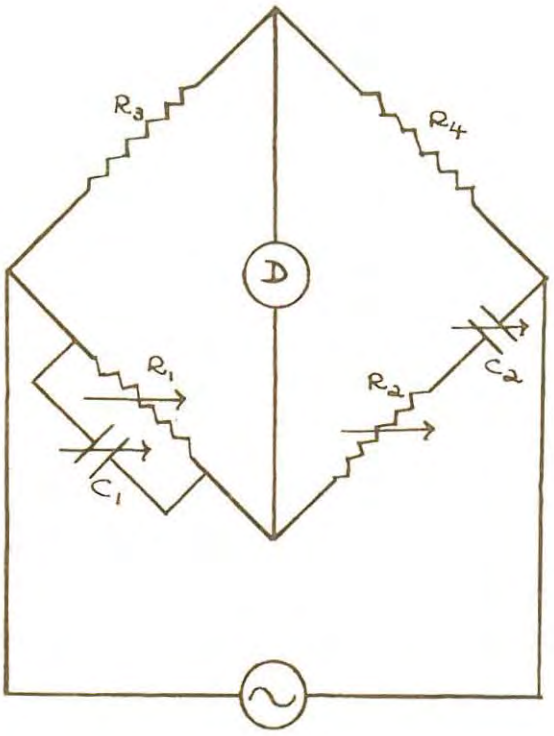

FIG. 22 CIRCUIT of WIEN BRIDGE

The bridge network is shown in Fig. 22.

Applying the general equation for balance, we have

$$(1/R_1 + j\omega C_1)(R_2 + 1/j\omega C_2) = R_4/R_3$$

and, if R_4 is made equal to R_3, we may write

$$R_2/R_1 + j\omega C_1 R_2 + C_1/C_2 + 1/j\omega C_2 R_1 = 1$$

On equating reals and imaginaries, we get

$$R_2/R_1 + C_1/C_2 = 1 \quad \text{.....(1)}$$

and $$\omega^2 = 1/C_1 C_2 R_1 R_2 \quad \text{.....(2)}$$

or $$f = 1/2\pi(C_1 C_2 R_1 R_2)^{\frac{1}{2}}$$

whence the second condition for balance is seen to be dependent on frequency. Hence, by noting the values of C_1, C_2, R_1 and R_2 at balance, the frequency may be calculated from equation (2).

When calibrating the beat-frequency oscillator, therefore, the Wheatstone Bridge was converted to the Wien Bridge as follows:

The G.R. resistance box and one of the decade condenser boxes - both previously calibrated - were connected in series in the cell arm to represent R_2 and C_2 respectively (see Fig. 22). The other calibrated condenser box was connected across the measuring arm as C_1 - thus, giving the parallel C_1R_1 combination. The ratio arms were regarded as R_3 and R_4.

By observing Lissajous figures on a Du Mont oscilloscope (which had been especially introduced for frequency-checking), the tuning condenser was set at a particular value of the

beat-frequency. The bridge was then rapidly balanced, and the frequency checked by glancing at the Du Mont oscilloscope. A slight re-adjustment of the tuning condenser - to obtain a steady pattern - became necessary, if a drift in the frequency was detected. Thereupon, balancing was rapidly repeated, and from the values of C_1, C_2, R_1 and R_2 noted, the frequency was computed. For frequencies up to 10 kc/s, the signal from a calibrated G.R. 1000 c/s oscillator was applied to the X-plates of the Du Mont oscilloscope; thereafter, the signal was replaced with the output from the crystal oscillator.

A sample of the readings obtained for frequencies up to 75 kc/s is given in the table on p. 57.

Note: The 10 kc/s frequency-measurement was determined firstly with the 1000 c/s oscillator, and subsequently with the 100 kc/s output (from the crystal oscillator). Hence a correction term was applied to all calculated frequencies below 10 kc/s. The corrected frequencies are recorded in the column under f'.

$\Delta f/f''\%$ represents the deviation of the calculated value from the frequency as given by the Lissajous figures (i.e. f''). The results, as shown in the table, were obtained for the following settings of the frequency: 500 c/s, 1 kc/s, 2 kc/s, 3 kc/s, 5 kc/s, 7 kc/s, 10 kc/s, 20 kc/s, 25 kc/s, 50 kc/s, 75 kc/s. It will be seen that frequencies in the range 2 kc/s to 50 kc/s can be set to an accuracy of, at least, 0.1%.

R_1 ohms	R_2 ohms	C_1 μF	C_2 μF	f kc/s	f' kc/s	$\frac{\Delta f}{f''}$ %
8692.1	5095.2	0.030895	0.075335	0.4957	0.4967	-0.66
6539.4	2518.1	.030783	.050325	.9964	.9984	-0.16
5749.3	1799.3	.020520	.030005	1.9942	1.9982	-0.09
3825.2	1199.1	.020525	.030005	2.9943	3.0002	+0.00
2282.0	729.93	.020380	.030005	4.9863	4.9963	-0.07
1643.3	509.91	.020645	.030005	6.9855	6.9995	-0.00
1148.0	359.92	.020535	.030005	9.9737	9.9943	-0.05
1112.0	719.91	.010555	.030005	9.9943		-0.05
810.01	370.00	.010680	.019965	20.018		+0.09
607.70	300.01	.010595	.020996	24.989		-0.04
318.50	150.00	.010610	.019965	50.023		+0.05
178.02	100.00	.010555	.024014	74.919		-0.11

1.7 SUGGESTED IMPROVEMENTS TO THE BRIDGE

Measurements effected with the conductance bridge show that the double-heterodyne principle has been applied with a fair degree of success. Attention is now drawn to a few ways in which the apparatus might be improved in its performance, particularly if it is intended to carry out measurements over a wider range of frequencies:

(a) The present phase-shifter should be replaced, since it is found to operate over only a restricted range of frequencies. Circuits are known which are capable of giving a phase-shift of 360°; although many of these are of elaborate design, it would be worthwhile if a suitable one were incorporated in the bridge.

(b) Recent research (55) has established that polystyrene is far superior to mica as a dielectric for precision capacitors. It possesses very nearly ideal characteristics, viz: a dielectric constant and low dissipation factor which are practically invariant with frequency. Mica, it is maintained, exhibits marked polarisations at frequencies below the audio range, and measurements on high-quality silvered-mica capacitors show rises in capacitance as much as 30% while similar measurments on polystyrene ones indicate increases of only a few tenths per cent. The latter, therefore, make excellent components for measuring circuits, filters and tuned circuits.

Now capacitance measurements made with the bridge cannot be guaranteed to the same degree of accuracy as the resistance measurements, and there is no doubt that some errors have been introduced through the use of the G.R. decade condensers which consist chiefly of mica-dielectric capacitors. {This observation has also been made by A. Faure (25)}. It is suggested, therefore. that polystyrene units be used instead.

(c) A suitable electronic switching device should be included to give a double-beam oscilloscope. This would facilitate rapid measurements since measuring arms and Wagner Earth can then be balanced simultaneously.

(d) An automatic gain control in the bridge-output amplifier would serve to limit the maximum signal when the bridge is far from balance. At present, this is effected by means of the potentiometer R_1 (in Fig. 12), but it is inconvenient to adjust R_1 repeatedly while balancing.

Although the last two recommended additions are not absolutely essential, the author feels that they would, nevertheless, prove to be useful.

In conclusion, it is suggested that the cause of unstable oscillations below 500 c/s be investigated.

AN INVESTIGATION

OF

POLARISATION ERRORS

IN

CONDUCTANCE MEASUREMENTS

2.1 INTRODUCTION

Electrolytic polarisation is frequently described as the departure of the electrode potential from its equilibrium value, when a current is passed through a chemical cell. The formation of gas films at the electrodes and concentration changes due to transport phenomena are, in many instances, the causes of polarisation; whilst other contributing factors are believed to be electron transfer or some other slow step at the electrode surface.

Modern research in electrochemistry has directed its efforts to investigating the true state of affairs at the electrode-solution interface. It will be realised, that a thorough understanding of electrode effects is necessary to account for polarisation errors in conductance measurements. So far, the problem has been dealt with from two experimental viewpoints. Grahame and others (56, 57) have found electrocapillarity measurements particularly rewarding. In a classical review, Grahame gives a strikingly clear account of the so-called ''electrical double layer'' on the basis of the theory of electrocapillarity. On the other hand, Frumkin and his school (58, 59) have tried to elucidate the structure of the double layer from studies of hydrogen overvoltage phenomena. In spite of the prevailing uncertainty as to the rate-determining step in overvoltage phenomena, much valuable data on the nature of polarisation is being gained from such investigations.

An interesting feature of these researches is the development of a schematic representation of electrode processes - commonly referred to as ''the equivalent circuit of the half-cell''. According to Grahame (60), the circuit may be depicted as shown in Fig. 23. Since the double layer behaves like a capacitor when a potential is applied across it, C_d is called the ''double layer capacitance'' or the ''differential capacitance''. C_d is, however, unlike an ordinary physical capacitance since it is a function of the applied voltage. Chemical transformations, brought about by an applied voltage, are represented in the ''faradaic branch''. Here θ is the ''transfer'' or ''transition'' resistance which is that component of the polarisation resistance due to slow electron transfer at the electrode. W is included as the ''Warburg impedance'' which results from the diffusion of primary reaction products away from the electrode. It is sometimes expressed as a series combination of a diffusion resistance and a diffusion capacitance. The element R_L has been added to the equivalent circuit by Remick and McCormick (61) who, from their experimental studies of platinum electrodes in a poised ferrocyanide-ferricyanide solution, showed the existence of electrode layer resistance.

From investigations into the electrochemical reaction at an amalgam electrode, when subjected to a small alternating potential, Randles (62) has proposed a circuit similar to that suggested by Grahame. Rozental and Ershler (63) and

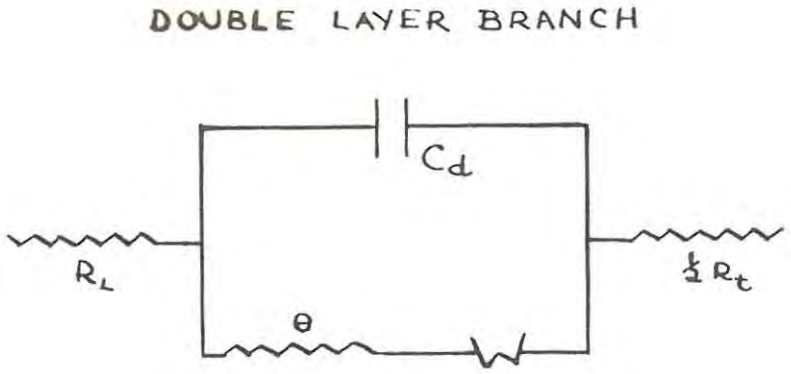

FIG. 23 EQUIVALENT CIRCUIT of the HALF - CELL

FIG. 24 FARADAIC BRANCH (after Grahame)

Gerischer (64) have been led to similar conclusions. It is worth mentioning that Breyer and Gutmann (65) introduced the terms ''dynamic resistance'' and ''dynamic capacitance'' in their electrical network representing the electrochemical process when a small a.c. potential, superimposed onto the direct potential, is applied to a reversible electrode. In later papers by Breyer and Hacobian (66), a quantity, giving the thickness of the ''active space'' wherein the electrode process is believed to occur, is derived from considerations of the diffusion process. Although, as the authors maintain, ''the quantity has been given a rather firm theoretical foundation'', the concept does not appear to have gained favour.

The ''faradaic branch'' is found to have special value in reaction mechanism studies. Applying the mathematical theory of the faradaic impedance, developed by Grahame, et al (60, 63), it is possible to calculate θ and the Warburg impedance for certain classes of substances defined by Grahame. Randles (62) has used θ for calculating the rate constants of rapid electrode processes, while Parsons (67) finds θ values helpful in computing the heats of activation for reactions involving hydrogen evolution on platinum electrodes. Remick (68) states that ''in order to demonstrate that the mechanism of an electrochemical reaction falls in any given mechanistic class, the mathematical requirements of that mechanism must first be deduced from basic principles (often an imposing task!) and then the reaction must be shown experimentally to be in accord

with these requirements. In working toward this goal, Grahame has considered a number of different classes of substances and has shown that Fig. 24 conveniently represents the faradaic branch of the equivalent circuit .....'' This circuit illustrates reactions involving certain classes of substances and ''the additional impedance X is not a conventional circuit impedance'' and has ''different mathematical properties for each different class of substances''.

In order to measure accurately the conductances of electrolytes, workers have attempted, amongst other things, to reduce electrode effects - polarisation - to a minimum. The use of platinised platinum electrodes,to reduce the frequency dependence of platinum electrodes, has been the standard procedure for some time past. Modern conductance research is now producing ingenious methods of eliminating electrode effects altogether. Amongst these may be mentioned:

(a) The use of electrodeless conductance cells

This has called for radicle departure from normal cell design. Griffiths (69) does this by employing the principle of a three-terminal transformer ratio-arm bridge. Measurements are made by using a loop of the solution contained in one arm of an annular cell as the transformer core. A somewhat similar method is resorted to by Gupta and Hills (70) who also make use of a transformer bridge. Here, coupling between two toroidal transformers is provided by a closed

loop which threads both coils - the loop containing the solution whose conductance is required. The coupling is found to depend directly on the conductivity of the loop and hence, on the conductivity of the solution, which is determined by comparing it with a standard. Lavagnino and Alby (71) have also devised a similar method. Hinkelmann (72), on the other hand, describes a probe for conductance measurements which consists essentially of two coils, hooked up in such a way that differences in conductivity are transformed into frequency differences of an auxiliary oscillating circuit.

Another method, which virtually eliminates electrodes, is achieved by the double cell design of Feates, Ives and Pryor (73). Two cells are constructed with identical electrodes but with different lengths of solution between them. The difference in the resistances of the two cells measured, is found to show only a small residual frequency dependence.

The author has noted two further methods devised by Huber and Cruse (74) and by Salomon and Svitok (75) where measurements are made without the use of electrodes. Details of these methods could not, however, be obtained

Note: As far back as 1930, Shedlovsky (29) designed a cell in which electrode effects were successfully eliminated. He used a cylindrical cell which was fitted with electrodes of the ordinary type at each end and, in addition, two (or more) platinum loops were sealed to the inner surface of the cell

at intermediate positions. The cell was connected to the bridge in such a way (by connecting the detector between the junction of the ratio arms and one of the loops) that the four arms of the bridge consisted of two ratio arms, a known resistance plus part of the electrolyte resistance and the remainder of the cell. When the bridge was balanced, no current flowed through the detector loop which was presumably free from electrode effects, while the two conducting electrodes were in opposite branches of the bridge. If the disturbances at these two electrodes gave rise to errors of equal magnitude, the resistance found in this way would be free from errors due to electrode effects. Even if they were not equal, their effect could be eliminated by taking a second resistance reading with a different loop in use and combining the two. Every such electrode combination was, of course, calibrated with a solution of known conductance.

(b) The d.c. method of conductance measurements

Since reactances only become significant with a.c., this method is free of impedance difficulties associated with electrode processes. Thus, Lim (76) obtained fairly accurate conductance values for sodium chloride and potassium chloride solutions. Gordon and his collaborators (77, 78) have developed the method to yield high precision data on dilute halide solutions in water and in methanol. However, the method is restricted in its applicability to solutions for which suitable reversible electrodes are available.

2.2 DESCRIPTION OF APPARATUS

2.21 THE CONDUCTANCE CELLS

Two types of Pyrex conductance cells, with bright platinum electrodes, were used during the course of the present research:

(a) THOMAS-GLEDHILL CELL - hereinafter, referred to as the T-G Cell. See Fig. 25.

Complete descriptions of the design of this cell and its construction are given by Gledhill (23) and P.K. Faure (37). The latter had the nitrogen inlet capillary tube brought in to a point eccentric to the bottom of the electrode vessel. This served to promote better stirring and also to minimise the risk of nitrogen bubbles displacing the electrodes.

Measurements carried out by various workers in this laboratory have shown the cell to be free from the Parker effect and, possibly, other errors arising from faulty cell design. However, it was noted that A. Faure (25) makes mention of inaccurate readings obtained when the cell was used for measuring the conductance of dilute potassium chloride solutions. The author has made similar observations (see Section 2.5).

Two T-G cells were used: one was reserved for measurements on conductance water, while the other was employed only for measurements on potassium chloride solutions.

(b) NICHOL-FUOSS CELL - hereinafter, referred to as the N-F Cell. See Plate 6.

In order to obtain reliable conductance data on very dilute non-aqueous systems, Nichol and Fuoss (31) found that a departure from normal cell design was necessary. The design incorporates electrodes which are concentric cylinders, with the lead to the outer electrode being a platinum tube which acts as an electrical shield for the lead to the inner electrode. Thus, it is maintained, stray electrical paths are eliminated.

The contemplated measurements at high frequencies - when stray electrical paths assume greater significance - warranted the use of such a cell and, it was felt, that it would be worthwhile constructing one along the lines suggested by Nichol and Fuoss.

Two factors were borne in mind while designing the cell, viz: the desired cell constant and the dimensions of the electrodes. The latter had to be such that the assembly would fit easily into an electrode vessel such as that which was used for the T-G Cell. Now for a cell of the N-F type, the cell constant is given by the approximate relationship

$$Q = (1/2\pi h)\ln(b/a)$$

where h is the length of the cylinders and b and a are the radii of the outer and inner electrodes respectively. Hence, for a cell constant of 0.15 - which was the value desired -

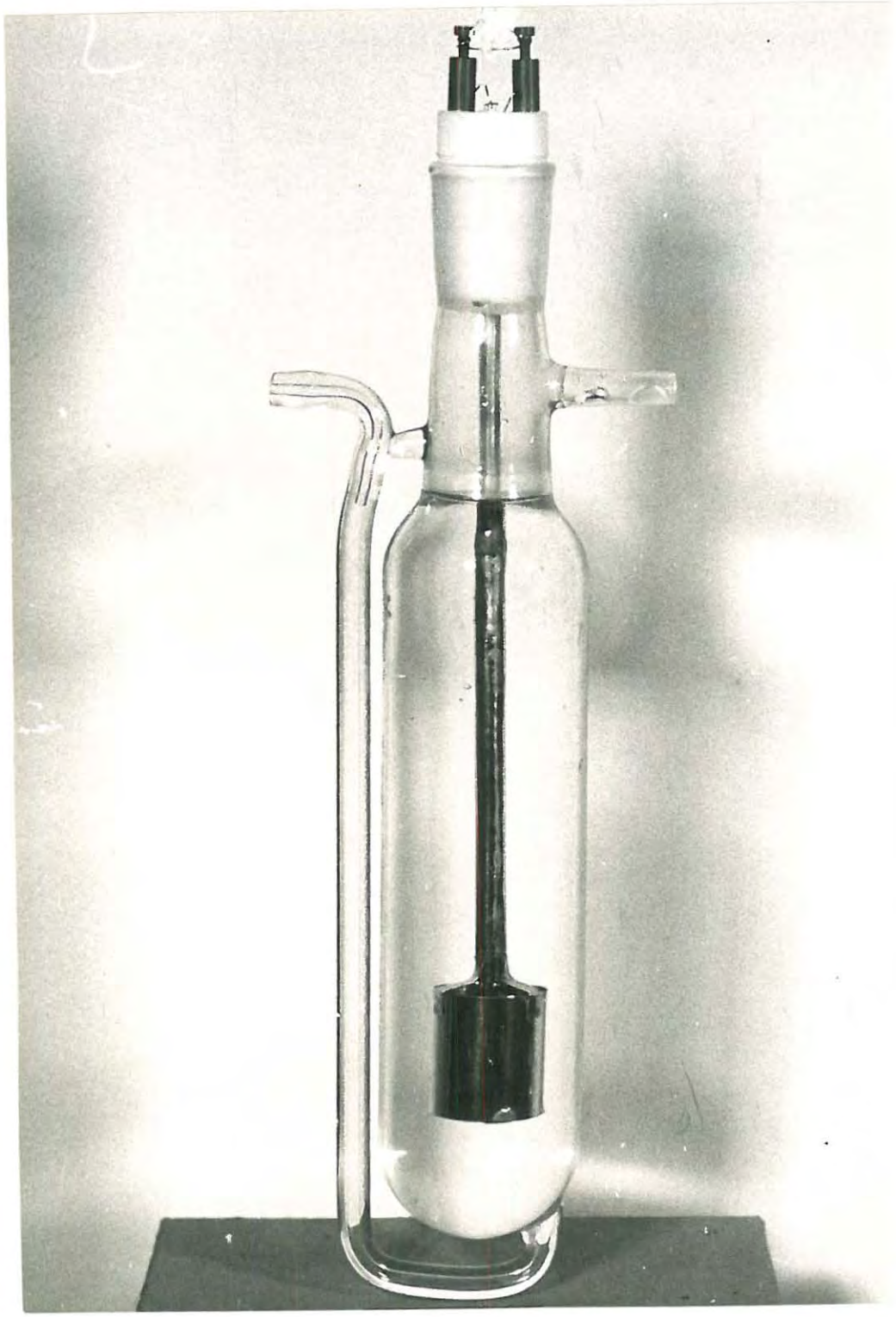

PLATE 6

it was required to have $\underline{h}$ = 3 cms and $\underline{b}$ = 1 cm. Much care was taken in constructing the assembly so that the inner electrode would not be easily displaced with respect to the outer one. A Teflon plug, carrying the electrode assembly, was machined to fit the electrode vessel which had a standard ground-glass joint. Fig. 26 shows the electrode assembly in diagrammatic form. With one set of electrodes, therefore, measurements could be made on conductance water and potassium chloride solutions contained in two different electrode vessels.

Note:

(1) This cell was used with satisfactory results by Clur (79) for the determination of the solubility of mercurous chloride in water.

(2) A search of the abstracts revealed that coaxial, concentric, cylindrical electrodes have also been incorporated in cells used by Nagaura and Karaki (80), Uggla (81) and Munson (82). Unfortunately, their papers were not available for study.

(3) Nichol and Fuoss have shown that their type of cell has excellent frequency characteristics if $Q < 0.1\ cm^{-1}$. For solutions having low specific conductance values, such cells would give too low a resistance to be measured with precision. Hence Brody and Fuoss (32) have designed two new types of cells with dipping electrodes, and with a view to increasing Q, while, at the same time, maintaining the satisfactory performance

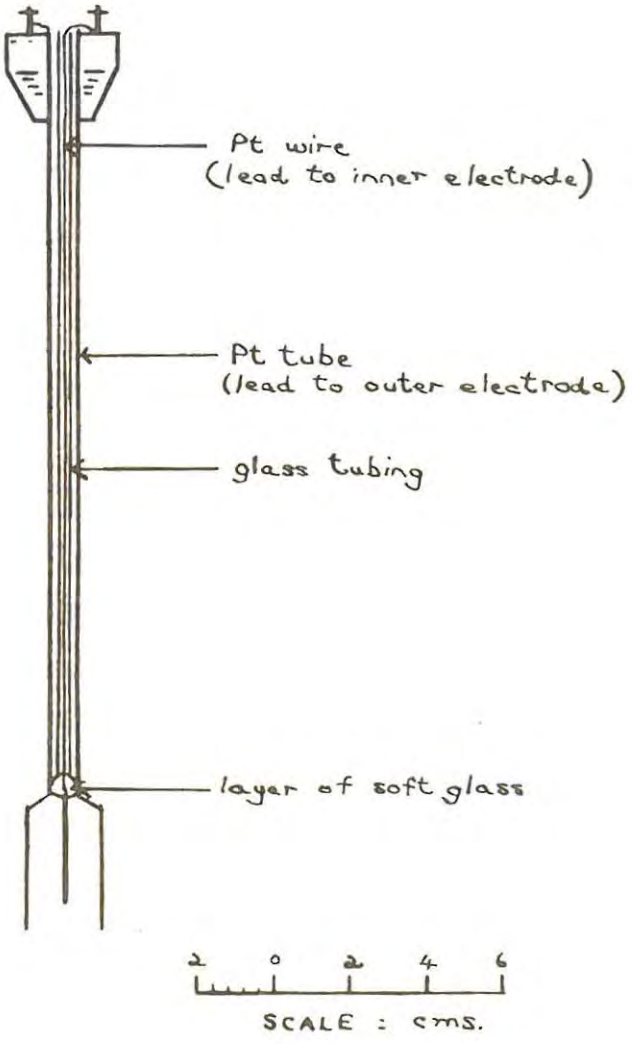

FIG. 26 ELECTRODE ASSEMBLY of NICHOL-FUOSS CELL

of the N-F type of cell. A brief description follows: The electrodes are flat rings of bright Pt mounted on an insulating tube (which was glass in the one type and Teflon in the other). The electrode assembly fits into a cylindrical vessel which is slightly larger than the outer diameter of the electrodes. The electrolyte is located in the annular space between the tube and the cylinder. By varying the electrode spacing and/or the electrolyte layer, Q could be made to assume any value betweem 0.3 and 4.0 cm^{-1}. The Parker effect is negligible (except for very high cell resistances) since the lead to the lower electrode is shielded by the cylindrical lead to the top electrode, and both are made to run inside the central insulating tube.

2.22 TEMPERATURE CONTROL APPARATUS

In view of the fact that many electrolyte solutions have a temperature coefficient of conductivity greater than 2% per degree at 25°C, a high degree of temperature control is required, so that measured conductance values can be guaranteed to an accuracy of at least 0.01%. Past workers in this laboratory have achieved this by housing the conductance bridge and the thermostat in a room maintained at a temperature of 24°C $\pm$ 0.2°.

2.221 ROOM CONTROL

The present investigations were, as mentioned, carried out in a constant-temperature room built by Gledhill.

The room temperature had, originally, been controlled by means of a paraffin thermoregulator based on a design by Deighton (83). Much difficulty was experienced by the author, however, in operating the regulator successfully since the main source of trouble lay in the presence of air bubbles in the tube. Goddard and Faure (24, 25), who attempted the same type of control in a room which they built, encountered similar difficulties. They then resorted to the use of an electronic thermoregulator adapted from a circuit by Sturtevant (84). Although the system is much more elaborate, it is easier to put into operation and requires less maintenance. For these reasons, it was decided to change over to the electronic method of control. During the course of experimentation, it was found that two minor changes could be made without lessening the degree of control. Consequently, the regulator constructed differs from that of Goddard and Faure in the following respects:

(a) The amplifier was coupled to the thyratron by a resistance-capacitance combination instead of a transformer. This did not cause the relay to chatter - as was reported by Faure (loc. cit.).

(b) Six wooden frames - onto which copper wire (No. 35 S.W.G., 0.33 ohm per foot) had been wound - were distributed about the ceiling of the room, and these made up the temperature sensitive arm. This arrangement, it was felt, afforded a better means of controlling the over-all temperature of the

room.

Observations made from time to time showed that the room could be maintained at 24°C ± 0.2° for long periods, and without any difficulty.

2.222 THE THERMOSTAT

The construction of the thermostat and the method of temperature control is adequately described by A. Faure (25), amongst others. To prevent corrosion, the outer thermostat - used for the present series of measurements - was made of copper instead of galvanised iron, which had been used by previous workers. The temperature was checked on a 5°C Beckmann thermometer which was periodically compared with a Baird and Tatlock solid-stem, mercury in glass thermometer (No. 55312), calibrated by the S.A. National Physical Laboratory. Since, according to Benson and Gordon (85), the temperature coefficients of conductivity of potassium chloride solutions of various concentrations are very nearly the same, it was not necessary to set the temperature to 25.000°C. A temperature reading of 4.108° on the Beckmann was found to correspond to 24.972°C ± 0.002° on the calibrated thermometer. At this temperature, conductance measurements could still be made with the desired accuracy of 0.01%, as long as the temperature remained constant. The temperature variation of the inner thermostat was observed to be not more than ± 0.003°C.

2.23 BALANCES AND WEIGHTS

The following balances and sets of weights were used for the preparation of potassium chloride solutions:

B I is a Sartorius microbalance (Model MD4). Maximum load: 20 g, accuracy: 0.001 mg with loads > 2 mg

B II is a large Sartorius balance, with a maximum load of 1400 g.

W I is a box of Grade A Sartorius weights (10 mg to 100 g). This was used with B I.

W II is a box of brass weights (10 mg to 1000 g) which was used with B II.

W III is a set of riders supplied with B I, consisting of a beam rider (10 mg) and ring riders (10 mg to 50 mg).

Note:

(1) All the weights were calibrated by the method of inter-comparison.

(2) A box of Oertling micro-weights (1 mg to 500 mg) whose calibrated values were known, was used for calibrating the riders supplied with B I.

(3) The difference in the length of arms of each balance was determined by the double-weighing method.

2.24 FLASKS AND BURETTES

Four flasks, varying in capacity from 250 ml to 1 litre, were used for preparing and storing the solutions. The flasks were fitted with ground-glass joints and stoppers. Two 50 ml

Normax Grade A burettes were also used - but with ungreased taps to prevent contamination of the conductance water.

2.3. EXPERIMENTAL

2.31 PURIFICATION OF MATERIALS

2.311 POTASSIUM CHLORIDE

About 300 g of Merck G.R. potassium chloride were crystallised, once from distilled water and twice from conductance water. Prior to the first recrystallisation, the hot solution was filtered through clean glass wool. The final recrystallised product was collected in a platinum dish and dried in an electric oven, initially at 150°C and then at 250°C. Since investigations into the removal of water from potassium chloride by Addink (86) showed that heating to 900°C was unnecessary, the usual procedure of fusing the salt was dispensed with. Instead, small amounts of potassium chloride, as required, were placed in a platinum boat and heated in a silica tube to about 600°C in an atmosphere of pure, dry nitrogen.

2.312 WATER

Ultra-pure conductance water was obtained from a still contrived and set up by Gledhill, Faure and Faure (87). The water was stored in Pyrex flasks fitted with ground-glass stoppers. The flasks had previously been leached out with conductance water.

2.313 NITROGEN

Nitrogen was rendered pure and dry, by passing it through a train consisting of pure sulphuric acid to remove traces of moisture, then through soda-lime to remove carbon dioxide, and finally over meta-phosphoric acid to remove ammonia.

To prevent the dry gas from absorbing water, and thus altering the concentration of the solutions in the cell, it was allowed to bubble through conductance water at 24°C so as to saturate it with water vapour at that temperature, and subsequently through potash bulbs in the thermostat to saturate it at 25°C.

2.32 PREPARATION OF POTASSIUM CHLORIDE SOLUTIONS

In order to determine the conductance of solutions with an accuracy of, at least, 0.01%, it is important that, amongst other things, the concentrations of the solutions be known to an equal degree of accuracy. Much care and special techniques are, therefore, essential. Shedlovsky (88), Jones and Bradshaw (89) and - in this laboratory - A. Faure and P.K. Faure were able to obtain highly accurate results by developing cautious weighing procedures and minimising errors due to loss of solution by evaporation during transfer. As far as necessary, the recommended precautions were observed.

Solutions of the following nominal concentrations were made up for the preliminary runs: 0.1N, 0.05N and 0.001N. For the accurate runs, an approximately 0.01D solution was prepared

according to Jones and Bradshaw (loc. cit.), and subsequently, solutions of the following nominal concentrations were used: 0.005N, 0.001N and 0.0005N.

All solutions were prepared by weight. The barometric pressure and room temperature were recorded during the course of weighing for conversion of weights to vacuo. This was done according to a simple procedure published by Gledhill and Faure (90).

Except for the 0.01D solution, all concentrations were expressed in gram-equivalents per litre. In making up the solutions, Li and Fang's formula (91) for the density d of potassium chloride solutions was used:

$$d \simeq 0.99707 + 0.00635f \text{ g per ml}$$

where f = weight per cent of KCl

2.33 CONDUCTANCE MEASUREMENTS

2.331 POTASSIUM CHLORIDE SOLUTIONS

As has already been mentioned, preliminary measurements were carried out before the accurate runs were attempted. Thus, it was hoped to:

(a) develop a standard procedure for taking readings;
(b) see whether both types of cells gave reproducible readings over the whole frequency range;
(c) gain some idea as to the extent of polarisation.

From the experience gathered, the following procedure

was adopted when taking readings:

At the outset, the room fan was switched off to prevent loss of solution by evaporation. The cell was rinsed once with the solution in question (after having been 'seasoned' with a solution of roughly the same concentration), filled to the mark and placed in the thermostat. Nitrogen was then allowed to pass over the top of the solution and, after a while, it was bubbled through at the rate of five bubbles per second. This was continued for two to three hours. About an hour before the actual readings were taken, the oscillator and accessory units were switched on. The thermostat temperature was noted, and the oscillator set at the desired frequency. Thereafter, the bridge was rapidly balanced, the frequency checked and the balancing repeated. In this sequence, resistance and capacitance readings were taken over the whole frequency range. On the average, a run lasted for about 25 minutes, after which the thermostat temperature was rechecked.

Readings were taken, first with the solution in, say, the T-G cell and, immediately thereafter, with a solution of the same concentration in the N-F cell - since it was desirable to obtain results with both cells under the same conditions.

2.332 CONDUCTANCE WATER

Following the method standardised by Malan (92) and Faure (37), the resistance was measured at various time intervals, at one frequency only, viz: 2 kc/s. From the resistance-

time curve so obtained, the conductance of the water was determined.

2.4 RESULTS

2.41 POTASSIUM CHLORIDE SOLUTIONS

Measurements were effected over a series of 15 to 20 frequencies from 250 c/s to 75 kc/s. To check for reproducibility, the readings were repeated at about 5 frequencies over this range.

The results are given in the Appendix.

Note:

(a) Unfortunately, the readings obtained for the 0.005N solution in the N-F cell were found to be in error due to a slight film of the solution having been, somehow, introduced between the leads to the electrodes. Hence, these results were discarded.

(b) Since an approximately 0.01D solution was prepared, the value used in calculating the cell constants was found by making a proportional correction to the value 0.00140877 $ohm^{-1}cm^{-1}$ (given by Jones and Bradshaw) for an exactly 0.01D solution.

2.42 CONDUCTANCE WATER

The water used in making up the solutions had conductance values ranging from 70 to 105 nm per cm.

Note:

Conductance readings were also taken at a number of different frequencies over the range. However, since only one such

run was attempted, the results were not considered conclusive enough to merit their inclusion in this thesis.

2.5 DISCUSSION

2.51 PRELIMINARY OBSERVATIONS

While the measurements taken during the preliminary runs showed that reproducible results could be obtained with cells of both types, it became clear that:

(a) the extent of polarisation was greater with the N-F cell;

(b) with the more dilute solutions, and at higher frequencies, the T-G cell behaved in a peculiar manner.

These results were to be expected for, with regard to the N-F cell, Nichol and Fuoss (31) observed a marked increase in polarisation when the diameter of the inner cylindrical electrode was reduced to dimensions such as that which obtains in the cell constructed; whilst A. Faure (25) detected significant errors in the equivalent conductance values for dilute potassium chloride solutions when the T-G type of cell was used.

2.52 R - f^{-1} Graphs

Following the procedure adopted by P.K. Faure, A. Faure and Taylor (37, 25, 93) for conductance measurements with bright Pt electrodes, all readings were, at first, plotted on graphs of R vs f^{-1}. The observed resistances had, of course, been corrected for bridge calibration, bridge lead and cell lead resistances. In addition, a frequency correction term was applied to each reading. (See Appendix).

Figs. 27 - 33 are such graphs for the results obtained from the accurate runs. On examining these curves, the following characteristics are revealed:

(a) With the T-G cell: Figs. 27 - 30

The graph for the approx. 0.01D KCl solution shows that, up to 3 kc/s, the points lie on a fairly straight line; thereafter, a distinct negative slope is observed which becomes more pronounced at the higher frequencies. In the 0.005N KCl graph, there is a sudden upward trend at about 10 kc/s, while the 0.001N KCl graph shows the negative slope commencing at 2 kc/s, with the minimum once again appearing in the region of 10 kc/s. Lastly, the 0.0005N KCl graph exhibits marked curvature throughout - the upward slope starting at an even lower frequency, viz: 4 kc/s.

(b) With the N-F cell: Figs. 31 - 33

All the graphs illustrating the behaviour of this cell show that the apparent resistance changes rapidly with frequency. In the case of the 0.0005N KCl solution, a steep downward plunge is found to occur at about 10 kc/s.

It is obvious, therefore, that none of the curves can be extrapolated to $f^{-1} = 0$, with any degree of confidence. An interesting point, however, is that when the readings at the higher frequencies are ignored and, the best straight line - drawn through the points at the lower frequencies - is extrapolated to infinite frequency, the T-G cell is found to have

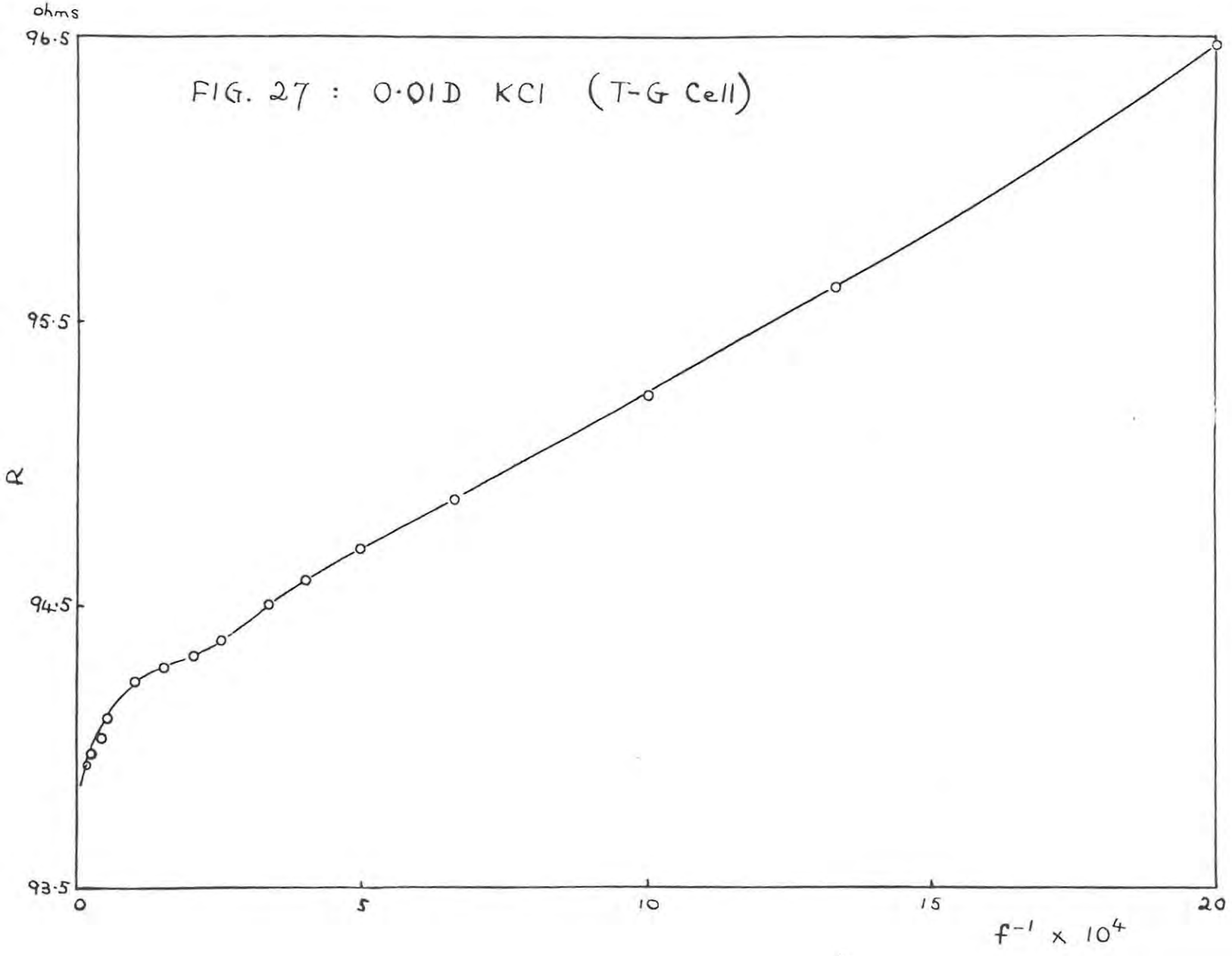

FIG. 27 : 0·01D KCl (T-G Cell)

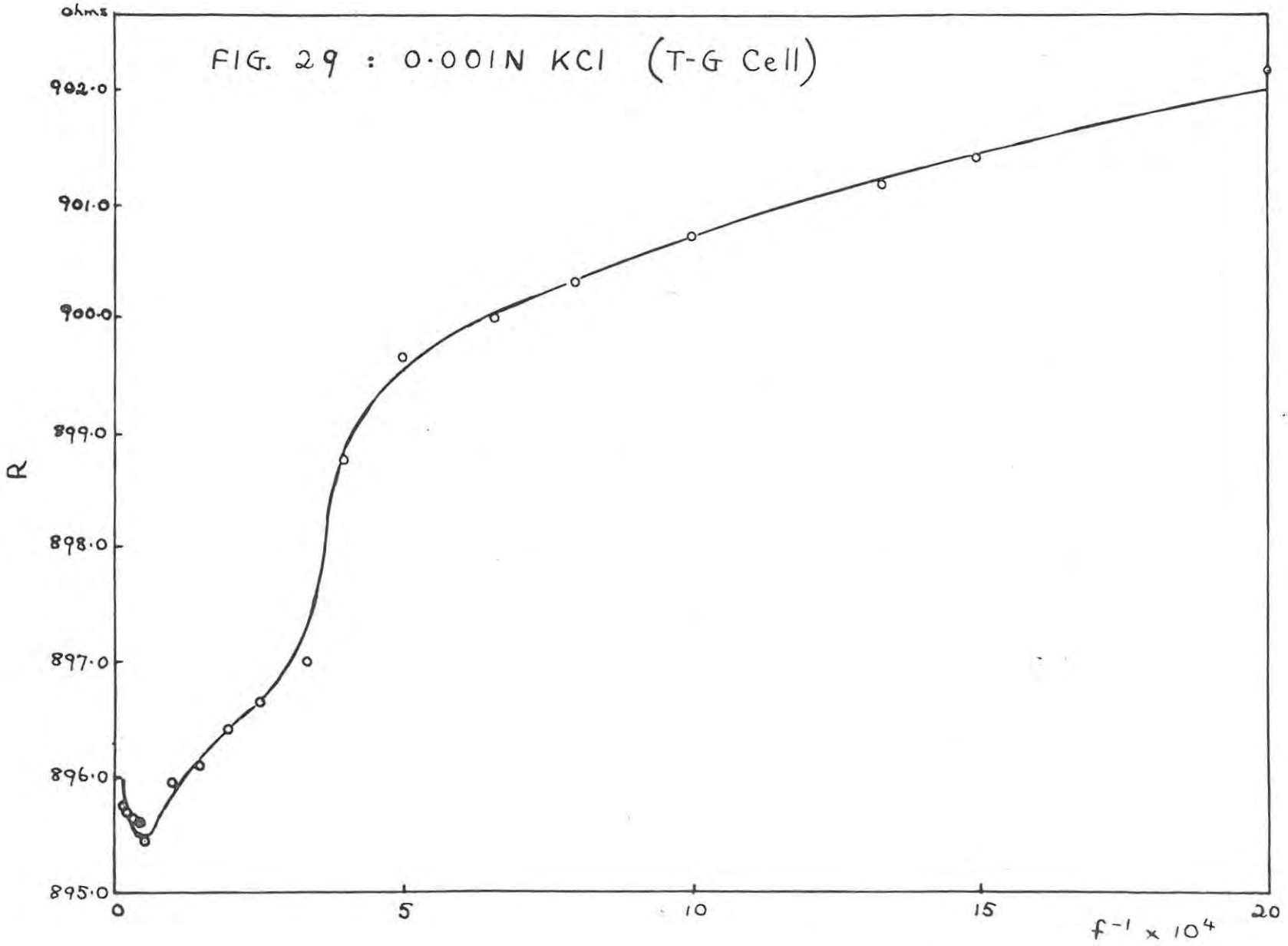
ohms
FIG. 29 : 0·001N KCl (T-G Cell)
902·0
901·0
900·0
899·0
898·0
897·0
896·0
895·0
R
0
5
10
15
20
f⁻¹ × 10⁴

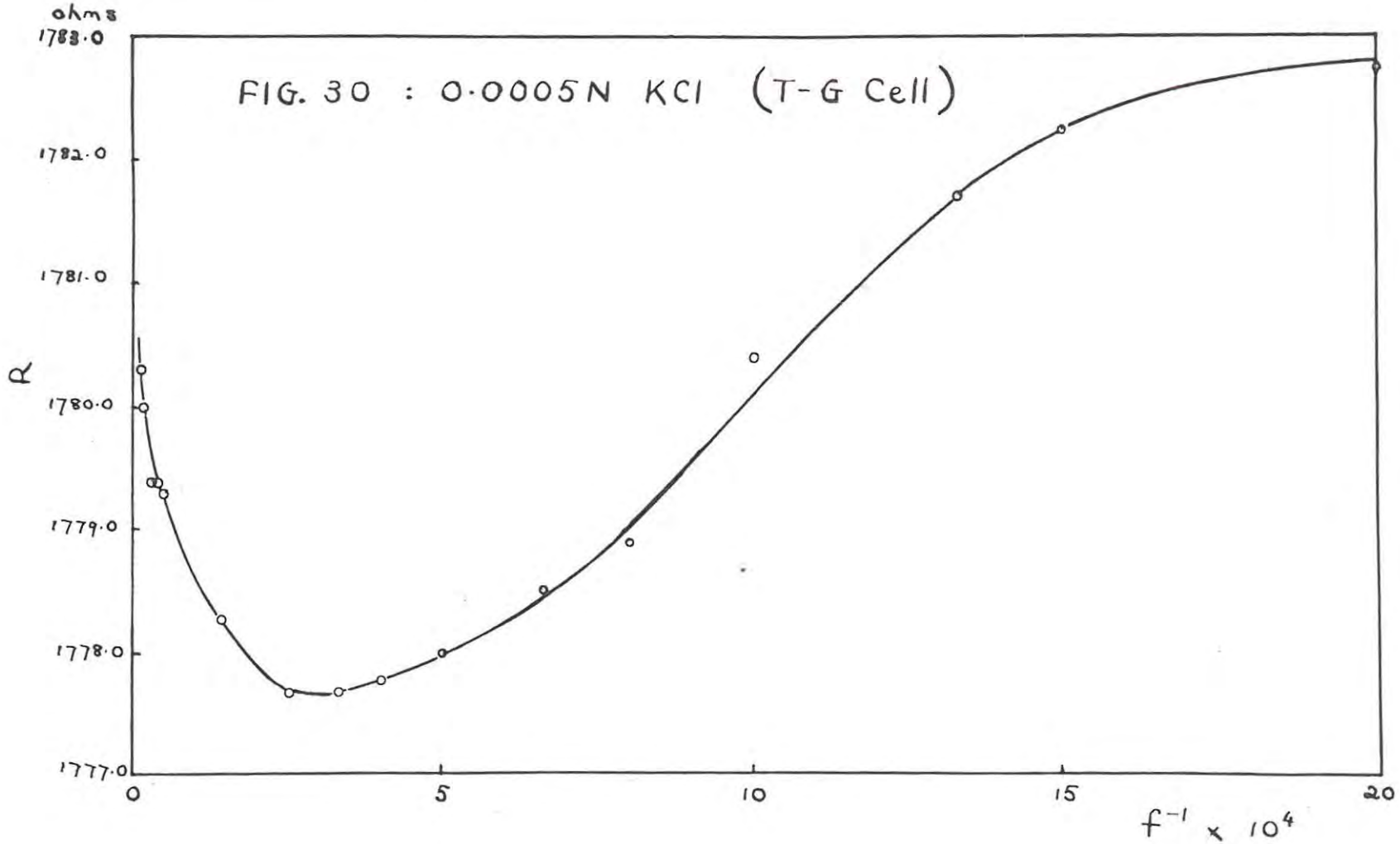

FIG. 30 : 0·0005N KCl (T-G Cell)

Q = 0.1320. This was determined from Fig. 27. (cf Q = 0.1319 which was the value obtained by other workers who used the same cell in conjunction with the Goddard-Faure bridge). Similarly from Fig. 31, the N-F cell was found to have Q = 0.1451.

2.53 R - X Diagrams

Since the Jones and Christian extrapolation procedure is seen to fail hopelessly when applied to readings taken over an extended frequency-range, the problem of determining the true resistance was approached by way of R - X diagrams. This is a method commonly used in the analysis of electrical networks. By plotting a graph showing the resistance and reactance at each frequency, the response of a network - containing resistive and reactive elements - to a.c. can be accurately demonstrated.

2.531 THEOREMS

The method may best be illustrated by considering the following theorems which deal with various combinations of resistances and capacitances:

1. SERIES R - C CIRCUIT {See Fig. 34 (a)}.

On applying the normal vector method, and in terms of a.c. notation, the complex impedance of the circuit is given by

$$Z = R_1 + 1/j\omega C_1$$

whence, the effective resistance and reactance are, respectively

$$R = R_1 \qquad \text{and} \qquad X = -1/\omega C_1$$

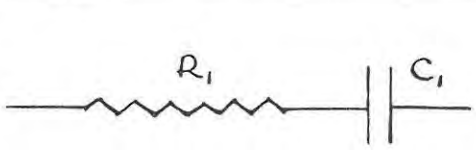

FIG. 34 (a)

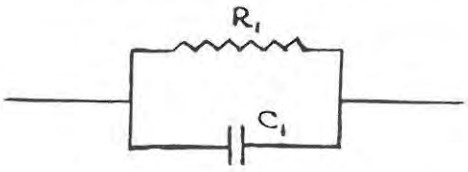

FIG. 35 (a)

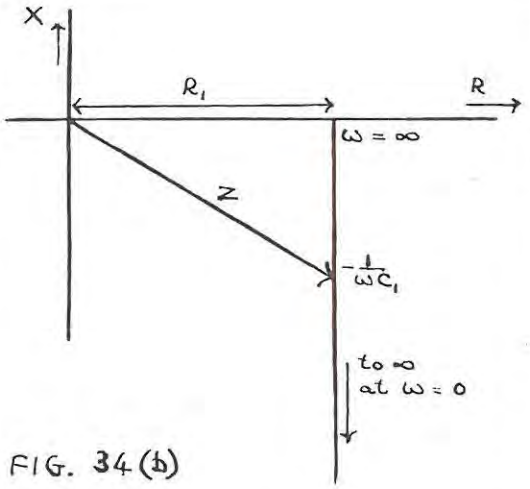

FIG. 34 (b)

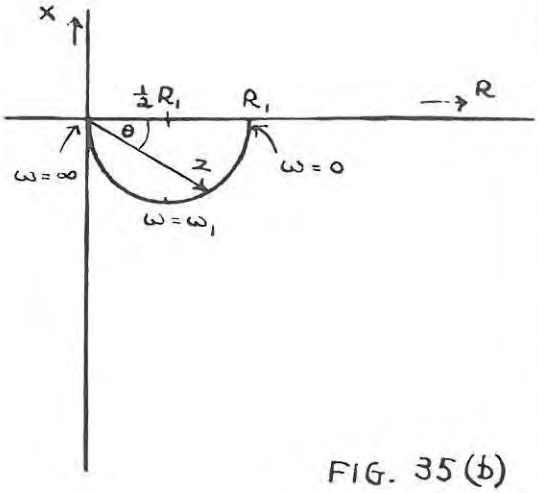

FIG. 35 (b)

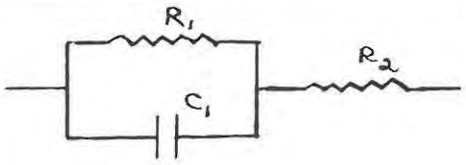

FIG. 36 (a)

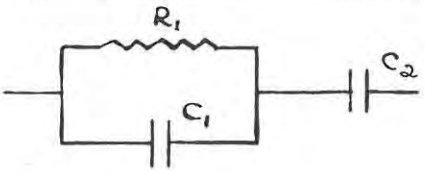

FIG. 37 (a)

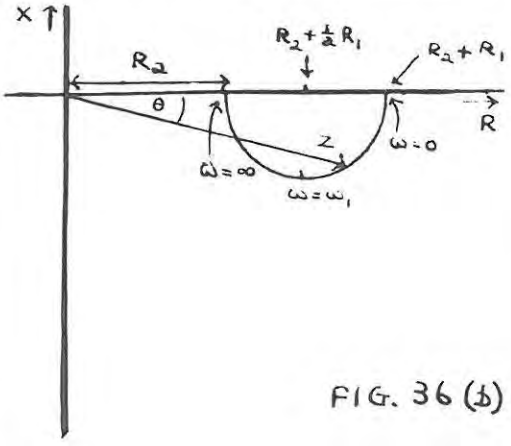

FIG. 36 (b)

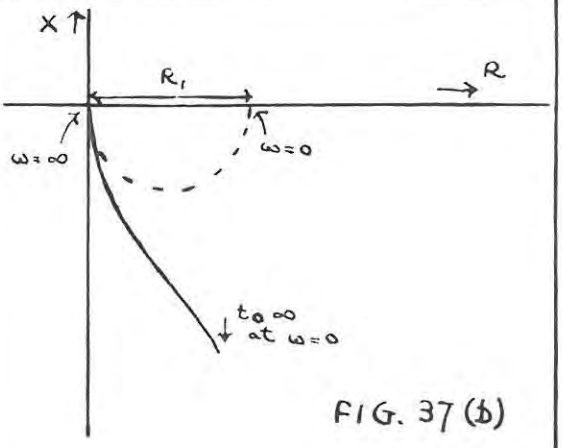

FIG. 37 (b)

If now, for this circuit, R and X values are plotted for various frequencies, a diagram such as that shown in Fig. 34 (b) will be obtained. The locus is seen to be a straight line parallel to the X axis, passing through $R = R_1$ and lying only on the negative side of the X axis. We may represent the impedance Z by the vector shown, the head of which lies on the locus at $-1/\omega C_1$.

It is obvious from the equations on p. 81 that,

as $\omega \to 0$, $X \to -\infty$ and $Z \to -\infty$

and as $\omega \to \infty$, $X \to 0$ and $Z \to R_1$

II PARALLEL R - C CIRCUIT {See Fig. 35 (a)}

The impedance of this circuit may be expressed in the form

$$\frac{1}{Z} = \frac{1 + j\omega C_1 R_1}{R_1}$$

On inverting this, and realising the denominator, we find

$$Z = \frac{R_1 - j\omega C_1 R_1^2}{1 + \omega^2 C_1^2 R_1^2}$$

$$= \frac{\frac{1}{C_1^2 R_1} - j\omega \frac{1}{C_1}}{\frac{1}{C_1^2 R_1^2} + \omega^2}$$, dividing through by $C_1^2 R_1^2$

Now let the relaxation frequency, ω_1, for this circuit be defined as

$$\omega_1 = 1/C_1 R_1$$

$$Z = \frac{\frac{1}{C_1}\omega_1 - j\omega\frac{1}{C_1}}{\omega_1^2 + \omega^2}$$

$$\text{i.e. } R + jX = \frac{1}{C_1}\cdot\frac{\omega_1}{\omega_1^2 + \omega^2} - j\frac{1}{C_1}\cdot\frac{\omega}{\omega_1^2 + \omega^2}$$

We have thus $$R = \frac{1}{C_1}\cdot\frac{\omega_1}{\omega_1^2 + \omega^2} \quad \ldots\ldots\ldots\ldots\ldots\ldots(1)$$

$$= \frac{1}{\omega_1 C_1}\cdot\frac{\omega_1^2}{\omega_1^2 + \omega^2}$$

$$= R_1\cdot\frac{\omega_1^2}{\omega_1^2 + \omega^2} \quad \ldots\ldots\ldots\ldots\ldots\ldots(2)$$

and $$X = \frac{1}{C_1}\cdot\frac{\omega}{\omega_1^2 + \omega^2} \quad \ldots\ldots\ldots\ldots\ldots\ldots(3)$$

From equations (1) and (3), we find,

$$X = \frac{\omega}{\omega_1}\cdot R \quad \ldots\ldots\ldots\ldots\ldots\ldots(4)$$

Hence $$^2 = \omega_1^2\cdot\frac{X^2}{R^2}$$

and, on substituting for ω^2 in equation (2), we see

$$R = R_1\frac{\omega_1^2}{\omega_1^2 + \omega_1^2 X^2/R^2}$$

$$= R_1\frac{1}{1 + X^2/R^2}$$

$$= R_1\frac{R^2}{R^2 + X^2}$$

$$\text{i.e.} \qquad 1 = \frac{R_1 R}{R^2 + X^2}$$

$$\text{or} \qquad R^2 + X^2 - R_1 R = 0 \qquad \ldots\ldots\ldots\ldots\ldots\ldots(5)$$

This is the equation of a circle, with origin on the circumference and centre on the R axis at the point $R = \frac{1}{2}R_1$.
See Fig. 35 (b)

The phase angle θ is given by

$$\theta = \tan^{-1}\frac{X}{R} = \tan^{-1}-\frac{\omega}{\omega_1}$$

Note: Inspection of equation (3) shows that if $\omega << \omega_1$,

$$X = -\frac{1}{C_1}\cdot\frac{\omega}{\omega_1}$$

i.e. $X \propto \omega$

III PARALLEL R - C and SERIES R {See Fig. 36 (a)}

For the total impedance of this circuit, we may write

$$Z = R_2 + R_1\frac{\omega_1^2}{\omega_1^2 + \omega^2} - j\frac{1}{C_1}\cdot\frac{\omega}{\omega_1^2 + \omega^2}$$

using equations (2) and (3).

The resistive and reactive components are, respectively

$$R = R_2 + R_1\frac{\omega_1^2}{\omega_1^2 + \omega^2} \qquad \ldots\ldots\ldots\ldots\ldots\ldots(6)$$

$$\text{and} \quad X = -\frac{1}{C_1}\cdot\frac{\omega}{\omega_1^2 + \omega^2} \qquad \ldots\ldots\ldots\ldots\ldots\ldots(7)$$

As it can be seen from Fig. 36 (b), the effect is to add R_2 to all previous R values, while leaving X unchanged.

IV PARALLEL R - C and SERIES C {See Fig. 37(a)}

The total impedance of this circuit is given by

$$Z = R_1 \frac{\omega_1^2}{\omega_1^2 + \omega^2} - j \frac{1}{C_1} \cdot \frac{\omega}{\omega_1^2 + \omega^2} - j \frac{1}{\omega C_2}$$

whence, the resistive and reactive components are seen to be

$$R = R_1 \frac{\omega_1^2}{\omega_1^2 + \omega^2} \qquad \ldots\ldots\ldots\ldots\ldots\ldots\ldots\ldots (8)$$

and $$X = -\left[\frac{1}{C_1} \cdot \frac{\omega}{\omega_1^2 + \omega^2} + \frac{1}{\omega C_2}\right] \ldots\ldots\ldots\ldots\ldots\ldots\ldots\ldots (9)$$

Thus we see that, while R is left unchanged, the effect is to add $\frac{1}{\omega C_2}$ values to all previous X values. Also as $\omega \to 0$, $X \to -\infty$.

This is illustrated in Fig. 37 (b)

V SERIES R - C and PARALLEL R {See Fig. 38 (a)}

The expression for the total impedance of this circuit is

$$\frac{1}{Z} = \frac{1}{R_2} + \frac{1}{R_1 + 1/j\omega C_1}$$

$$= \frac{1 + j\omega C_1 (R_1 + R_2)}{R_2 (1 + j\omega C_1 R_1)}$$

Inverting this, and realising the denominator gives

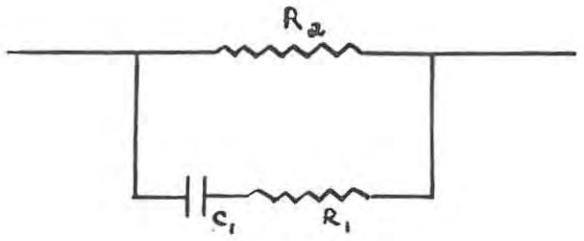

FIG. 38 (a)

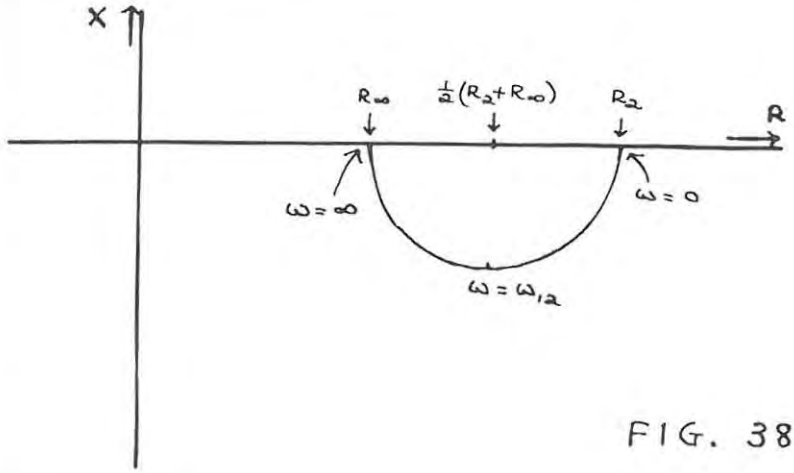

FIG. 38 (b)

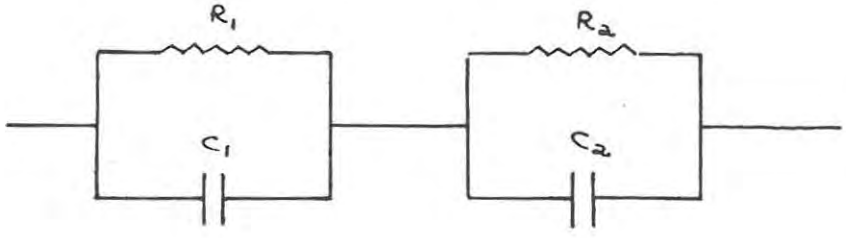

FIG. 39 (a)

$$Z = R_2 \frac{1 + \omega^2 C_1^2 R_1^2 (R_1 + R_2) - j\omega C_1 R_2}{1 + \omega^2 C_1^2 (R_1 + R_2)^2}$$

Let us write for the relaxation frequency

$$\omega_{12} = \frac{1}{C_1(R_1 + R_2)}$$

Then $Z = R + jX$

$$= R_2 \cdot \frac{\omega_{12}^2 + \omega^2 \frac{R_1}{R_1 + R_2} - j\omega \frac{R_2}{C_1(R_1 + R_2)^2}}{\omega_{12}^2 + \omega^2}$$

Hence, we find

$$R = R_2 \cdot \frac{\omega_{12}^2 + \omega^2 \frac{R_1}{R_1 + R_2}}{\omega_{12}^2 + \omega^2} \quad \ldots\ldots\ldots\ldots\ldots\ldots(10)$$

and $$X = R_2 \cdot \frac{\omega\omega_{12} \frac{R_2}{R_1 + R_2}}{\omega_{12}^2 + \omega^2} \quad \ldots\ldots\ldots\ldots\ldots\ldots(11)$$

Now at $\omega = \infty$, $X = 0$ and $R = R_\infty = \frac{R_1 R_2}{R_1 + R_2}$

Then $$R = R_2 \cdot \frac{\omega_{12}^2 + \omega^2 \frac{R_\infty}{R}}{\omega_{12}^2 + \omega^2} \quad \ldots\ldots\ldots\ldots\ldots\ldots(12)$$

and $$X = -R_2 \cdot \frac{\omega\omega_{12} \cdot \frac{R_\infty}{R_1}}{\omega_{12}^2 + \omega^2} \quad \ldots\ldots\ldots\ldots\ldots\ldots(13)$$

From equation (12), we see that

$$R(\omega_{12}^2 + \omega^2) = R_2(\omega_{12}^2 + \omega^2 \frac{R_\infty}{R_2})$$

whence $$\omega^2 = \omega_{12}^2 \cdot \frac{R_2 - R}{R - R_\infty}$$

Now on substituting for ω^2 in equation (13) and simplifying, we find that

$$X = -\{(R_2 - R)(R - R_\infty)\}^{\frac{1}{2}}$$

$$X^2 = -R^2 + R(R_2 + R_\infty) - R_2R_\infty$$

or $$R^2 + X^2 - (R_2 + R_\infty)R + R_2R_\infty = 0 \quad \ldots\ldots\ldots(14)$$

This is the equation of a circle with the centre at $\frac{1}{2}(R_2 + R_\infty)$ and radius $\frac{1}{2}(R_2 - R_\infty)$. See Fig. 38 (b).

The minimum in X may be found from equation (13) to occur at

$$\frac{dX}{d\omega} = -R_2 \cdot \frac{\omega_{12} \frac{R_\infty}{R_1}}{\omega_{12}^2 + \omega^2} + R_2 \cdot \frac{2\omega^2\omega_{12} \frac{R_\infty}{R_1}}{(\omega_{12}^2 + \omega^2)^2} = 0$$

i.e. at $\omega = \omega_{12}$

VI SERIES COMBINATION OF TWO PARALLEL R - C CIRCUITS

{See Fig. 39 (a)}

Using equations (2) and (3), we find that the net effective resistance and reactance of this combination

are respectively,

$$R = R' + R'' = R_1 \frac{\omega_1^2}{\omega_1^2 + \omega^2} + R_2 \frac{\omega_2^2}{\omega_2^2 + \omega^2} \quad \ldots\ldots(15)$$

$$X = X' + X'' = -\frac{1}{C_1} \frac{\omega}{\omega_1^2 + \omega^2} - \frac{1}{C_2} \frac{\omega}{\omega_2^2 + \omega^2} \quad \ldots\ldots(16)$$

Note:

(a) Suppose that $R_1 > R_2$, each parallel R-C circuit may be represented graphically as shown in Fig. 39 (b) and Fig. 39 (c) with vectors Z_1 and Z_2 respectively. The series combination effect of these is shown in Fig. 39 (d) where Z is the resultant vector.

(b) The resultant locus will depend on the values of ω_1 and ω_2.

If $\omega_1 >> \omega_2$, the vector Z_1 has almost got round semicircle 2 before it starts to move round semicircle 1. See Fig. 39 (e).

If $\omega_1 > \omega_2$, but $\omega_1 \not>> \omega_2$, the R-X diagram will be as shown in Fig. 39 (f).

If $\omega_1 = \omega_2$, we get a semicircle, with centre at $\frac{1}{2}(R_1 + R_2)$ and radius $\frac{1}{2}(R_1 + R_2)$, since

$$R = 2R_1 \frac{\omega_1^2}{\omega_1^2 + \omega^2}$$

$$X = -\frac{2}{C_1} \frac{\omega}{\omega_1^2 + \omega^2}$$

See Fig. 39 (g).

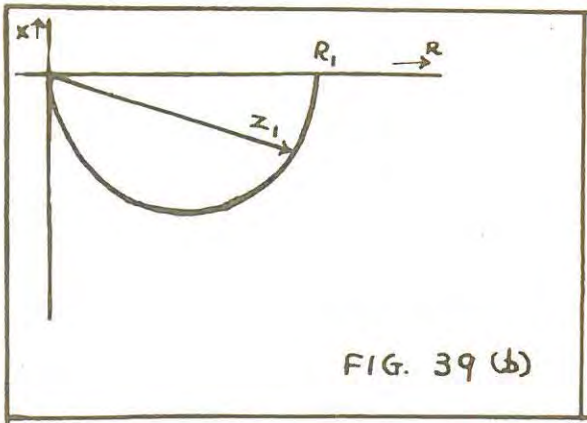

FIG. 39 (b)

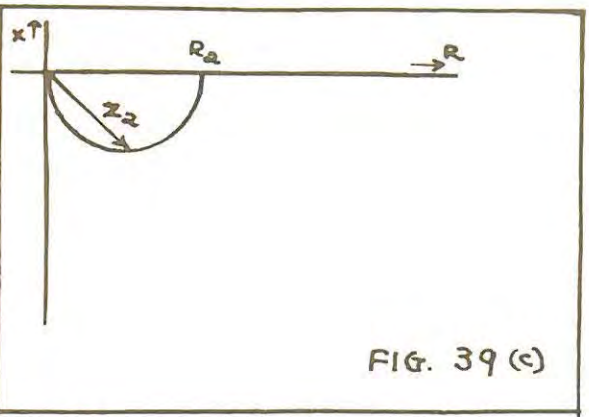

FIG. 39 (c)

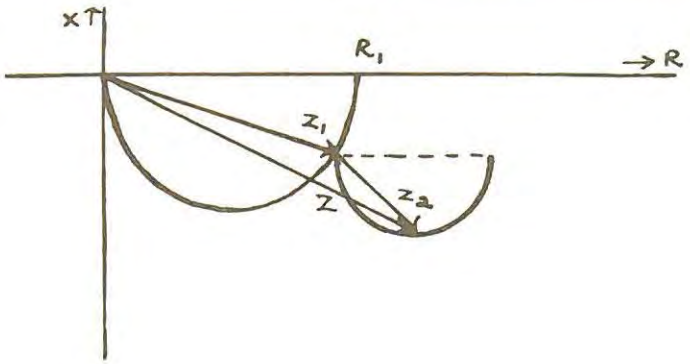

FIG. 39 (d)

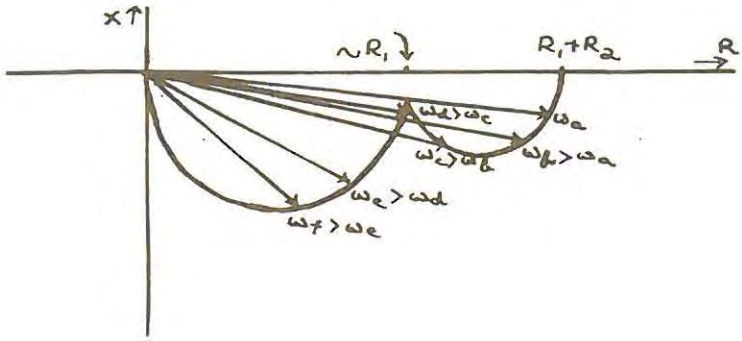

FIG. 39 (e)

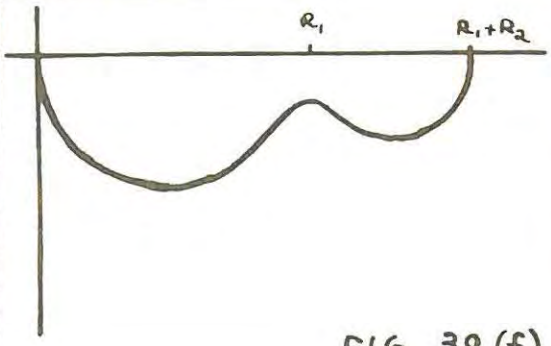

FIG. 39 (f)

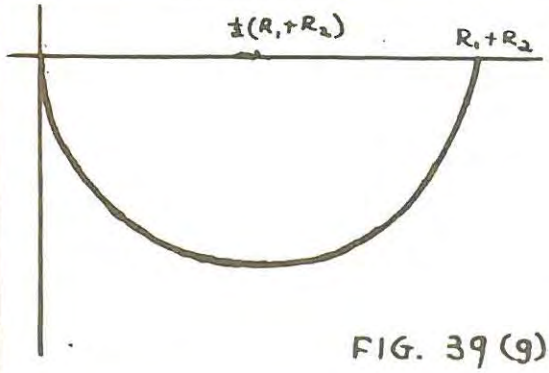

FIG. 39 (g)

2.532 APPLICATION TO EXPERIMENTAL VALUES OF R and X

In the course of investigating the response of a conductance cell to long pulses, Allison (94) proposed a number of various R - C networks which, it was hoped, would simulate cell behaviour. The present approach can be recognised as an alternative method for elucidating cell behaviour, since R - X diagrams were drawn for the experimental readings and correlated with the different types of R - C combinations just considered. It may be noted that, since the measuring arm of the bridge is a parallel R - C circuit, the effective resistance and reactance values - used in plotting the diagrams - were calculated from the following well-known relationships:

$$R = \frac{R'}{1 + \omega^2 C^2 R'^2}$$

$$X = -\frac{\omega C R'^2}{1 + \omega^2 C^2 R'^2}$$

where R' is the observed resistance corrected for bridge calibration and for bridge and cell lead resistances; C is the observed capacitance corrected for capacitance in the cell-arm of the bridge.

On carefully scrutinising the diagrams (see Figs. 40 - 45), the following interesting features became obvious:

(a) A minimum is found to occur in each case.

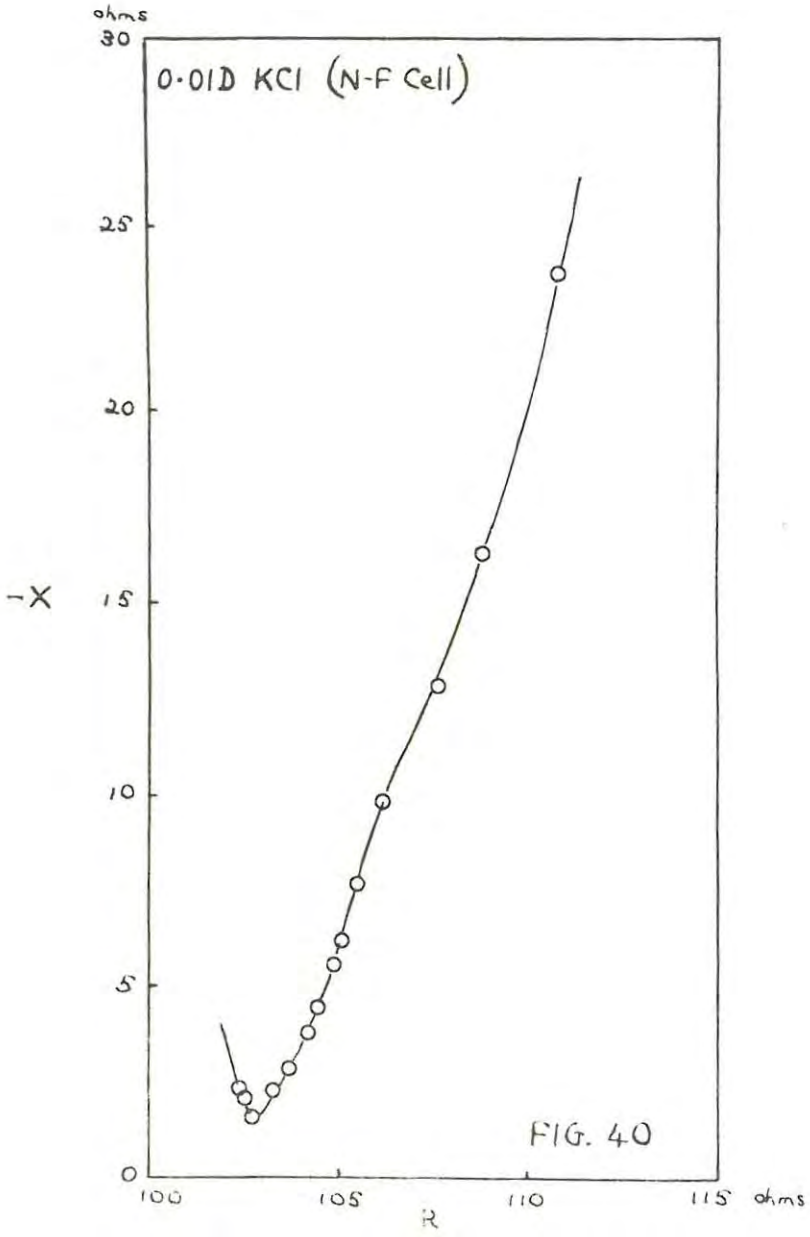
ohms
30
0·01D KCl (N-F Cell)
25
20
15
10
5
0
-X
100
105
110
115 ohms
R

FIG. 40

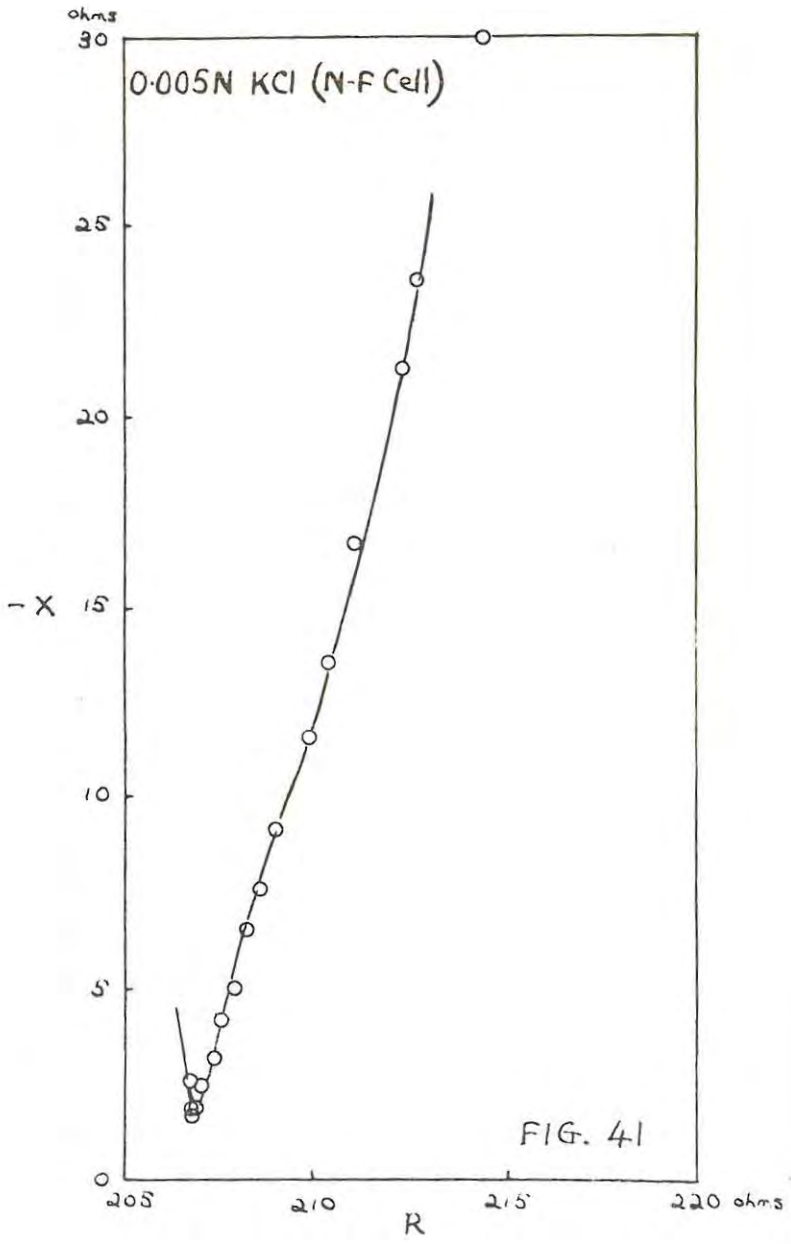
ohms
30
0·005N KCl (N-F Cell)
25
20
15
10
5
0
-X
205
210
215
220 ohms
R

FIG. 41

(b) Each diagram is seen to consist of two 'branches'; but this is not very clear in Figs. 44 and 46 (diagrams depicting the behaviour of 0.005N and 0.0005N solutions in the T-G cell), where a peculiar type of curve is obtained at the high frequencies - which seems to confirm the observations made during the course of preliminary measurements.

(In order to distinguish between the branches, the terms 'high relaxation frequency branch' and 'low relaxation frequency branch' are introduced).

(c) For measurements made in the N-F cell, the minimum appears to be in the region of 7 kc/s in the case of the 0.0005N solution and hence, there is much more of the high relaxation frequency branch here, than there is for the approx. 0.01D and 0.005N solutions where the minimum occurs in the region of 30 to 40 kc/s.

(d) A striking resemblance is observed between the low relaxation frequency branch and Fig. 37 (b), whilst the high relaxation frequency branch is strongly suggestive of Fig. 35 (b). The R-X diagram illustrating the behaviour of the 0.0005N solution in the N-F cell (i.e. Fig. 42) is a clear demonstration of these similarities.

2.54 EQUIVALENT CIRCUITS

In view of the foregoing observations, it was felt that it would be justifiable to assume that , for all the solutions investigated in the N-F cell and also for the approx. 0.01D

solution - and to a lesser extent - the 0.001N solution in the T-G cell, the experimental curves represent the combined effect of two networks, viz: a parallel R-C and a parallel R-C with series C. Thus, the circuit shown in Fig. 47 was tentatively proposed as a basis for explaining the results obtained.

2.541 METHODS FOR DEDUCING NEAREST TYPE OF EQUIVALENT CIRCUIT

Initial attempts in this direction were made by the method of trial and error, but this proved to be too tedious. Nevertheless, much useful information was gained as regards the relative magnitudes of the relaxation frequencies. Thus, C_1 (in Fig. 47) was found to be of the order of picofarads, whilst C_2 and C_3 were of the order of microfarads - indicating that the high and low relaxation frequencies were of the order of megacycles and kilocycles, respectively.

Subsequently, a more exact method was developed by analysing the circuit (Fig. 47) along the following lines:

Consider measurements carried out at frequencies high compared with the low relaxation frequency i.e. $\omega >> \omega_2$. Equations (15) and (16) - see p. 88 - show that, under these conditions, the effects of the low relaxation frequency branch become negligible. As a result, the circuit is reduced to the parallel R_1-C_1 combination, whose effective resistance is given by

$$R = \frac{R_1}{1 + \omega^2 C_1^2 R_1^2} \quad \text{.....(17)}$$

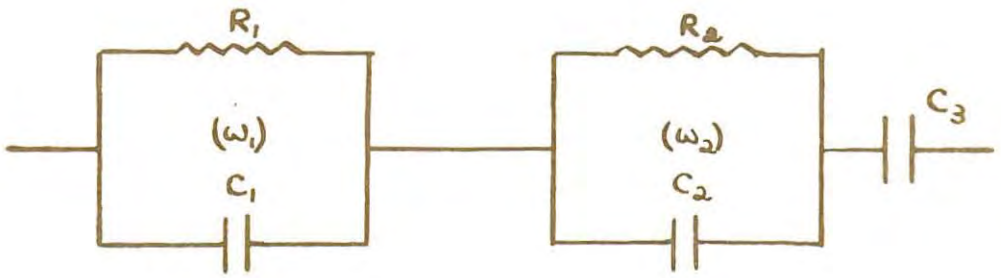

FIG. 47 PROPOSED EQUIVALENT CIRCUIT

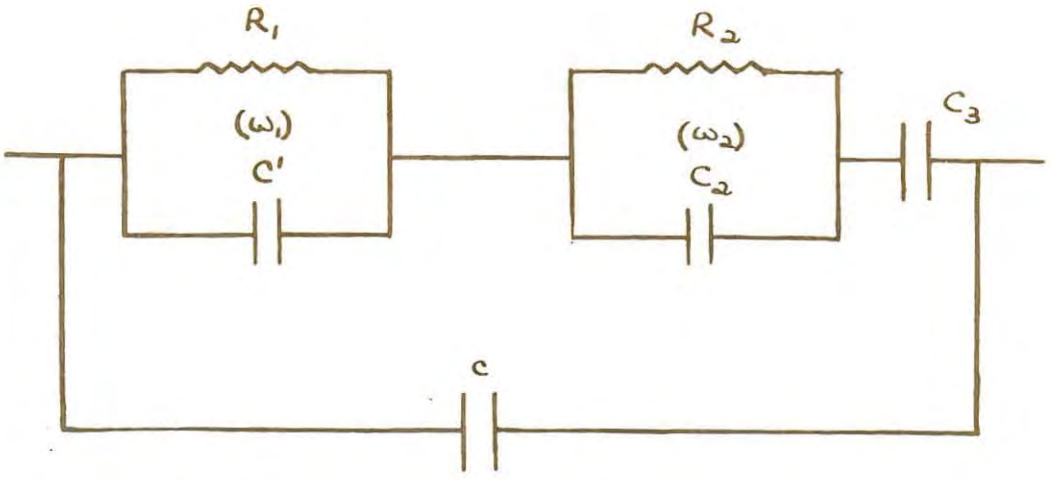

FIG. 48 EQUIVALENT CIRCUIT (modified)

Writing equation (17) in its reciprocal form, we find

$$1/R = 1/R_1 + \omega^2 C_1^2 R_1 \quad \ldots\ldots\ldots\ldots (18)$$

Now, this is the equation of a straight line with slope $C_1^2 R_1$ and intercept $1/R_1$. Hence, by plotting reciprocal values of the observed resistances against corresponding ω^2 values, R_1 can be computed from the intercept and C_1 from the slope.

For measurements at low frequencies i.e. when $\omega \ll \omega_1$ but $\omega \not\ll \omega_2$, the reactance due to the high relaxation frequency branch is negligible i.e. the effect of C_1 may be ignored. The equivalent circuit, therefore, becomes effectively R_1 in series with parallel R_2-C_2 with series C_3. The complex of this network may be shown to be

$$Z = R_1 + \frac{R_2}{1 + \omega^2 C_2^2 R_2^2} - j\left[\frac{\omega C_2 R_2^2}{1 + \omega^2 C_2^2 R_2^2} + \frac{1}{\omega C_3}\right]$$

whence, the resistive and reactive components are respectively,

$$R = R_1 + \frac{R_2}{1 + \omega^2 C_2^2 R_2^2} \quad \ldots\ldots\ldots\ldots\ldots\ldots (19)$$

$$X = -\left[\frac{\omega C_2 R_2^2}{1 + \omega^2 C_2^2 R_2^2} + \frac{1}{\omega C_3}\right] \ldots\ldots\ldots\ldots\ldots\ldots (20)$$

The reciprocal of equation (19) may be written in the form

$$\frac{1}{R - R_1} = \frac{1}{R_2} + \omega^2 C_2^2 R_2 \quad \ldots\ldots\ldots\ldots (21)$$

which is the equation of a straight line with slope $C_2^2 R_2$ and intercept $1/R_2$. Hence, C_2 and R_2 can be determined from the graph, drawn by plotting reciprocal values of the difference between R (the observed resistance) and R_1 (whose value has already been determined) versus the corresponding ω^2 values.

It will be seen that C_3 can be calculated from equation (20) provided that a value for X (the observed reactance) is chosen at a relatively low frequency, say, 1 kc/s.

2.542 PROPOSED CIRCUITS

Applying the methods outlined above, the circuits suggested in the following pages were derived for all the solutions, except the 0.005N, 0.001N and 0.0005N solutions measured in the T-G cell. No reasonable explanation - in terms of an equivalent circuit - could be found to account for the behaviour of the latter solutions at the high frequencies; some resemblance was, however, noted between these curves and those for the other solutions - there appears to be a very definite probability that the curves have low relaxation frequency branches, which can also be represented by a parallel R-C with series C network.

Attention is drawn to a slight modification made to the equivalent circuit originally proposed. In order to include the inter-electrode capacitance of the conductance

cell, Fig. 47 was changed to the form shown in Fig. 48. Here c represents the inter-electrode capacitance, which is significant only at high frequencies i.e. when the high relaxation frequency branch becomes operative. It should be remembered, however, that this electrostatic capacitance constitutes only part of the shunting capacitance in the high relaxation frequency branch, and that it has a constant value as long as measurements are carried out with the same cell. We may write, therefore

$$C' + c = C_1$$

According to a theorem derived by A. Faure (25), the inter-electrode capacitance is related to the cell constant by the formula:

$$c = \frac{k}{4\pi Q}$$

where k is the dielectric constant of the solvent and c is in absolute e.s.u.

Using this equation, the respective values of c for the N-F and T-G cells were found to be 49 pF and 53 pF.

Note:

In the Tables that follow, the behaviour of the proposed circuit over the range of frequencies, at which measurements were effected, is compared with the experimental readings in order to show how closely the cell containing the solution in question is simulated.

SOLUTIONS INVESTIGATED IN THE N-F CELL

0.0005N KCl

The results obtained for this solution were subjected to analysis first, since the R-X diagram drawn was found to show both branches clearly. Fig. 49 shows the graph used for determining R_1 and C_1 and Fig. 50 that for R_2 and C_2.

The equivalent circuit thus derived is given in Fig. 51.

T A B L E 1

f kc/s	RESISTANCE ohms		REACTANCE ohms	
	Calculated	Observed	Calculated	Observed
0.5	2025.0	2024.9	47.152	45.712
1.0	2019.8	2019.8	35.301	26.125
1.5	2017.8	2017.8	21.505	21.491
2.0	2016.9	2017.1	18.325	19.073
3.0	2016.2	2016.4	16.057	17.091
5.0	2015.8	2015.9	16.778	16.980
10.0	2015.5	2015.3	25.055	24.755
20.0	2014.6	2014.4	45.816	43.873
25.0	2014.1	2014.0	56.711	51.638
50.0	2009.5	2009.3	111.36	103.00
75.0	2002.0	2001.6	165.91	153.83

High relaxation frequency: 5.703×10^6 c/s (ω_1)

Low relaxation frequency: 3.679×10^3 c/s (ω_2)

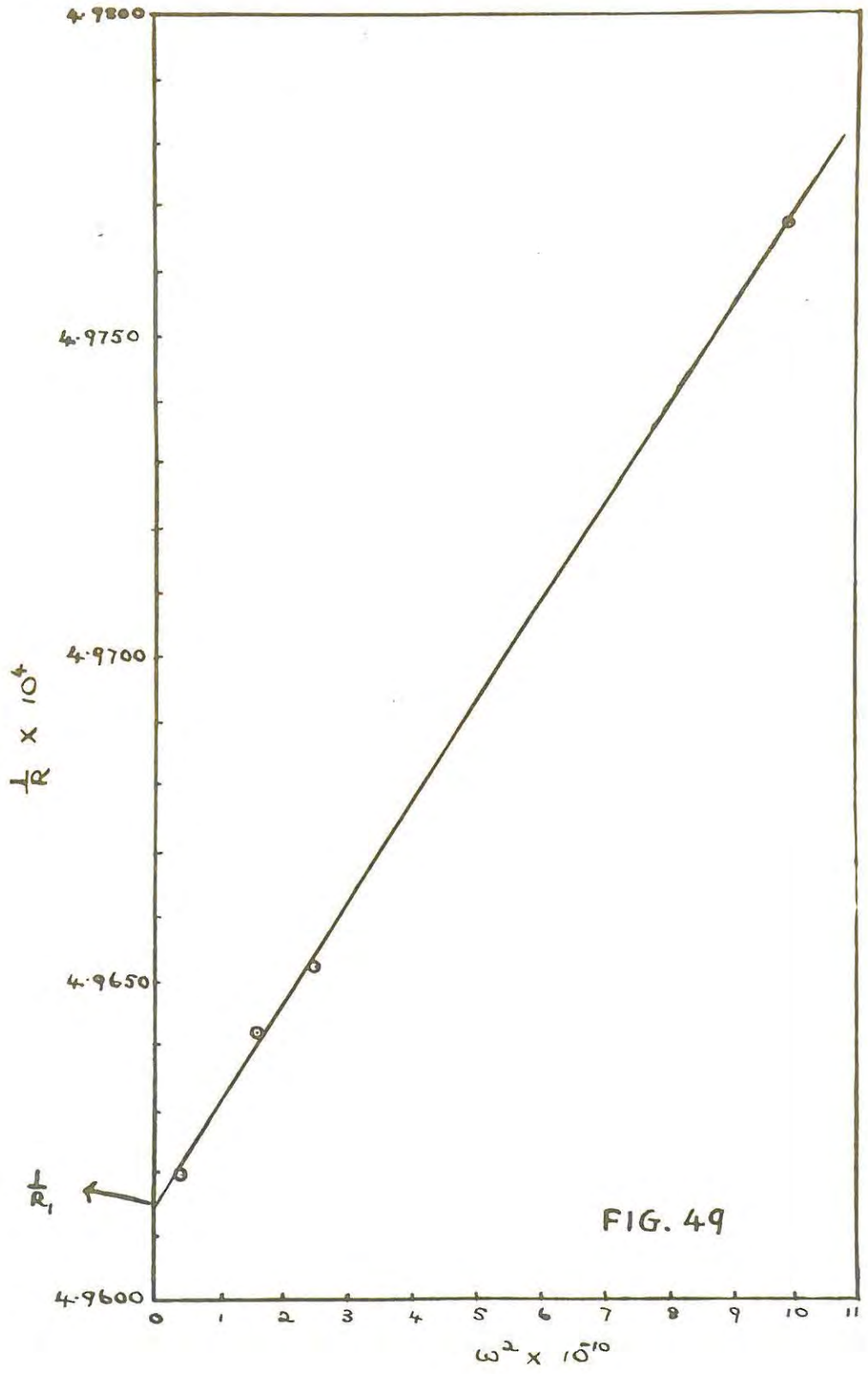
4·9800
4·9750
4·9700
4·9650
4·9600
$\frac{1}{R} \times 10^4$
$\frac{1}{R_1}$
0
1
2
3
4
5
6
7
8
9
10
11
$\omega^2 \times 10^{10}$

FIG. 49

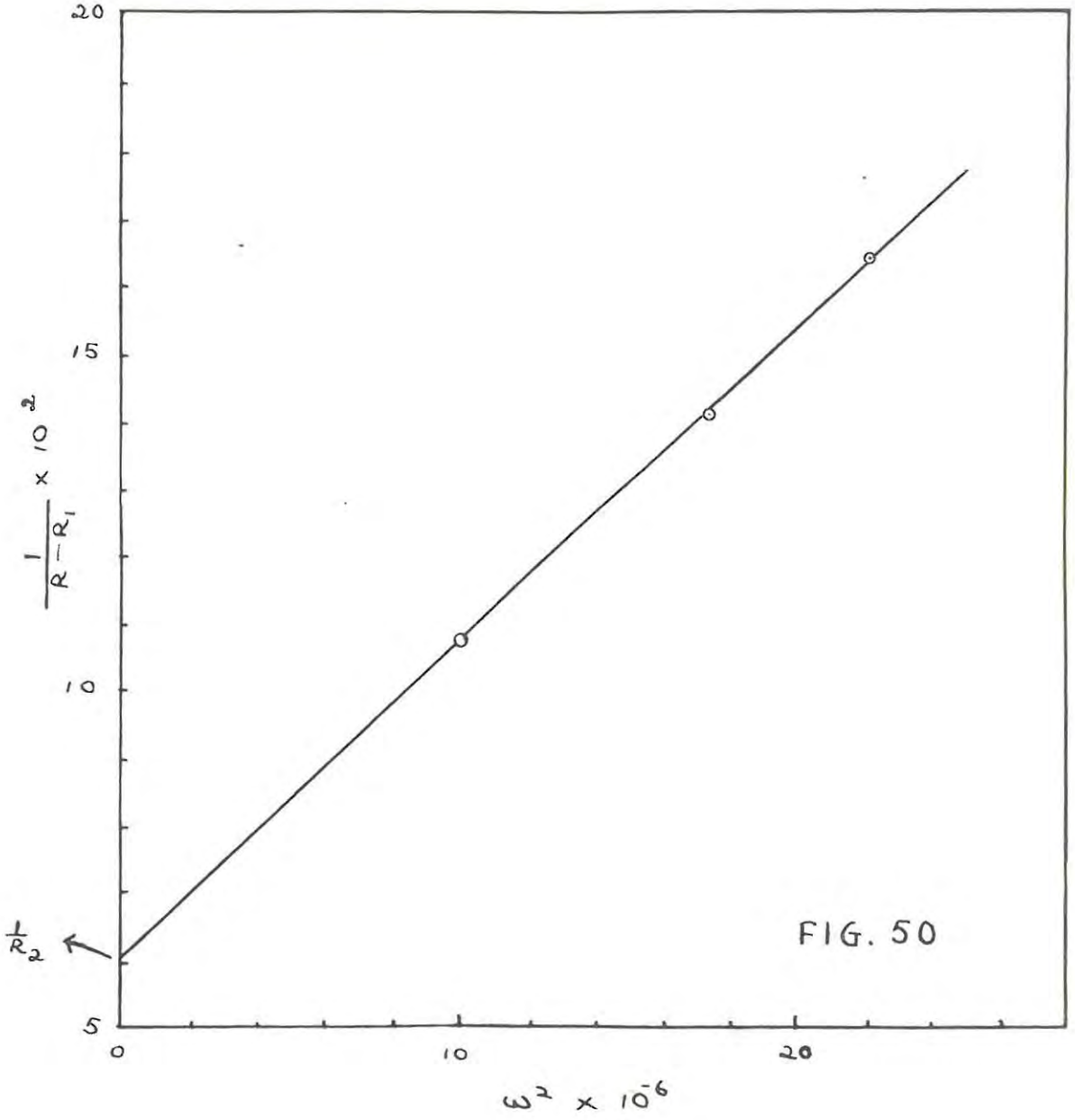

FIG. 50

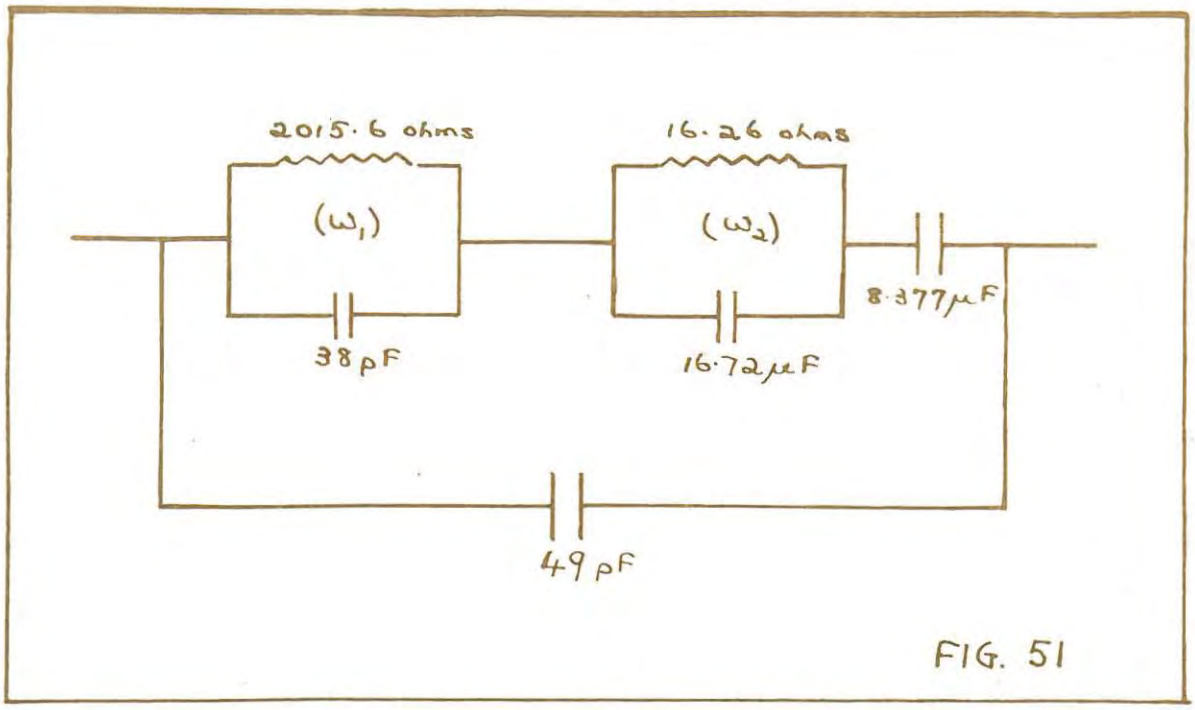
2015.6 ohms
16.26 ohms
(ω1)
(ω2)
38 pF
16.72 μF
8.377 μF
49 pF

FIG. 51

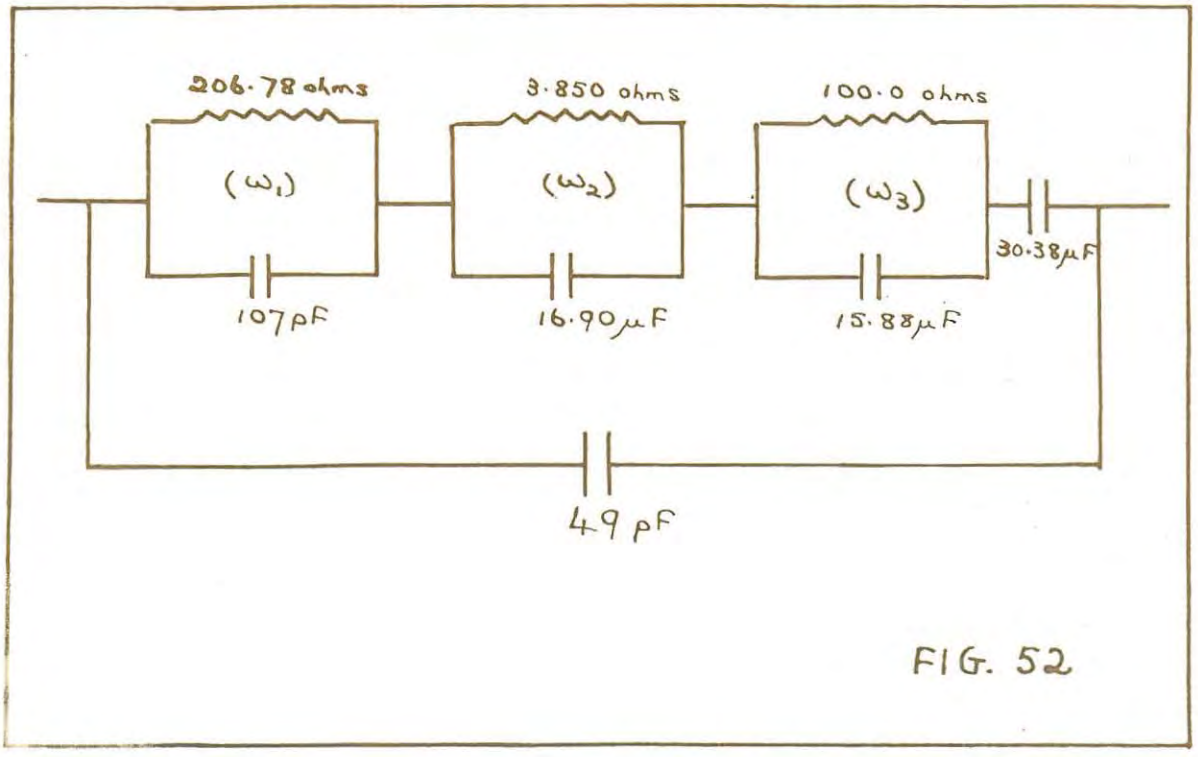
206.78 ohms
3.850 ohms
100.0 ohms
(ω1)
(ω2)
(ω3)
107 pF
16.90 μF
15.88 μF
30.38 μF
49 pF

FIG. 52

0.005N KCl

Fig. 52 shows the equivalent circuit derived for this solution. The network may now be seen to consist of three parallel R-C combinations. With the additional R_3-C_3 circuit, a better fit was obtained over the low frequencies.

T A B L E 2

f kc/s	RESISTANCE ohms		REACTANCE ohms	
	Calculated	Observed	Calculated	Observed
0.5	214.34	214.41	30.53	30.04
1.0	211.07	211.08	16.55	16.70
3.0	208.43	208.23	7.11	6.57
5.0	207.56	207.63	4.78	4.23
10.0	207.01	207.00	2.82	2.45
25.0	206.82	206.83	2.01	1.73
50.0	206.77	206.76	2.59	2.57
75.0	206.74	206.74	3.47	2.48(?)

High relaxation frequency: $\omega_1 = 3.100 \times 10^7$ c/s

Low relaxation frequencies: $\omega_2 = 1.537 \times 10^4$ c/s

$\omega_3 = 6.298 \times 10^2$ c/s

0.01D KCl

The equivalent circuit derived for this solution may be seen in Fig. 53. Here too, the addition of a further R-C network improved the behaviour of the circuit at the low frequencies.

T A B L E 3

f kc/s	RESISTANCE ohms		REACTANCE ohms	
	Calculated	Observed	Calculated	Observed
0.5	110.89	110.80	20.51	23.72
1.0	107.65	107.65	12.43	12.95
3.0	105.11	104.85	5.62	5.63
5.0	104.33	104.17	4.28	3.75
10.0	103.32	103.29	3.11	2.34
25.0	102.67	102.66	2.54	1.62
50.0	102.49	102.45	3.32	2.07
75.0	102.38	102.36	4.47	2.41

High relaxation frequency : $\omega_1 = 1.190 \times 10^7$ c/s

Low relaxation frequencies: $\omega_2 = 3.895 \times 10^4$ c/s

$\omega_3 = 3.554 \times 10^3$ c/s

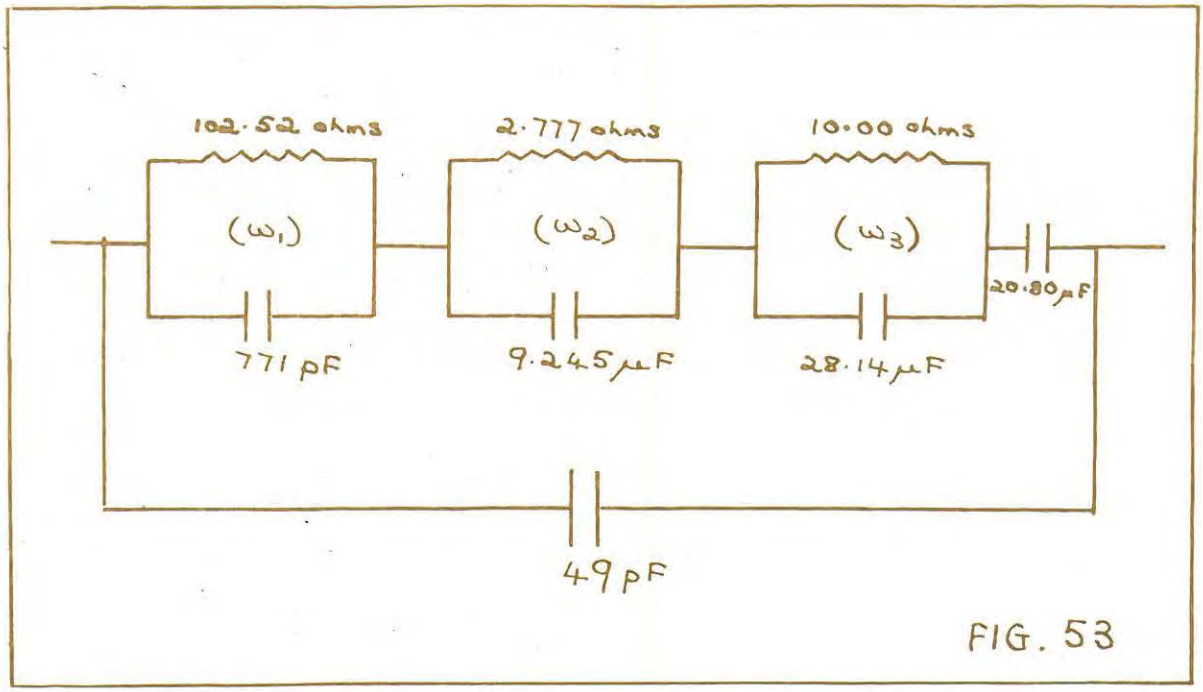
102.52 ohms
2.777 ohms
10.00 ohms
(ω_1)
(ω_2)
(ω_3)
20.80μF
771 pF
9.245μF
28.14μF
49 pF

FIG. 53

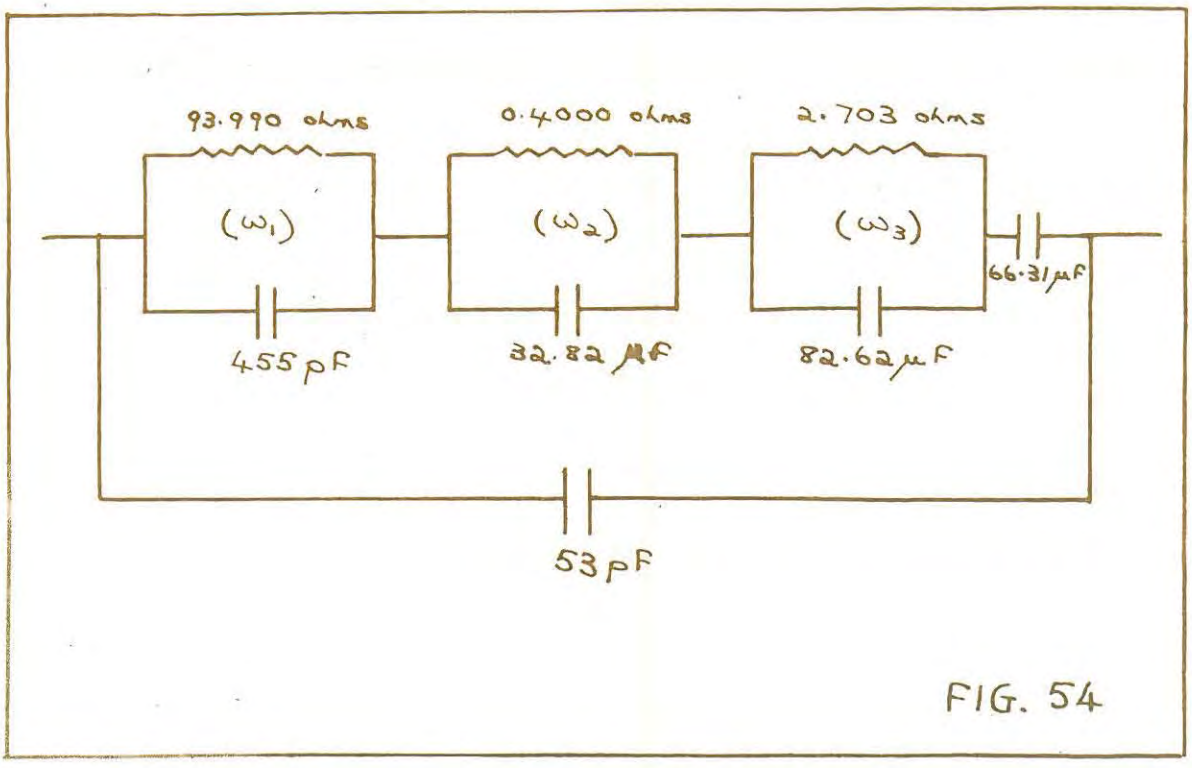
93.990 ohms
0.4000 ohms
2.703 ohms
(ω_1)
(ω_2)
(ω_3)
66.31μF
455 pF
32.82 μF
82.62μF
53 pF

FIG. 54

SOLUTION MEASURED IN THE T-G CELL

0.01D KCl

The equivalent circuit derived for this solution is shown in Fig. 54.

T A B L E 4

f kc/s	RESISTANCE ohms		REACTANCE ohms	
	Calculated	Observed	Calculated	Observed
0.5	96.200	96.474	6.09	5.87
1.0	95.298	95.236	3.74	3.73
3.0	94.511	94.504	1.59	1.51
5.0	94.386	94.322	1.14	1.05
10.0	94.242	94.232	0.910	0.697
20.0	94.096	94.085	0.957	0.699
50.0	93.991	93.968	1.59	1.28
75.0	93.952	93.940	2.24	1.83

High relaxation frequency : $\omega_1 = 2.094 \times 10^7$ c/s

Low relaxation frequencies: $\omega_2 = 7.615 \times 10^4$ c/s

$\omega_3 = 4.477 \times 10^3$ c/s

Note:

(a) Despite the addition of a further R-C network, there is still a relatively large discrepancy between the calculated and observed resistance at 500 c/s.

(b) Tables 1 - 4 show that the deviation of the observed reactances from the calculated values is greater than in it is in the case of the resistances, since the Wheatstone Bridge is primarily designed to take accurate readings of resistance.

2.6 CONCLUSION

From the foregoing discussion, we may infer that:

(a) Conductance cells of the N-F type - and to a degree those of the T-G type - may be simulated by an electrical network of resistive and capacitive elements, the equivalent circuit being such as that shown in Fig. 48. The circuits derived, however, only approximate to actual cell behaviour. With the more concentrated solutions and at the lower frequencies, additional R-C combinations are essential to obtain a better fit with the experimental data. Hence, it may be assumed that only an infinite number of R-C networks could completely describe the behaviour of the conductance cell.

As regards the R-X diagrams for the 0.005N and 0.0005N solutions in the T-G cell, where the curve turns over completely and then approaches the R axis, it appears that only the introduction of an inductive element can account for this behaviour. Until confirmation has been obtained for this peculiar type of graph, no satisfactory explanation can be offered.

(b) The increase of reactance with frequency - at the high frequencies - is clearly due to the shunting of the electrolyte resistance by the capacitance in the high relaxation frequency branch, which - it must be remembered - includes the inter-electrode capacitance of the cell. This may, however, be only one of the contributing factors, since the measured

reactances are not strictly proportional to the frequency in this region. Perhaps, the Parker effect is also responsible for this behaviour. No confirmation of this can be advanced from the present series of investigations.

(c) Since the inter-electrode capacitance is the same as long as measurements are carried out with the same cell, the high relaxation frequency must be inversely proportional to the electrolyte resistance. One would, therefore, expect the minimum to occur at progressively lower frequencies as the solution becomes less concentrated. This is certainly borne out by observation.

(d) The Jones and Christian extrapolation procedure is of doubtful validity - when bright platinum electrodes are used. Only if one can extrapolate out the residual effects of the high relaxation frequency branch can the method be considered to be satisfactory. Consequently, we see why the extrapolation for polarisation sometimes works if we plot R vs $f^{-\frac{1}{2}}$, at other times R vs f^{-1} and even R vs $f^{-\frac{1}{4}}$ in a few cases. It depends on the relative magnitudes of the relaxation frequencies of the two branches, both of which are seen to change from solution to solution and from cell to cell. Consider, for example, the R-X diagram for the 0.0005N solution in the N-F cell. If the low relaxation frequency were of the order of 2 to 3 kc/s, we should be near the maximum of the low relaxation frequency branch when the high relaxation frequency branch takes over, and it is understandable that

the resistance-frequency graphs would not look the same. Hence, it may be deduced that there is no simple relationship between R and f.

(e) In general, the high frequency branch is decided mainly by the configuration of the cell, while the low frequency branch represents the effects of the electrode processes i.e polarisation.

(f) The occurrence of a minimum in the diagrams may be explained along the following lines: measurements indicate that the cell geometry effect reaches its maximum at high frequencies (of the order of 10 megacycles per second or more) whereas the electrode processes have relaxation frequencies of the order of seconds. Between these two limits, therefore, there must be a region where these effects are reduced to a very small value, viz: at the minimum of the graph. The determining factors in this connection would obviously be: cell design, the nature of the electrolyte and the electrode material.

(g) The problem of how to find the true resistance of the electrolyte does now appear to be solved - at least, for solutions investigated in cells of the N-F type. An R-X diagram of the readings is plotted, and a very good approximation to the true resistance of the electrolyte is given by the value of R at the minimum of the graph. Alternatively, if readings are taken at high frequencies i.e. where the low relaxation frequency branch has negligible effect, the

following methods may be employed:

(i) Accurately fit a semicircle onto the points on an R-X diagram, and the point of intersection on the R axis will give the true resistance of the electrolyte.

(ii) Plot $1/R$ (where R is the observed resistance) vs ω^2. The true resistance may then be determined from the intercept (see p. 92 and Fig. 49). As has already been shown, this method was applied with a fair measure of success.

(h) Finally, it can now be stated with certainty that the equivalent circuit of the conductance cell contains non-linear elements - which confirms the conclusion reached by Gledhill and Allison (95).

2.7 SUGGESTIONS FOR FURTHER WORK

Since the data collected during the course of the present series of measurements can be regarded as a definite contribution towards the development of a satisfactory theory of the variation of observed resistance with frequency, it is suggested that future research be pursued along the following lines:

(1) Accurate measurements of resistance and capacitance should be carried out over an even wider range of frequencies. Thus, from readings taken at very low frequencies (in the region of 1 cycle per thousand seconds) useful information will be derived with regard to electrode processes, and the Warburg impedance

in particular. The very high frequency data (i.e. readings taken at 10 megacycles per second and more) can be used to provide additional information as regards the cell geometry.

Note: Extension of the frequency-range would, no doubt, call for modification in the design of the bridge.

(2) It is recommended that factors, in addition to the frequency of the a.c., be varied in order to gain further insight into the behaviour of the cell. This would involve:

(a) Varying the potential applied to the cell - which will permit a study of the non-linear elements.

(b) Varying the electrode spacing - so as to throw more light on the effects of the cell geometry.

(c) Varying the temperature at which measurements are effected - which should enable one to investigate the rate of the electrode processes.

(3) Lastly, all the effects mentioned should be investigated with various electrolytes, at different concentrations, contained in various forms of conductance cells and with different electrode materials.

A P P E N D I X

OPTIMUM OPERATING VOLTAGES

The Table below will be found useful in making any adjustments which may become necessary, or in cases of 'trouble-shooting'.

UNIT	TUBE	PLATE	SCREEN	GRID
CRYSTAL OSCILLATOR	½6SL7	180v	-	-4.4v
CATHODE-FOLLOWER	½6SL7	180v	-	-10v
V-F OSCILLATOR	½6SL7	160v	-	-0.5v
CATHODE-FOLLOWER	½6SL7	160v	-	-2.5v
FIRST MIXER	6SA7	115v	100v	-5.8v (1) -1.5v (3)
BRIDGE-INPUT AMP.	6AC7	150v	130v	-3.0v
CATHODE-FOLLOWER	6V6	185v	170v	-21v
BRIDGE-OUTPUT AMP.	6AC7	145v	130v	-3.2v
SECOND MIXER	6SA7	150v	110v	-5.6v (1) -1.4v (3)
CRYSTAL FILTER				
1st Stage of Amp.	6SJ7	150v	100v	-2.1v
2nd Stage	6SJ7	150v	100v	-2.1v
100 kc/s HORIZONTAL AMPLIFIER	6SJ7	150v	100v	-2.1v

BRIDGE CALIBRATION

The values given below were obtained when the resistances in the measuring arm were calibrated 'in situ' by the method of intercomparison (see Section 1.61).

DECADE RESISTANCES (G.R. Type 510-A, -B, -C, -D, -E)

TENTHS	CORRECTION
1	+ 0.0005 ohm
2	+ 0.0010
3	+ 0.0015
4	+ 0.0010
5	+ 0.0025
6	+ 0.0020
7	+ 0.0035
8	+ 0.0021
9	+ 0.0026
10	+ 0.0031

UNITS	CORRECTION
1	- 0.0008 ohm
2	- 0.0005
3	- 0.0023
4	- 0.0030
5	- 0.0048
6	- 0.0046
7	- 0.0064
8	- 0.0071
9	- 0.0059
10	- 0.0057

TENS	CORRECTION
1	+ 0.0049 ohm
2	+ 0.0050
3	+ 0.0090
4	+ 0.0013
5	- 0.0004
6	+ 0.0073
7	+ 0.0094
8	+ 0.0142
9	+ 0.0182
10	+ 0.0270

HUNDREDS	CORRECTION
1	+ 0.099 ohm
2	+ 0.139
3	+ 0.214
4	+ 0.265
5	+ 0.311
6	+ 0.335
7	+ 0.377
8	+ 0.404
9	+ 0.431
10	+ 0.457

THOUSANDS	CORRECTION
1	- 0.04 ohm
2	- 0.20
3	- 4.65
4	- 4.80
5	- 4.94
6	- 4.69
7	- 5.24
8	- 5.10
9	- 5.66
10	- 7.31

THE SLIDE-WIRE

The values given below are set out in the same way as in logarithm tables:

ohms x 10^{-4}

0	0	1	2	3	4	5	6	7	8	9
0	0000	0010	0019	0029	0039	0049	0058	0068	0078	0088
1	0097	0107	0116	0126	0135	0145	0155	0164	0174	0184
2	0193	0203	0213	0222	0232	0241	0251	0261	0270	0280
3	0290	0299	0309	0319	0328	0338	0347	0357	0367	0376
4	0386	0396	0405	0415	0425	0434	0444	0453	0463	0473
5	0483	0492	0502	0511	0521	0531	0540	0549	0559	0569
6	0579	0589	0598	0608	0617	0627	0636	0646	0655	0665
7	0675	0685	0695	0704	0714	0723	0733	0742	0752	0762
8	0771	0781	0791	0801	0810	0819	0829	0839	0849	0859
9	0868	0877	0887	0897	0907	0916	0926	0935	0945	0955
10	0965	0974	0983	0993	1003	1013	1023			

CALIBRATION OF DECADE CONDENSERS

G.R. Type 219-K: effective zero capacitance: 35 pF

THOUSANDTHS	CORRECTION
1	- 0.000004 μF
2	+ 0.000007
3	- 0.000002
4	+ 0.000014
5	+ 0.000015
6	+ 0.000006
7	- 0.000008
8	- 0.000027
9	- 0.000011
10	- 0.000020

HUNDREDTHS	CORRECTION
1	+ 0.000050 μF
2	- 0.000070
3	- 0.000030
4	+ 0.000310
5	+ 0.000290
6	+ 0.000270
7	+ 0.000250
8	+ 0.000230
9	+ 0.000210
10	+ 0.000100

G.R. Type 219-M: effective zero capacitance: 30 pF

THOUSANDTHS	CORRECTION
1	- 0.000002 μF
2	- 0.000016
3	- 0.000020
4	+ 0.000006
5	+ 0.000007
6	- 0.000022
7	- 0.000021
8	- 0.000040
9	- 0.000039
10	- 0.000053

HUNDREDTHS	CORRECTION
1	+ 0.000022 μF
2	- 0.000178
3	+ 0.000182
4	- 0.000003
5	- 0.000023
6	- 0.000073
7	+ 0.000132
8	+ 0.000112
9	+ 0.000035
10	- 0.000083

BRIDGE LEAD RESISTANCE

Readings taken with Cell Selector on R.H.S: + 0.013 ohm

RATIO ARMS INEQUALITY

Readings taken with the ratio arms reversed were found to be 0.026% higher than those with the ratio arms direct. Hence all observed resistances (taken with the ratio arms direct) were increased by 0.013%.

CALIBRATION OF WEIGHTS

W I

Nominal Wgt (g)	Correction (mg)
100	+ 0.62
50	+ 0.04
20	+ 0.02
10	+ 0.06
10•	+ 0.15
5	- 0.01
2	+ 0.05
1	0.00
1•	+ 0.02
1••	+ 0.03

Nominal Wgt (mg)	Correction (mg)
500	0.060
200	+ 0.045
100	+ 0.011
100•	+ 0.032
50	+ 0.010
20	- 0.050
10	- 0.021
10•	- 0.070

W II

Nominal Wgt (g)	Correction (mg)
1000	- 5.8
500	- 3.5
200	- 2.6
100	- 0.5
100°	- 1.2
50	+ 1.5
20	0
10	0
10°	0
5	0
2	0
1	0
1°	0

Nominal Wgt (g)	Correction (mg)
0.5	+ 1.0
0.2	0
0.1	0
0.1°	0
0.05	0
0.02	0
0.01	0
0.01°	0

W III

Beam Rider (10 mg): Correction: + 0.041 mg

Ring Riders

Nominal Wgt (mg)	Correction (mg)
90	- 0.028
80	- 0.025
70	- 0.036
60	- 0.026
50	- 0.019

Nominal Wgt (mg)	Correction (mg)
40	- 0.009
30	- 0.006
20	- 0.017
10	- 0.007

CORRECTIONS FOR INEQUALITY OF LENGTH OF BALANCE ARMS

B I : - 0.003%

B II : + 0.003%

EXPERIMENTAL READINGS

In the readings that follow:

R' = observed resistance corrected for bridge calibration, bridge and cell lead resistances and ratio arms inequality.

C = observed capacitance corrected for capacitance in the cell arm of the bridge and G.R. decade condenser calibration.

R and X are the effective resistance and reactance - calculated from values of R' and C as shown in Section 2.532.

SOLUTIONS MEASURED IN THE N-F CELL

0.01D KCl

f kc/s	R' ohms	R ohms	C μF	X ohms
0.50	115.87	110.80	0.588203	23.722
0.75	111.28	108.81	.287222	16.388
1.00	109.21	107.65	.175265	12.946
1.50	107.08	106.16	.092217	9.8799
2.00	106.09	105.53	.055305	7.7803
2.50	105.51	105.11	.037161	6.4736
3.00	105.16	104.85	.027080	5.6285
4.00	104.68	104.48	.016374	4.5009
5.00	104.31	104.17	.010991	3.7521
7.00	103.79	103.71	.006129	2.9017
10.00	103.34	103.29	.003491	2.3413
25.00	102.68	102.66	.000976	1.6161
50.00	102.49	102.45	.000628	2.0716
75.00	102.41	102.36	.000488	2.4104

0.005N KCl

f kc/s	R' ohms	R ohms	C μF	X ohms
0.25	233.75	219.92	0.683228	55.170
0.50	218.61	214.41	.204014	30.041
0.66	215.35	212.74	.122928	23.566
0.75	214.39	212.27	.099199	21.273
1.00	212.41	211.08	.059279	16.699
1.25	211.30	210.42	.038959	13.607
1.50	210.54	209.89	.027903	11.621
2.00	209.45	209.03	.016761	9.2216
2.50	208.89	208.6[illegible]	.011126	7.6162
3.00	208.43	208.23	.008031	6.5699
4.00	207.99	207.86	.004712	5.1200
5.00	207.71	207.63	.003121	4.2285
7.00	207.40	207.36	.001711	3.2364
10.00	207.02	207.00	.000910	2.4502
20.00	206.88	206.86	.000348	1.8715
25.00	206.85	206.83	.000258	1.7339
33.33	206.82	206.80	.000210	1.8811
50.00	206.81	206.76	.000191	2.5658
75.00	206.76	206.74	.000123	2.4777

0.0005N KCl

f kc/s	R' ohms	R ohms	C μF	X ohms
0.25	2037.7	2034.5	0.012485	81.302
0.50	2025.9	2024.9	.003547	45.712
0.66	2023.3	2022.7	.002110	36.134
0.75	2022.2	2021.7	.001694	32.635
1.00	2020.2	2019.8	.001019	26.125
1.25	2018.8	2018.5	.000738	23.626
1.50	2018.0	2017.8	.000560	21.491
2.00	2017.3	2017.1	.000373	19.073
2.50	2016.8	2016.7	.000274	17.506
3.00	2016.5	2016.4	.000223	17.091
4.00	2016.1	2016.0	.000168	17.161
5.00	2016.0	2015.9	.000133	16.980
7.00	2015.7	2015.5	.000113	20.220
10.00	2015.5	2015.3	.000097	24.755
20.00	2015.3	2014.4	.000086	43.873
25.00	2015.2	2014.0	.000081	51.638
33.33	2015.0	2012.6	.000081	68.800
50.00	2014.5	2009.3	.000081	103.00
66.66	2014.3	2005.0	.000081	136.89
75.00	2013.4	2001.6	.000081	153.83

SOLUTIONS MEASURED IN THE T-G CELL

0.01D KCl

f kc/s	R' ohms	R ohms	C μF	X ohms
0.25	99.481	98.293	0.705015	10.829
0.50	96.830	96.474	.200000	5.8695
0.75	95.825	95.615	.102998	4.5507
1.00	95.377	95.236	.065285	3.7261
1.50	94.951	94.866	.032968	2.7988
2.00	94.740	94.692	.019039	2.1464
2.50	94.623	94.586	.013048	1.8344
3.00	94.532	94.504	.008989	1.5137
4.00	94.393	94.374	.005398	1.2085
5.00	94.329	94.322	.003766	1.0527
7.00	94.284	94.276	.002400	.93828
10.00	94.240	94.232	.001249	.69692
20.00	94.094	94.085	.000628	.69863
33.33	94.023	94.016	.000493	.91274
50.00	93.984	93.968	.000462	1.2818
75.00	93.974	93.940	.000440	1.8303

0.005N KCl

f kc/s	R' ohms	R ohms	C μF	X ohms
0.25	188.39	187.23	0.265285	14.698
0.50	185.39	185.00	.079239	8.5380
0.66	184.62	184.38	.047302	6.7449
0.75	184.38	184.18	.037943	6.0719
1.00	183.68	183.55	.022928	4.8569
1.25	183.45	183.35	.015338	4.0521
1.50	183.18	183.11	.011342	3.5855
2.00	183.02	182.98	.006302	2.6522
2.50	182.84	182.80	.004487	2.3557
3.00	182.76	182.74	.003131	1.9710
4.00	182.64	182.62	.001904	1.5962
5.00	182.45	182.45	.001036	1.0834
7.00	182.42	182.42	.000733	1.0728
10.00	182.35	182.35	.000406	0.84826
20.00	182.19	182.19	.000233	0.97190
25.00	182.19	182.19	.000210	1.0950
33.33	182.34	182.34	.000145	1.0095
50.00	182.36	182.36	.000113	1.1806
66.66	182.54	182.54	.000091	1.2702
75.00	182.58	182.58	.000058	0.95957

0.001N KCl

f kc/s	R' ohms	R ohms	C μF	X ohms
0.25	905.00	904.54	0.016189	20.817
0.50	902.35	902.18	.004672	11.949
0.66	901.47	901.40	.002685	9.1392
0.75	901.23	901.18	.002170	8.3052
1.00	900.77	900.74	.001313	6.6935
1.25	900.34	900.34	.000901	5.7362
1.50	900.01	900.01	.000688	5.2523
2.00	899.67	899.67	.000417	4.2414
2.50	898.77	898.77	.000308	3.9080
3.00	897.02	897.02	.000243	3.6856
4.00	896.66	896.66	.000168	3.3948
5.00	896.43	896.43	.000133	3.3191
7.00	896.11	896.11	.000103	3.6378
10.00	895.95	895.95	.000083	4.1862
20.00	895.48	895.44	.000070	7.0536
25.00	895.69	895.62	.000068	8.5682
33.33	895.74	895.64	.000063	10.583
50.00	895.89	895.69	.000058	14.621
66.66	895.99	895.70	.000058	17.144
75.00	896.02	895.75	.000058	15.129

0.0005N KCl

f kc/s	R' ohms	R ohms	C μF	X ohms
0.25	1787.3	1787.0	0.004857	23.272
0.50	1782.8	1782.7	.001355	13.529
0.66	1782.2	1782.2	.000828	11.005
0.75	1781.7	1781.7	.000713	10.666
1.00	1780.4	1780.4	.000448	8.9221
1.25	1778.9	1778.9	.000328	8.1542
1.50	1778.5	1778.5	.000253	7.5424
2.00	1778.0	1778.0	.000188	7.4685
2.50	1777.8	1777.8	.000138	6.8511
3.00	1777.7	1777.7	.000123	7.3270
4.00	1777.7	1777.7	.000103	8.1808
5.00	1777.9	1777.9	.000090	8.9374
7.00	1778.4	1778.3	.000083	11.546
10.00	1779.3	1779.1	.000080	15.913
20.00	1779.6	1779.3	.000070	27.852
25.00	1779.7	1779.4	.000070	34.815
33.33	1779.8	1779.4	.000070	46.412
50.00	1780.2	1780.0	.000070	69.588
66.66	1780.4	1780.3	.000070	92.624
75.00	1780.5	1780.3	.000070	104.22

CONCENTRATIONS OF POTASSIUM CHLORIDE SOLUTIONS PREPARED

Nominal	Actual
0.005N	0.0050465N
0.001N	0.00099392N
0.0005N	0.00049860N

Note:

The specific conductance of the approx. 0.01D solution

$$= 1.4027 \times 10^{-3} \text{ ohm}^{-1} \text{ cm}^{-1}$$

DATA re CONDUCTANCE CELLS

CELL	LEAD RESISTANCE ohm	Q cm^{-1}
NICHOL-FUOSS	0.046	0.14381
THOMAS-GLEDHILL	0.060	0.13184

Note:

The true resistance values for the approx. 0.01D KCl solutions measured in the N-F and T-G cells were determined by the proposed graphical method mentioned on p. 102 (i.e. by plotting $1/R$ vs ω^2). Hence

In the N-F cell, true resistance : 93.990 ohms
In the T-G cell, true resistance : 102.52 ohms

These values were used in calculating the Q values given above.

S U M M A R Y

(1) Developments in a.c. conductance techniques during the past ninety years have been reviewed, and a brief outline is given of the older theories regarding electrolytic polarisation.

(2) A conductance bridge - incorporating the double heterodyne principle - has been constructed, capable of giving resistance readings to an accuracy of 0.01% over a range of frequencies covering the best part of 100 kc/s. It has also been found possible to calibrate the oscillator so that frequency settings can be guaranteed to an accuracy of , at least, 0.1% in the range: 2 kc/s to 50 kc/s.

(3) The Wheatstone Bridge Network has been slightly modified to enable measurements at the high frequencies.

(4) Resistances in the measuring arm of the bridge have been calibrated 'in situ' by the method of intercomparison.

(5) A brief description is given of the modern theories regarding electrode processes and modern methods of eliminating electrode effects.

(6) Two types of conductance cells, with bright Pt electrodes, have been used to carry out measurements on potassium chloride solutions: (a) Thomas-Gledhill Cell (b) Nichol-Fuoss Cell. The latter incorporates concentric, cylindrical electrodes with the lead to the outer electrode acting as an electrical shield for the lead to the inner electrode. This cell was constructed and used for the first time in this laboratory.

(7) From resistance-frequency graphs plotted, it is shown that the Jones and Christian extrapolation procedure cannot be applied (with any degree of confidence) to obtain the true resistance, when measurements are effected over an extended range of frequencies.

(8) The method of resistance-reactance diagrams is discussed and applied to various networks of resistances and capacitances.

(9) By drawing resistance-reactance diagrams for the experimental readings obtained, equivalent circuits have been derived - for all the solutions investigated in the N-F cell, and for the approx. 0.01D solution in the T-G cell - which approximate to cell behaviour in the range: 500 c/s to 75 kc/s. The less concentrated solutions in the T-G cell show peculiar behaviour at the high frequencies.

(10) Probable reasons are advanced for deviations from linearity on resistance-frequency graphs.

(11) A new method is proposed for determining the true resistance of solutions measured in cells of the N-F type.

REFERENCES

(1)	Kohlrausch	Wied. Ann.	11,	653, (1880)
(2)	Washburn and Bell	J.A.C.S.	35,	177, (1913)
(3)	Taylor and Curtis	Phys. Rev.	6,	61, (1915)
(4)	Taylor and Acree	J.A.C.S.	38,	2396, (1916)
(5)	Morgan and Lammert	ibid.	48,	1220, (1926)
(6)	Hall and Adams	ibid.	41,	1515, (1919)
(7)	Ulich	Z. Phys. Chem.	115,	377, (1925)
(8)	Woolcock and Murray-Rust	Phil. Mag.	5,	1130, (1928)
(9)	Jones and Josephs	J.A.C.S.	50,	1049, (1928)
(10)	Lamson	Rev. Sci. Inst.	9,	272, (1938)
(11)	Jones, Mysels and Juda	J.A.C.S.	62,	2919, (1940)
(12)	Ulrey	Physics	7,	97, (1936)
(13)	Breazeale	Rev. Sci. Inst.	7,	250, (1936)
(14)	Garman	Rev. Sci. Inst.	8,	327, (1937)
(15)	Koehler	ibid.	8,	540, (1937)
(16)	Quirk and Hall	Electronics	18,	147, (1945)
(17)	Hague, ''A.C. Bridge Methods'' p. 540 5th Edition (Pitman and Sons, Ltd., London)			(1957)
(18)	Campbell	Elec. World	43,	647, (1904)
(19)	Morecroft and Turner	Proc. Inst. Rad. Eng.	13,	497, (1925)
(20)	Shedlovsky	J.A.C.S.	52,	1793, (1930)
(21)	Astin	Bur. Stds. J. Research	21,	425, (1938)
(22)	Luder	J.A.C.S.	62,	89, (1940)

(23) Gledhill, M.Sc. Thesis (Univ. of S.A.) (1943)

(24) Goddard, M.Sc. Thesis (Univ. of S.A.) (1948)

(25) Faure,A. Ph.D. Thesis (R.U.) (1953)

(26) Washburn J.A.C.S. 38, 2431, (1916)

(27) Parker ibid. 45, 1366, (1923)
ibid. 45, 2017, (1923)

(28) Randall and Scott ibid. 49, 636, (1927)

(29) Shedlovsky ibid. 52, 1806, (1930)

(30) Jones and Bollinger ibid. 53, 411, (1931)

(31) Nichol and Fuoss J. Phys. Chem. 58, 696, (1954)

(32) Brody and Fuoss J. Phys. Chem. 60, 177, (1956)

(33) Wien Wied. Ann. 58, 37, (1896)
ibid. 59, 269, (1896)

(34) Warburg ibid. 67, 493, (1899)

(35) Jones and Christian J.A.C.S. 57, 272, (1935)

(36) Miller Phys. Rev. 22, 622, (1933)

(37) Faure, P.K., Ph.D. Thesis (R.U.) (1956)

(38) Taylor Ph.D. Thesis (to be submitted)

(39) Baker Rev. Sci. Inst. 22, 34, (1951)

(40) Herold Proc. I.R.E. 30, 84, (1942)

(41) R.C.A. Rec. Tube Manual (1955)

(42) G.R. Experimenter June,(1954)

(43) Zobel Bell System Tech. J. 2, 1, (1923)

(44) Langford-Smith, Radio Designer's Handbook, 4th Ed. (Iliffe and Sons,London) p.183 (1954)

(45) Wheeler Proc. I.R.E. 27, 429, (1939)

(46) Everest Electronics 11, 16, (1938)

(47) Terman,	Radio Engineer's Handbook 1st Ed. (McGraw-Hill)		p. 418	(1950)
(48) Stanesby		British P.O.E.E.J	28,	4,(1942)
(49) Mason		B.S.T.J.	13,	405,(1934)
(50) G.R. Experimenter				June,(1933)
(51) Everest		Electronics	14,	46,(1941)
(52) Dike		Rev. Sci. Inst.	2,	379,(1931)
(53) Robinson		J.P.O.E.E.	16,	171,(1924)
(54) Kurokawa and Hoashi		J.I.E.E. Japan	437,	1132,(1924)
(55) G.R. Experimenter				July,(1956)
(56) Grahame		Chemical Review	41,	441,(1947)
(57) Koenig		J. Phys. Chem.	38,	111,(1934)
(58) Frumkin		Acta Physicochim. U.R.S.S.	18,	23,(1943)
(59) Vorsina and Frumkin		ibid.	18,	242,(1943)
(60) Grahame		J. Electrochem. Soc.	99,	370,(1952)
(61) Remick and McCormick		ibid.	102,	534,(1955)
(62) Randles		Disc. Faraday Soc.	1,	11,(1947)
(63) Rozental and Ershler		Zhur. Fiz. Khim.	22,	1344,(1948)
(64) Gerischer		Z. Physik. Chem.	198,	286,(1951)
(65) Breyer and Gutmann		Disc. Faraday Soc.	1,	19,(1947)
(66) Breyer and Hacobian		Aust. J. of Sc.	14,	118,(1952)
		ibid.	14,	153,(1952)
(67) Parsons		Trans. Faraday Soc.	56,	1340,(1960)
(68) Remick		J. Chem. Ed.	33,	564,(1956)

(69)	Griffiths	Anal. Chim. Acta	18,	174,	(1958)
(70)	Gupta and Hills	J. Sc. Instr.	33,	313,	(1956)
(71)	Lavagnino and Alby	Ann. Chim. (Rome)	49,	1272,	(1959)
(72)	Hinkelmann	Z. Angew. Phys.	10,	500,	(1958)
(73)	Feates, Ives and Pryor	J. Electrochem. Soc.	103,	580,	(1956)
(74)	Huber and Cruse	Angew. Chim.	68,	178,	(1956)
(75)	Salomon and Svitok	Chem. Prumyol	6,	10,	(1956)
(76)	Lim	Aust. J. Chem.	9,	443,	(1956)
(77)	Gordon and Gunning	J. Chem. Phys.	10,	126,	(1942)
(78)	Jervis, Muir, Butler and Gordon	J.A.C.S.	75,	2855,	(1953)
(79)	Clur, M.Sc. Thesis	(R.U.)			(1959)
(80)	Nagaura and Karaki	J. Inst. Polytech. Osaka City Univ.	5,	7,	(1956)
(81)	Uggla	Naturwissenschaften	44,	391,	(1957)
(82)	Munson	Dissertation Abs. (Northwestern Univ. Evanston, Illinois)	20,	2043,	(1959)
(83)	Deighton	J. Sci. Instr.	13,	298,	(1936)
(84)	Sturtevant	Rev. Sci. Instr.	9,	277,	(1938)
(85)	Benson and Gordon	J. Chem. Phys.	13,	473,	(1945)
(86)	Addink	Rec. trav. Chim.	70,	205,	(1951)
(87)	Gledhill, Faure and Faure	J. of S.A. Chem. Inst. (New series)	4,	19,	(1951)
(88)	Shedlovsky	J.A.C.S.	54,	1411,	(1932)
(89)	Jones and Bradshaw	ibid.	55,	1780,	(1933)
(90)	Gledhill and Faure	Analytical Chem.	30,	1304	(1958)

(91) Li and Fang J.A.C.S. 64, 1544, (1942)

(92) Malan, Ph.D. Thesis (R.U.) (1953)

(93) Taylor, Ph.D. Thesis (to be submitted)

(94) Allison, M.Sc. Thesis (R.U.) (1953)

(95) Gledhill and Allison Trans. Faraday Soc. (in press)